To the Graduate Council:

I am submitting herewith a thesis written by Benjamin Kyle Bowlin entitled "Descriptive, Interpretive, and Quantitative Study of the Coarse Clastics of the Middle Ordovician Tellico Formation in the Vicinity of South Holston Dam, Tennessee." I recommend that it be accepted in partial fulfillment of the requirements for the degree of Master of Science, with a major in Geology.

Fred B. Keller

Fred B. Keller, Major Professor

We have read this thesis and recommend its acceptance:

Kenneth R. Walker

Otto C. Kopp

John B. Higgins

Accepted for the Council:

L Evans Roth

Vice Chancellor
Graduate Studies and Research

DESCRIPTIVE, INTERPRETIVE, AND QUANTITATIVE STUDY OF THE COARSE CLASTICS OF THE MIDDLE ORDOVICIAN TELLICO FORMATION IN THE VICINITY OF SOUTH HOLSTON DAM, TENNESSEE

A Thesis

Presented for the

Master of Science

Degree

The University of Tennessee, Knoxville

Benjamin Kyle Bowlin

December 1979

This thesis is dedicated

to the memory

of my beloved grandmother

Sarah Augustina Cantwell Brewer

(1902-1979)

Blessed are the dead which die in the Lord from henceforth: Yea, saith the Spirit, that they may rest from their labours; and their works do follow them. (Revelation 14:13)

ACKNOWLEDGMENTS

This thesis is the result of the assistance and encouragement of many people.

Fred Keller, my advisor, has been most generous with his assistance. I am especially grateful to him for the careful attention he has given to the organization and revision of this work. On him fell the unenviable task of editing earlier versions of the thesis. His suggestions have been both helpful and insightful.

Otto Kopp, Kenneth Walker, and John Higgins also contributed to this work. Professor Kopp has been quite helpful with the organization and writing of this thesis. Professor Walker has helped clarify the geological constraints on some of the quantitative models presented in this work. Professor Higgins has advised me with regards some of the quantitative aspects of the study.

My brother-in-law, Peter Mariolis, helped set up the design of the analysis of variance and the factor analysis. At each step he clarified the quantitative methodology and helped evaluate the results.

James Sledz assisted Dr. Mariolis and me in running the computer program for the factor analysis. I thank him for his kind assistance.

I thank Terry Raines, University of Virginia, for his help in untangling the complexities of Kolmogorov analysis.

Elliott and Mavis Barrett are acknowledged for their warm support and friendship during the completion of this work.

Juan Rodriguez is acknowledged for his support and assistance during the writing of this work. He helped me untangle numerous problems encountered in the completion of this thesis.

It is with good reasons that acknowledgments end with mention of one's family. For my parents, Dora and Kyle Bowlin; for my sister, Corinne Mariolis, her husband, Peter, and children, Michael and Margaret; for by beloved grandparents, both living and deceased, I owe the deepest debt of gratitude.

ABSTRACT

Coarse clastics of the Middle Ordovician Tellico Formation in the vicinity of South Holston Dam in northeast Tennessee are described by distinct sets of attributes which are thought to reflect the action of three transport mechanisms: fluid turbulence, grain dispersive pressure, and debris flow. Normal distribution grading, clast-supported fabric, erosive features, Bouma (1962) divisions, and relatively good sorting reflect fluid turbulence. Inverse grading and imbrication suggest the action of grain dispersive pressure. Chaotic, matrix-supported beds indicate debris flow. Coarse-fraction and distribution grading are distinguished on the basis of their standardized cumulative densities by the Kolmogorov-Smirnov Statistic. Distribution grading is studied by a one way analysis of variance. Vertical variation is shown to be significant but not adequately characterized by a linear model. Departures from linearity are related to competency-availability constraints.

The coarse clastics are divided into five lithotypes following Walker (1978): classical turbidites, massive sandstones, pebbly sandstones, clast-supported conglomerates, and matrix-supported beds. Each lithotype is characterized as to its descriptive features and possible transport mechanism. Certain distinct patterns of regular change, both within beds and between beds, are suggested by upward transition probability matrices.

Associational and sequential regularities in lithotypes and their properties provide evidence for distinct environments of deposition. Broadly, the six outcrops studied are best explained as deposits of a submarine fan. Markov analysis and smoothing procedures are used to study the sequential regularities in the rocks. Transitions in conglomerates and turbidites provide information on the environmental constraints that induced regularity in their probability matrices.

Factor analysis is used to objectively specify the common factors explaining variation in properties (R-mode) and beds (Q-mode). An iterative R-mode factor analysis disclosed five factors: a turbulence factor, a scale or parameter factor, a bed geometry factor, a time-competency factor, and a clast concentration factor. These factors explain property variance in the coarse clastic beds studied. Q-mode analysis uncovered one important factor that defines a seriation of the beds from proximal to distal environments. This seriation in turn can be used to stochastically ordinate the properties of the coarse clastic beds.

Kolmogorov (1951) analysis is used to investigate the interaction of accumulative and erosive processes in turbidite sedimentation. By extending shale thickness distributions into the negative region left of the ordinate, an approximation (p) to the stable probability value of shale accumulative events is achieved. A model of shale deposition is proposed for a stationary, independent time series. The convolution integral of the thickness distributions of pelagic and turbiditic shale in such a series yields a near normal, though erosion-truncated, density distribution. It is this distribution that is used to calculate Kolmogorov's coefficient and ratio. Autocorrelation coefficients, thickness ratios, and amalgamations provide some empirical evidence in favor of the theory. Compaction and phenomenological limitations suggest important qualifications to the values of the ratio and coefficient.

TABLE OF CONTENTS

LIST OF TABLES

TABLE | PAGE

LIST OF FIGURES

FIGURE PAGE

FIGURE PAGE

FIGURE PAGE

CHAPTER 1

INTRODUCTION

Purpose and Methods

Coarse clastic rocks of Middle Ordovician age are exposed at several localities in eastern Tennessee and southwestern Virginia. Particularly striking examples of conglomerates, massive sandstones, and sandstone-shale couplets crop out in a northeast-trending belt (Tellico Formation) in the vicinity of Bristol, Tennessee. A field study of several exposures of these rocks provided information which will be treated from three separate, though interrelated, standpoints in this study.

The deposits are described at successively more complex levels of organization: from the individual, within-bed properties (Chapter 2), the bed (Chapters 3 and 5), the outcrop (Chapters 4 and 6), to the basin (Chapters 4 and 6). Features such as bed thickness, grain size, sedimentary structures, and other noninferential properties are examples of this type of outcrop characterization. The outcrops fall into broadly different patterns and sequences of regularity based upon these observable properties.

The data and descriptive types ascertained from them at each level of organization (property, bed, outcrop, basin) have been interpreted for their significance as indicators of geological process and environment. Suites and association patterns of these parameters point strongly toward overall styles and facies of deposition. These broader relationships provide answers to questions of possible paleoenvironments and their changes through time.

Quantitative stratigraphic and sedimentologic methods have been applied at each level of organization to the data to suggest solutions to several problems dealing with coarse clastic sediments. The application of statistical and mathematical techniques to coarse clastic deposits constitutes the primary investigative method of this thesis. The problem of the definition and quantification of grading is reviewed and a linear statistical model (ANOVA) (Choi, 1978) suggests restrictions to the definitions and applications of grading terminology. The classification of coarse clastics has long been a serious problem and factor analysis (Rummel, 1970) has been applied to the rocks and their properties to examine whether a classification can be achieved based on natural divisions and not on arbitrary divisions based upon clast size alone. Markov analysis (Krumbein, 1967) has been used to unravel preferred successions of lithological states in these coarse clastic sediments. Finally, Kolmogorov analysis (Kolmogorov, 1951) has been used to quantify the interplay between erosive and accumulative processes in the dynamics of sedimentation as it evolved through time.

Regional History and Stratigraphic Nomenclature

Throughout much of the Cambrian and the Lower Ordovician, the Appalachian region was the site of shallow-water carbonate deposition with some admixture of terrigenous material from the North American craton. In the Middle Ordovician, this passive continental shelf experienced subsidence and a great influx of clastic sediments from a southeastern source area (Shanmugam and Walker, 1978). A sequence of clastic material, which coarsens upward and to the southeast, was deposited in a deep, rapidly subsiding basin. Within the study area, this Middle Ordovician sequence has been variously named and subdivided. Figure 1-1 shows a summary of the stratigraphic nomenclature applied to the rocks by workers in northeast Tennessee. Neuman's terminology (1955) is adopted in this work.

A major reason for the varying terminologies has been the very real difficulty of correlating across facies changes and different thrust belts as well as differences among outcrops in this particular area with those in the type localities of the several formations. In particular, the Tellico-Sevier belt of Neuman (1955) occurs in the strike belt west of the Pulaski fault, while the Bristol rocks are within the Pulaski thrust sheet. If, as this study will maintain, the clastics in this area are best interpreted in terms of a submarine fan model, the chances of working out a detailed stratigraphy are slim. Structural complications, poor exposures, shifting, abrupt facies changes are some of the factors which would militate against a detailed correlation of beds for any distance.

These complications are probably the reason why even the thickness of the sequence is a matter of dispute. Butts (1940) thought the sequence to be around 10,000 feet (3050 m) thick in the vicinity of South Holston Dam while Kellberg and Grant (1956) and King and Ferguson (1960) believe it to be between 5,000 and 8,000 feet (1500-2400 m). King and Ferguson

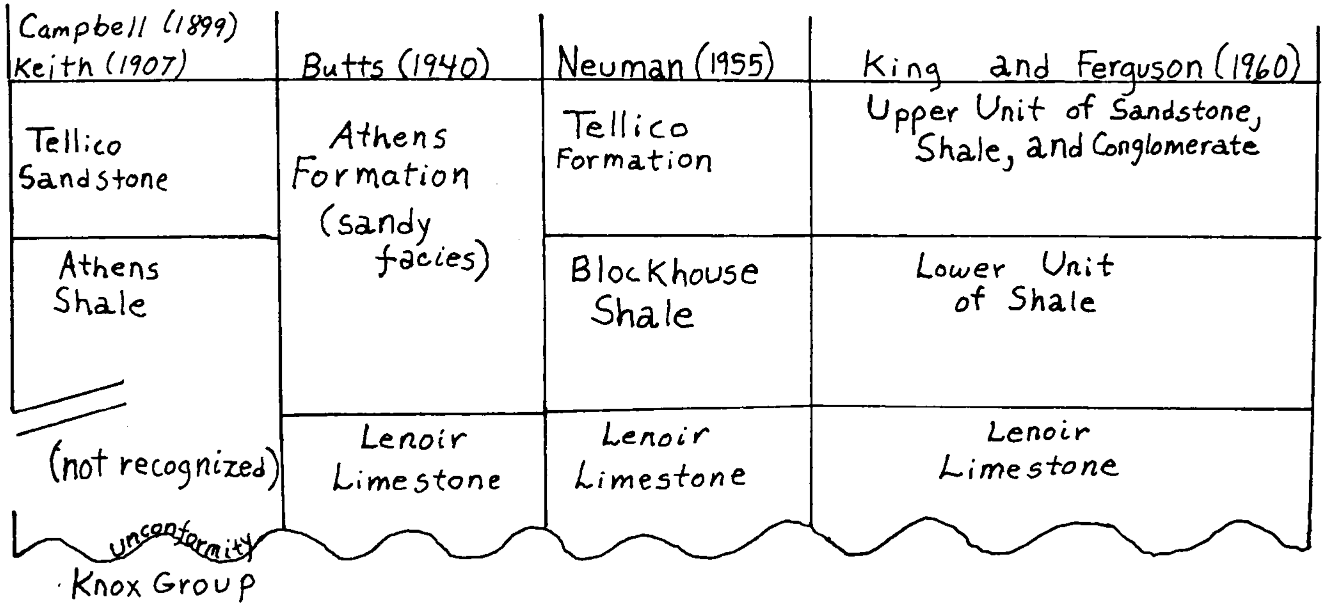

Figure 1-1. Stratigraphic nomenclature applied to the Middle Ordovician Series in northeastern Tennessee. Figure is after King and Ferguson (1960).

regard 5,000 feet (1500 m) as the minimal thickness estimate. This estimate will be accepted in this work.

Geology and Structure in the Study Area

The geological relationships within the study area are shown in Figure 1-2. The Middle Ordovician clastics under consideration form a synclinorium that is overriden on the southeast by Cambrian (Chilhowee Group) rocks along the Holston Mountain fault. They unconformably overlie the Knox Group (Jonesboro Limestone) to the northwest and are a part of the Pulaski thrust sheet. Typical of structure in the Appalachian Valley, the faults dip southeast at low angles and the rock formations define northeast-trending outcrop belts.

In the study area itself, the Middle Ordovician rocks in the South Holston Dam area generally strike northeast and dip from 30 to 50 degrees to the southeast. However, locally, the rocks are almost vertically dipping and are in places overturned. The broad structural pattern of the synclinorium is complicated by complexly faulted and folded strata in its interior. Shale sequences have been especially susceptible to deformation. Detailed structure sections, unfortunately, are not available. The complex relationship between various lithofacies, as well as the deformed nature of the strata, makes the construction of accurate structure sections difficult.

Location and General Description of the Outcrops

The six outcrops described in this work are located in the vicinity of South Holston Dam Reservoir, approximately 13 km southeast of Bristol,

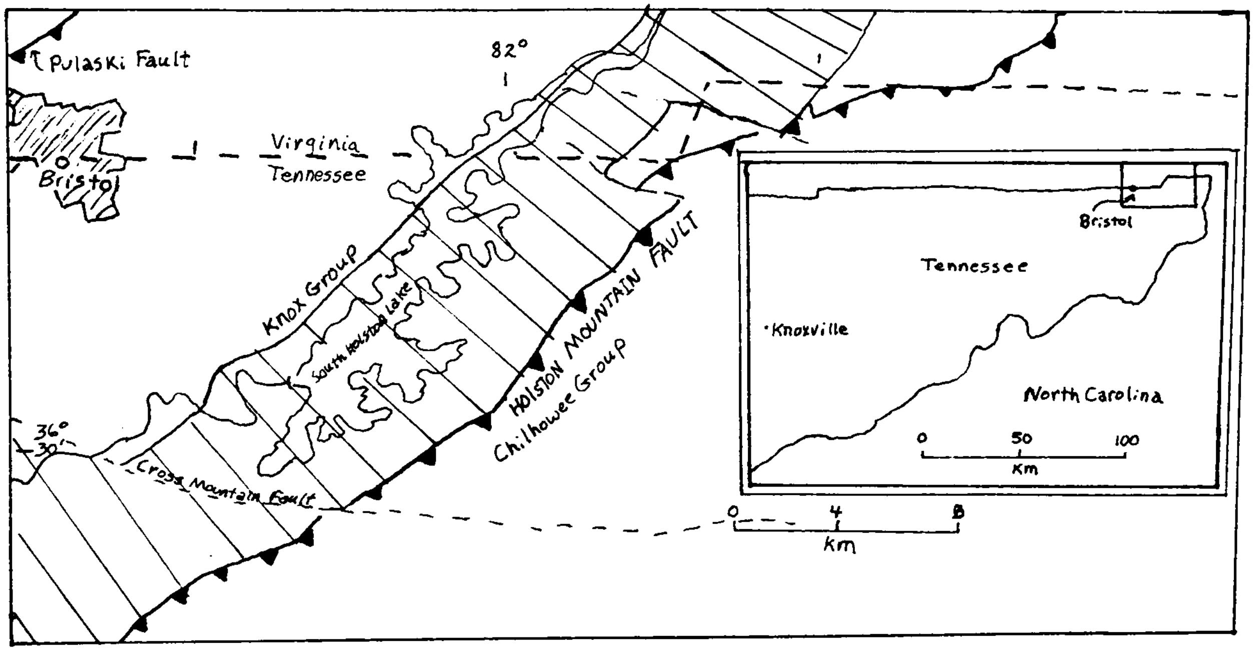

Figure 1-2. General geologic relationships in the study area. The hatchured area represents the Middle Ordovician clastic belt.

Virginia. Figure 1-3 shows the specific locations of the outcrops with the abbreviations by which each outcrop will be identified in the text. The outcrops occur in the Appalachian Valley portion of the Valley and Ridge Physiographic Province.

A spectrum of clastic rock types ranging from thick conglomerate beds containing clasts almost a meter in diameter to thinly laminated pelites is contained in the outcrops. Separately, however, each of the outcrops examined can be characterized by the dominance of one type (or closely related types) of deposit.

South Holston Dam (SHDC) and Avens Ferry (AFC) are dominated by conglomerates, diamictites, and massive sandstones. In both cases, these extremely coarse clastics rest on top of finer, thinner-bedded sediments. Beds from Lower South Holston Dam (LSHDS) and Upper South Holston Dam (USHDS) are primarily composed of sand and finer-sized material. Outcrop LSHDS is dominated by beds describable by the Bouma sequence (Bouma, 1962). Outcrop USHDS contains mostly massive sandstones and some fine pebbly sandstone for which the Bouma notation is not appropriate. Outcrops at Lower Lucy Creek and Upper Lucy Creek (LLCD and ULCD, respectively) both include large units of what are herein interpreted as debris flows (or transitional slump) deposits. In both cases, these thick, jumbled beds of coarse material are bounded, top and bottom, by beds of probable turbidity current origin.

Lithologically, the rocks at all outcrops are polymict. The conglomerate clasts are mostly carbonate (80.9% according to Kellberg and Grant for the SHDC outcrop, 1956) with a minor admixture of quartzite,

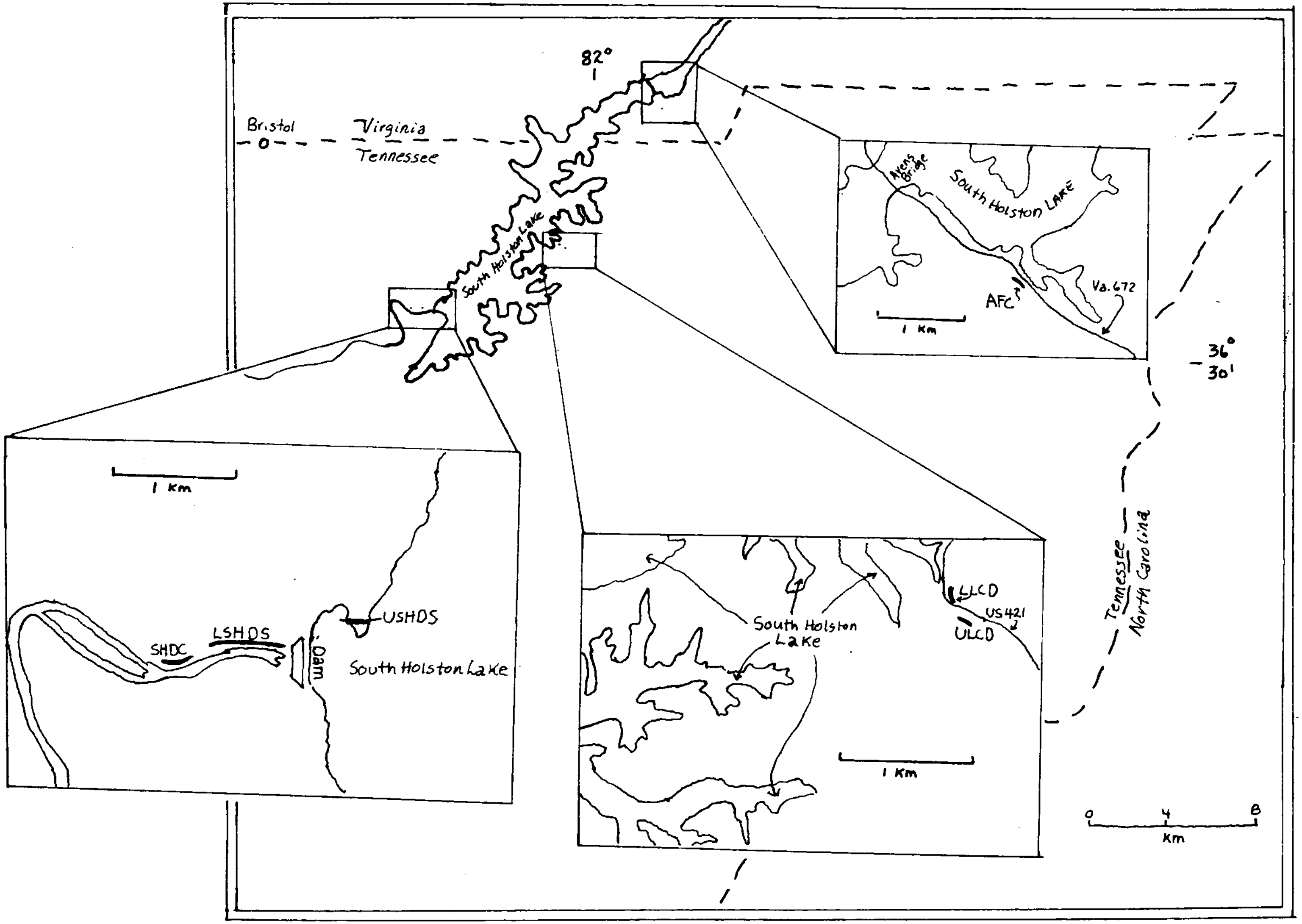

Figure 1-3. Outcrop locations. Abbreviations explained in the text.

chert, sandstone, and siltstone. The percentage of quartz is greater in the sandstones than in the conglomerates (Leible, 1975), but the rocks are still calcite cemented and have abundant carbonate rock fragments. It is thought (Kellberg and Grant, 1956; Leible, 1975) that the clastic material contained in these rocks was derived from the older rocks underlying the Middle Ordovician, perhaps including the Precambrian Mount Rogers Formation. Some material may have been derived from within the Tellico Formation itself.

Stratigraphic Relationships among Outcrops

The outcrops can be related to each other in only a most general fashion. SHDC rests upon the Blockhouse Shale. LSHDS lies above SHDC but is separated from it by a faulted, covered interval [approximately 50 m of section(?)]. USHDS lies approximately 330 m above the Blockhouse and is, hence, stratigraphically above LSHDS, the stratigraphic separation between the two being perhaps 125-130 m.

The outcrop at Avens Ferry (AFC) is estimated to be 215 m above the Blockhouse (King and Ferguson, 1960). The two outcrops at Lucy Creek (LLCD and ULCD) are thought to be near the top of the section approximately 1000 m above the top of the Blockhouse. Figure 1-4 shows the suggested stratigraphic relationships among the outcrops in the study area.

Previous Work

Early examinations of the Middle Ordovician clastics in the study area were motivated by questions of regional stratigraphy. (See King

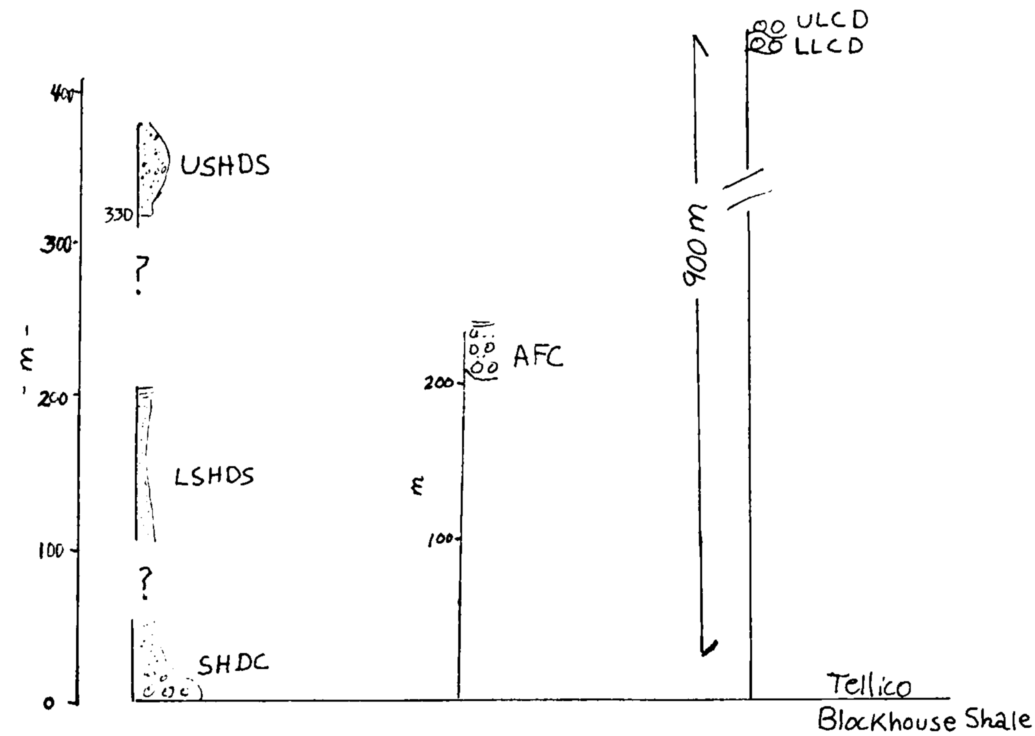

Figure 1-4. Stratigraphic relationships among outcrops. General lithology is schematically indicated in the diagram. The datum is the top of the Blockhouse shale.

and Ferguson, 1960, for a summary of these early investigations.) The descriptions are general; the main goal was regional correlation of larger stratigraphic packages. Kellberg and Grant (1956) and King and Ferguson (1960) provide more detailed descriptions of the rocks in the study area. In particular, Kellberg and Grant describe SHDC, USHDS, ULLD and AFC. King and Ferguson summarize these descriptions and describe ULCD in some detail. However, in these descriptions the outcrops were broken into units characterized only by broad lithologic terms (e.g., "conglomerate"). Further, these earlier investigators were hampered by the lack of theoretical models concerning the emplacement mechanisms and deposits of subaqueous gravity flows. Their descriptions reflect this lack and do not include measurements or descriptions of what other workers now regard as important properties of coarse clastics (e.g., maximum clast size, bed thickness, grading type, imbrication, etc.). Specification of depositional mode and environment, of course, could only be made in the most speculative sense in the absence of descriptive sedimentological models.

A more detailed study of AFC and SHDC with some ancillary comments on LSHDS was made by Leible (1975). Her descriptions, while somewhat vague, can be partially documented at the level of a bed-by-bed traverse across the outcrop. Unfortunately, her interpretation is suspect as the Bouma C interval of sandstones was misinterpreted as ripples formed by currents in shallow water. Turbidite beds, consequently, were not recognized as such. The sequence is described as resulting from some unspecified "high-energy" shallow water emplacement mechanism.

A more plausible interpretation of the sequence was given by Walker and Keller (1977). Reference was made in their work to the submarine fan model and mechanisms of clast transport (e.g., turbidity currents). While their interpretation is substantially correct, more documentation is necessary for the full interpretation of these deposits.

Methods of Data Collection

This study has been almost completely field oriented with respect to the amassing of data. Conglomerates, with their large clasts and thick beds, present almost insuperable difficulties regarding statistically valid sampling techniques for laboratory examination. Although thin-sections and polished slabs have been made, the majority of the information was derived from measurements and observations made at the outcrops themselves. A summary of the thickness and lithotype data on which much of the quantitative work is based is given in Appendix A. Other descriptive data appear at appropriate places within the text.

CHAPTER 2

DESCRIPTIVE PROPERTIES OF COARSE CLASTIC SEDIMENTS AND THEIR IMPLICATIONS AS TO GEOLOGICAL PROCESS

Introduction

In this chapter, the most basic descriptive properties of coarse clastic sediments are reviewed, and methods of statistical sedimentology are applied to the problem of defining grading. The chapter will close with a review of the types of transport mechanisms important in the formation of coarse clastic deposits and their properties.

Review of Terminology

Bed

This term refers to that thickness of sediments that was deposited under essentially the same physical conditions during a single depositional event (Otto, 1938). As such, it is both descriptive and interpretive. For most sediments, the identification of a bed (both senses) poses little problem. For coarse clastics, however, amalgamation of separate units, marked lateral changes in bed thickness and grain size, and incomplete understanding of the different structures possible from one depositional event make the breakdown of an outcrop into beds difficult. These problems are not pronounced in turbidite sequences (LSHDS). They appear more strongly in massive sandstone sequences (USHDS), and are worst in conglomerates (SHDC and AFC).

Bed Thickness

In all cases, maximum thickness is used as the bed thickness measurement parameter. Lateral diminution or disappearance is noted but not used in calculations. Since numerical values are assigned to each bed, bed thickness classifications (e.g., Ingram, 1954) are not used extensively. However, in qualitative descriptions, the conventions of Ingram are followed.

Clast Size

A variety of measurement parameters have been used for clasts in coarse deposits. At present, though, the physical significance of these measures is not clearly understood. For many of the coarse beds, three parameters--maximum clast size, D/10, and mean grain size--were recorded. These are treated below.

Maximum clast size. Maximum clast size indicates in a general way flow competency immediately prior to the deposition of the clast, but it does not specify the limits of competence. Two beds with identical maximum clast size may have been deposited from currents with quite different clast support mechanisms--for example, fluid turbulence and matrix strength--so that comparisons of "vigor" or "energy" based on maximum clast size may be invalid.

D/10. D/10 (mean diameter of the 10 largest clasts in a certain interval or in a bed) has been used extensively by Walker (1975, 1977) to show graphically the variation in graded beds. In many graded beds the main variation in clast size occurs in the very coarsest fraction as a result of changing flow velocities (Middleton, 1967). D/10 may thus tell us more about flow conditions and fluctuations than would a *bona fide* measure of central tendency, for example, the mean (Allen, 1968; Pett and Walker, 1971a,b). However, it may present a distorted picture of the variation in the population as a whole.

Mean grain size. Mean grain size and mean size of clasts above a certain size range (say, the mean size of material coarser than sand) give a better picture of the size distribution of the total population than either maximum grain size or D/10. But, again, whether we always want to know about the whole population or what such a measure tells us is an unsettled question.

Grading

Observations of grading within beds are problematic as there is not only variation in the types of systematic change shown by coarse clastics, but also no one set of measurement parameters has been shown to be best in quantifying this variability. Some beds show significant variation in mean grain size, some in the frequency of a given clast size class, others in the mean of the coarsest grains. Furthermore, there are several different variation patterns. What is and what is not called "graded" depends in many cases upon the approach, the rigor of the quantifying program (if there is one), the subjectivity of the field examiner, and the style of the variation pattern itself.

The rationale behind a close study of grading is that the presence of different systematic grain size variation patterns is good evidence of different sedimentation-emplacement mechanisms. In the following, several different types of grading observed in the study are described. Later, the author will treat these patterns quantitatively.

Normal grading. In this type of grading the magnitude of a grain measurement parameter (mean, D/10, etc.) shows a significant decrease with increasing vertical height from a given datum level (usually, but not always, the datum is the lower bedding surface). There is no implication that this trend is regular in a linear sense. There are two important varieties: distribution and coarse-fraction.

In normal distribution grading, the entire grain population shows a decline in size upward (Rocheleau and Lajoie, 1974). This variety is common in sands as well as coarser-grained beds.

Rocheleau and Lajoie (1974) distinguish two types of coarse-fraction grading: coarse-frequency grading, in which coarser grains maintain a relatively constant size but decline in simple abundance upward; and, coarse-tail grading, characterized by a diminution in the mean diameter of only the coarse fraction upward. In most examples that were examined in this study, neither type appears dominant as both generally appear alternately or irregularly within the same bed. The two have, consequently, been called coarse-fraction grading in this study.

Inverse grading. Inverse grading is a pattern of vertical variation in which the grain size parameter measured increases upward. It may be either distribution or coarse-fraction in variety. There are some other important differences between inverse grading and normal grading, however.

First, the datum from which an inversion is observed to commence is always a bedding surface. While normal grading may proceed from *within* a bed following an inversely graded interval, inversely graded intervals were always observed in the study area to proceed from the base of a bed.

In beds in which a normally graded interval follows an inversely graded interval, the thickness of the inversely graded interval is usually considerably less than the normally graded portion. For example, thickness proportions such as 7:38, 9:22, and 1:2 were observed in three inverse-to-normally graded units.

Inverse grading in sandstone is much more rare than in coarser material. Whether this is simply a bias introduced because inverse grading is less easily observed in finer material or whether its rarity indicates a real difference between the two is unclear. Inversion, however, was observed in some sandstone units. There cannot be, then, an absolute physical constraint against inverse grading in sand-sized material.

Textural Homogeneity

There are many beds or parts of beds in which homogeneity, not systematic variation, is the characteristic textural feature. Two end-member types of textural homogeneity can be distinguished in the study area on the basis of sorting.

Poorly-sorted texturally homogeneous beds. Beds of this category range from poorly sorted, matrix-rich sandstones to extremely thick beds in which large boulder-sized clasts are randomly dispersed in a sandy to muddy matrix. No well developed fabric or textural styles are discriminated. Field examination as well as laboratory examination of slabs cut along three mutually orthogonal planes show no significant or quantifiable trends or orientations. Whatever physical mechanisms served to emplace these beds did not develop that degree of discrimination necessary to size sort the material.

Fair-to-well-sorted texturally homogeneous beds or intervals. The best examples of this textural property are found in the massive sandstone lithotype (the term "massive" is used in this thesis solely as a textural term, not as a thickness term). Some units have nearly two meter thick intervals with homogeneous, nongraded texture in very well-sorted sand. In general, these beds are of medium or slightly finer sand. Usually, a texturally homogeneous interval occurs not as an entire bed but as the central portion of otherwise graded beds. It is bounded top and bottom by some form of graded interval.

Imbrication

Imbrication in coarse clastics refers descriptively to a clast fabric in which an overlapping of clasts, inclined at some preferred angle to bedding, is exhibited. However, for those coarse clastics thought to have been deposited by subaqueous density currents the orientation and implications of imbrication are very different from coarse clastics deposited by fluvial processes.

Imbrication occurs in fluvial sediments when the intermediate axis of a clast dips up-current and the long axis lies transverse to flow, assuming ellipsoidal-shaped clasts for simplicity (Rust, 1972). In the current process of bed load rolling, the most stable configuration is one in which the rotation of the clast occurs about the long axis. It is in this position that the center of gravity is lifted least as the clast rolls along the bed (Walker, 1975).

For subaqueous density current sediments, however, imbrication occurs as a result of up-current dip of long axes and alignment of these long axes parallel to flow (Davies and Walker, 1974). Both the orientation (plan view) and imbrication (vertical section cut parallel to long axes' orientation) are exhibited by the long axes, the orientation giving the trend and the dip giving the up-current direction of the emplacing flow (see Figure 2-1). Apparently, then, bed load rolling played little part in developing imbrication for these deposits. The clasts deposited from a dispersion or turbulent suspension assume a different statistically stable configuration. The reasons for this will be discussed in a later section on the grain flow mechanism.

Stratification

"Stratification" in the literature is used as a technical term referring to a within-bed size segregation of grains into bands or layers (strata). In this usage it is not synonymous with bedding. The term will be used in this work solely in this technical sense.

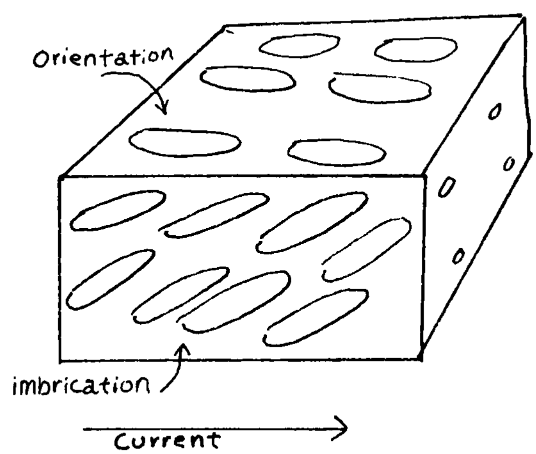

Figure 2-1. Imbrication in subaqueous density flows.

Stratification is a poorly understood property of coarse clastic deposits. It refers descriptively to the development of alternating coarser and finer grained layers that are segregated from each other, sharply or crudely, depending upon the difference in grain sizes between layers and the abruptness with which one layer ends and the next begins. This stratification of grain sizes appears in conglomerates (usually rather crudely), pebbly sandstones, and massive sandstones. It varies in scale from a few grains in thickness in some sandstones to 10-15 cm thick bands of coarse and medium sand in others. It may be parallel or oblique to bedding.

At present, there is no satisfactory explanation for the causes of stratification. Rocheleau and Lajoie (1974) postulate the origin of oblique stratification in the filling of holes in the underlying bed. The origin of these holes in not suggested, nor is their control on the occurrence of oblique stratification explained. Since oblique stratification usually occurs higher up in a bed, presumably the holes in the underlying bed would have already been filled earlier by the lower portions of the bed.

Walker (1975) thinks that stratification results when eddies from the upper part of the flow sweep finer material down into the coarser portion of the flow where it is trapped and kinetically sieved into a well-defined band. Repeated eddy sweeps result in the development of bands of stratification. However, the kinetic sieve mechanism results in inverse grading, not the sharply defined layers of size-segregated material we see in some beds (Middleton, 1970).

Hendry (1972) reports that oblique stratification is part of a preserved dune form. The oblique stratification was formed by dune migration. The segregation of sizes may thus have involved traction. It is doubtful, however, that dune migration can explain all the occurrences of stratification (Rocheleau and Lajoie, 1974).

Stratification is a real property exhibited by some coarse clastic beds. It is not clear what its significance is or what it indicates about flow mechanism. Indeed, there may be different causes for stratification in different beds. Eventually, however, a satisfactory explanation may be found. Until that time, it is important to at least notice and record the presence or absence of stratification in a bed.

Quantification of Grading

Field observations and measurements suggest that grading patterns introduced in the preceding section validly represent the grain size variation in coarse beds of the study area, though data was necessarily collected on weathered, irregular outcrop surfaces where the error of measurement is large. As a method of checking these patterns in a rigorous fashion, some slabs were examined to determine if the relationships established in the field are exhibited at a closer level of scrutiny.

Two slabs were chosen for closer examination. Slab A was thought in the field to be inverse-to-normally distribution graded (taken from SHDC-X). The other, B, was thought to be inverse-to-normally coarse-fraction graded (taken from AFC-33). The cut slab of B revealed it to be toward the coarse-frequency end of the coarse-fraction spectrum. Measurements of apparent long diameters on faces cut normal to bedding were made. Each slab was divided into one centimeter thick rows as nearly parallel to bedding as possible, and all clasts larger than 1 mm with centers within the confines of a particular row were measured and recorded in the tally for that row (1839 grains on A and 416 grains on B). Figure 2-2 shows a simple plot of the row means of the two distributions of grain sizes.

Distinction between Coarse-Frequency and Distribution Grading

In establishing that two distinct types of grading are represented by slabs A and B, two steps are required. First, statistical diversity in the cumulative density functions of the two populations must be shown; and, second, this diversity must be characterizable in such a way that the initial expectations regarding the distinction between coarse-frequency and distribution grading are confirmed.

Due to differences in mean grain size, it is not possible to compare the total cumulative distributions directly. If the differences due to the first two moments (mean and standard deviation) are removed by the calculation of z-scores (Choi, 1978), then the overall form (higher moments) of the two cumulative distributions can be compared. This will show whether the populations accumulate to 100% by basically different routes or styles. Since the density of the functions is not known, the nonparametric Kolmogorov-Smirnov test (Miller and Kahn, 1962) is applied to check for significant difference. Figure 2-3 shows a graphical

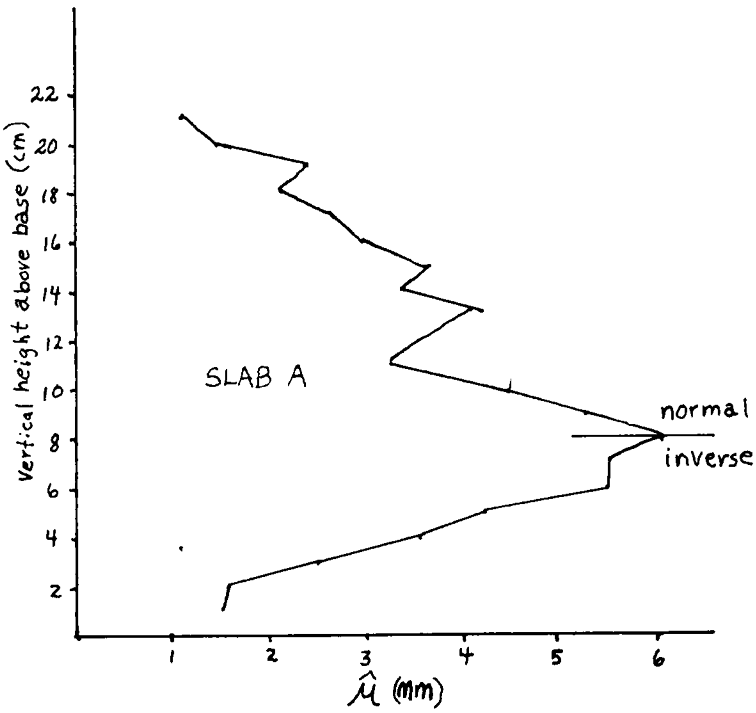

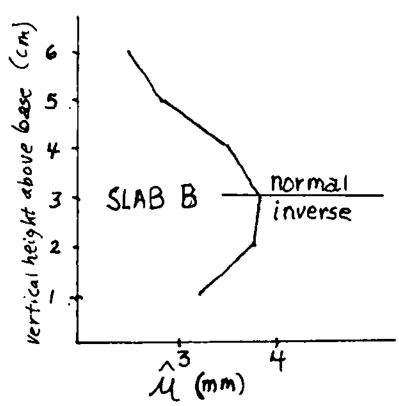

Figure 2-2. Plots of the clast means for two graded slabs, A and B. Plots are for grains greater than 1 mm in diamter in successive 1 cm thick rows.

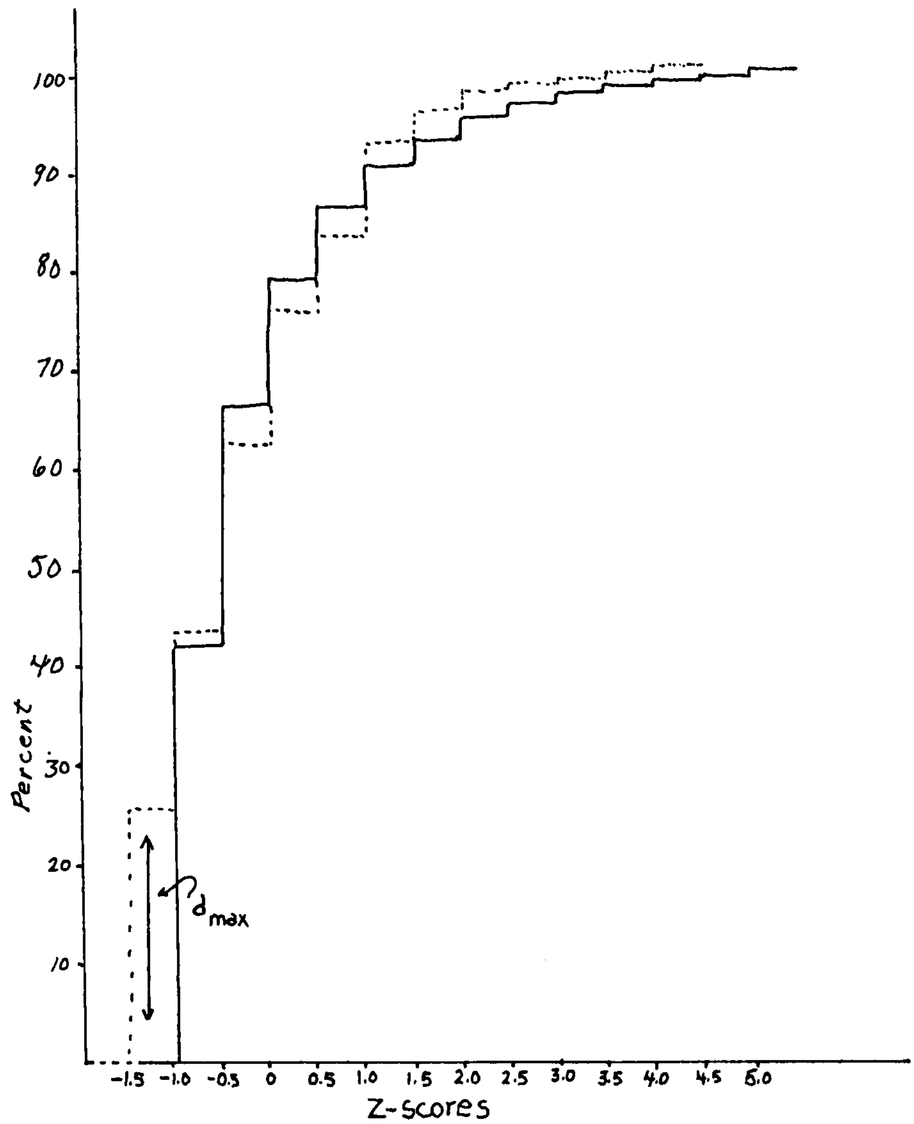

Figure 2-3. The Kolmogorov-Smirnov test. The maximum distance (d_{max}) is 25.26% (0.2526). The theoretical requirement for significant difference at the 0.99 confidence level is 9% (0.09). The populations are significantly different. The broken line is the cumulative density of Slab B. The solid line is the cumulative density for Slab A.

solution to the Kolmogorov-Smirnov test for the total data of A and B. Significant difference between the two is established at the 0.99 confidence level.

The differences in the styles of systematic variation between the two populations are best observed graphically. We expect that for distribution graded beds (slab A), D/10 and mean grain size are significantly graded, while for coarse-frequency graded beds (slab B), D/10 and mean grain size show relatively small changes. Since coarse-frequency grading is defined as a reduction in frequency (not size) of coarse grains, the expectation is that D/10 will not change a great deal vertically. The vertically varying proportions of coarser and finer particles in the bed tend to "buffer" the mean grain size against extremes of variation. The distribution-graded bed should lack these buffers since the variation is defined to be in the entire population. Figures 2-4 and 2-5 show that these expectations are met and that these statistically different populations do indeed exhibit different grading styles.

Statistical Treatment of Distribution Grading and Its Implications

For distribution grading, there is an explicit assumption that a significant systematic variability exists vertically in the *total* grain size population. While the previous section compared row means to ascertain difference between grading styles, an analysis of variance (ANOVA) was performed on the grain size data collected on sample A to characterize the variation of an entire population of grains (see, also,

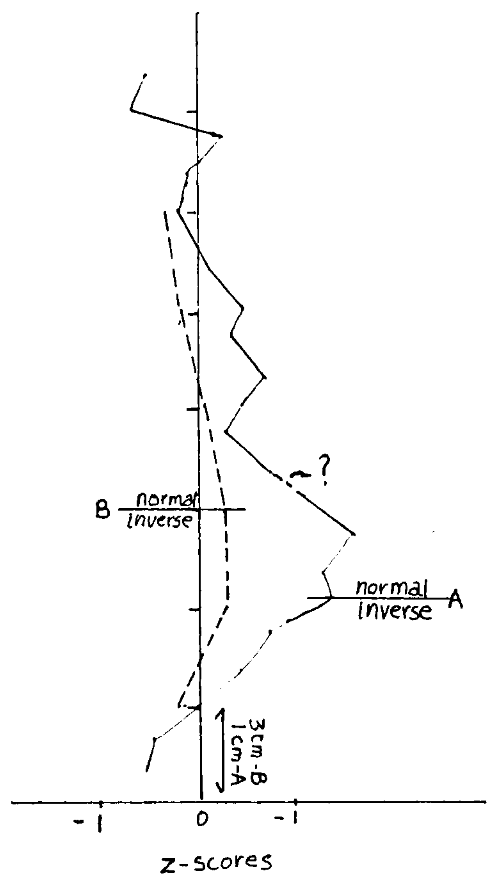

Figure 2-4. Comparison of grading in z-scores means. The question mark in the curve for Slab A indicates a layer that was broken during slabbing and hence not used for computation.

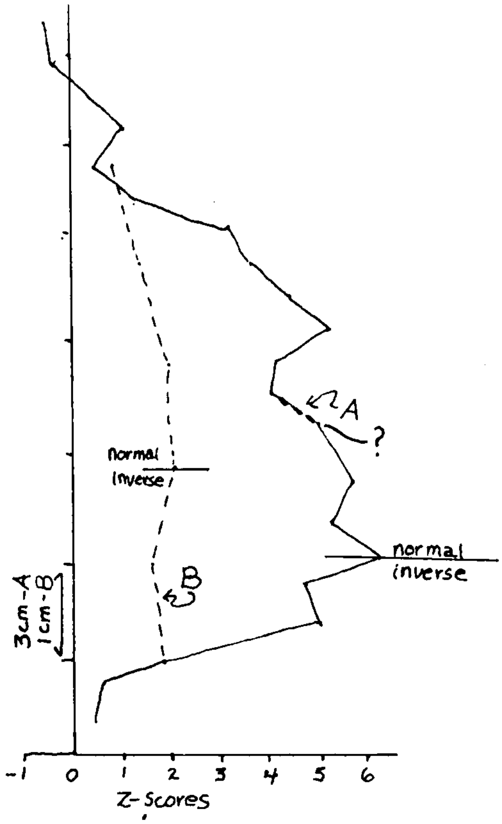

Figure 2-5. Comparison of D/10 z-scores for Slabs A and B. The question mark for the curve for Slab A indicates a layer that was broken during slabbing and hence not used for computation.

Dahlberg and Griffiths, 1967). In order to emphasize the overall size of the clasts, the radius of each clast was cubed to supply an indication of volume (assuming spherical clasts). The factor of spherical volume (4/3 π) was not used since assumption of isotropy of shape would cancel its effect in all subsequent computations.

The distribution of clast diameters and volumes was close to lognormal. To insure validity, the log of the volume of each clast was taken. The transformed distribution was much closer to normal as is required by an ANOVA (Choi, 1978). Means for each row μ_i and the grand sample mean $\bar{\bar{\mu}}$ were computed from the log-transformed data. Row means μ_i were, then, computed from raw diameters (d_i) by:

$$\bar{\mu}_i = \sum_{i=1}^{n} \frac{\log\left[\left(\frac{d_i}{2}\right)^3\right]}{n}$$

where n = the total number of grains in a row.

The row means μ_i of the transformed data were used to divide the sample into its inverse interval and its normal interval (differing by one row from the division determined from simple diameter means). A single centimeter interval which showed the largest mean μ_i was used both as the final row of the inverse layer and the starting row of the normal layer. The normal layer contained 14 rows; the inverse layer contained 7. The grand mean $\bar{\bar{\mu}}$ for each of these two intervals was calculated by summing the means μ_i and dividing by the number of rows in the respective grading type:

$$\bar{\bar{\mu}} = \sum_{i=1}^{n} \frac{\mu_i}{n}$$

where n = the number of rows in a given grading type.

Having computed this data, an ANOVA was performed on the two intervals. The question which an ANOVA is intended to answer is whether simple vertical position in the slab influences grain size. The fundamental assumption behind saying that the rock is graded is that vertical position and grain size are associated. Formally,

$$S_i = \bar{\bar{\mu}} + A_i + \varepsilon_i$$

where a particular grain size S_i is a combination of the grand mean $\bar{\bar{\mu}}$, the effect due to the i^{th} vertical level A_i, plus some random error ε_i for S_i. The null hypothesis is that all the means μ_i for the different rows are equal (i.e., that vertical level makes no difference in grain size). The first task will be to show that row means μ_i are significantly different "because" of vertical position. The second task is to find out what percent of the total variance of the population is explained by the effect of vertical position alone on grain size variation.

The general ANOVA table and the ANOVA tables for the two grading intervals are shown in Tables 2-1, 2-2, and 2-3. (The ANOVA tables are standard. Consult Choi, 1978, or Winkler and Hays, 1975, for elaboration of the computations involved.) Since for the inverse layer $F_{0.01}(6,564) = 2.8020 < 18.76$ and for the normal layer $F_{0.01}(13,1256) = 2.1077 < 17.609$, we reject the null hypothesis of no vertical influence on

Table 2-1. General ANOVA pattern

Source of Variation	Sum of Squares	Degrees of Freedom	Mean Squares	F
Between Rows	SS_b	P - 1	$MS_b = SS_b/P - 1$	MS_b/MS_w
Within Rows	SS_w	N - P	$MS_w = SS_w/N - P$	
Total	SS_t	N - 1		

P = number of rows.
N = number of observations.

Table 2-2. ANOVA results for Slab A, inversely graded layer

Source of Variation	Sum of Squares	Degrees of Freedom	Mean Squares	F
Between Rows	337.145	7 - 1 = 6	56.191	18.76
Within Rows	1689.095	570 - 6 = 564	2.995	
Total	2026.240	570 - 1 = 569		

Table 2-3. ANOVA results for Slab A, normally graded layer

Source of Variation	Sum of Squares	Degrees of Freedom	Mean Squares	F
Between Rows	728.414	14 - 1 = 13	56.032	17.609
Within Rows	3997.103	1269 - 13 = 1256	3.182	
Total	4725.517	1269 - 1 = 1268		

grain size at the 1% significance level. The analysis thus shows that the size of a clast and its vertical level are associated.

The F-test tells us only that vertical position *affects* grains size; it does not tell us about the overall strength of association between vertical position and clast size. The index ω^2 (Winkler and Hays, 1975) represents the proportion of variance in the clast size distribution which is accounted for by vertical position. This index is estimated as:

$$\text{est } \omega^2 = \frac{SS_b - Ms_w(P - 1)}{SS_t + MS_w}$$

where the symbols on the right are defined as to their value by the ANOVA table. For the inverse layer, $\omega^2 = 0.1573$; for the normal layer $\omega^2 = 0.1453$. Thus, even though there is definitely some relationship between vertical position and grain size (results of the F-test), vertical position explains only approximately 15% and 16% of the total grains size variance respectively for normal and inversely graded layers.

While the ANOVA shows a significant difference in grain size in a vertical direction, it does not establish directionality. A linear regression on row means and vertical position should indicate if there is a regular linear change and should give the sign of that change (direction). The plot of row means and their regression lines are shown in Figures 2-6 and 2-7. The signs of the correlation coefficients ($r = +0.870$ for the inverse layer and $r = -0.894$ for the normal layer) are what we would expect since a positive correlation is anticipated

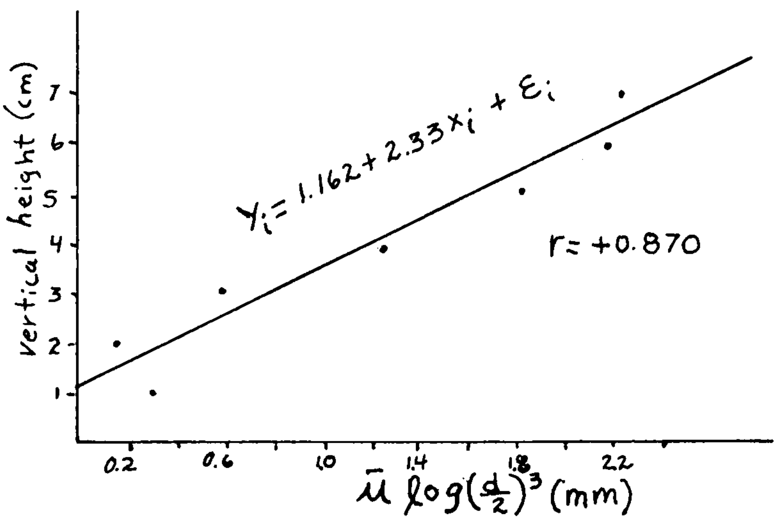

Figure 2-6. Regression on the row means of the inversely graded layer of Slab A.

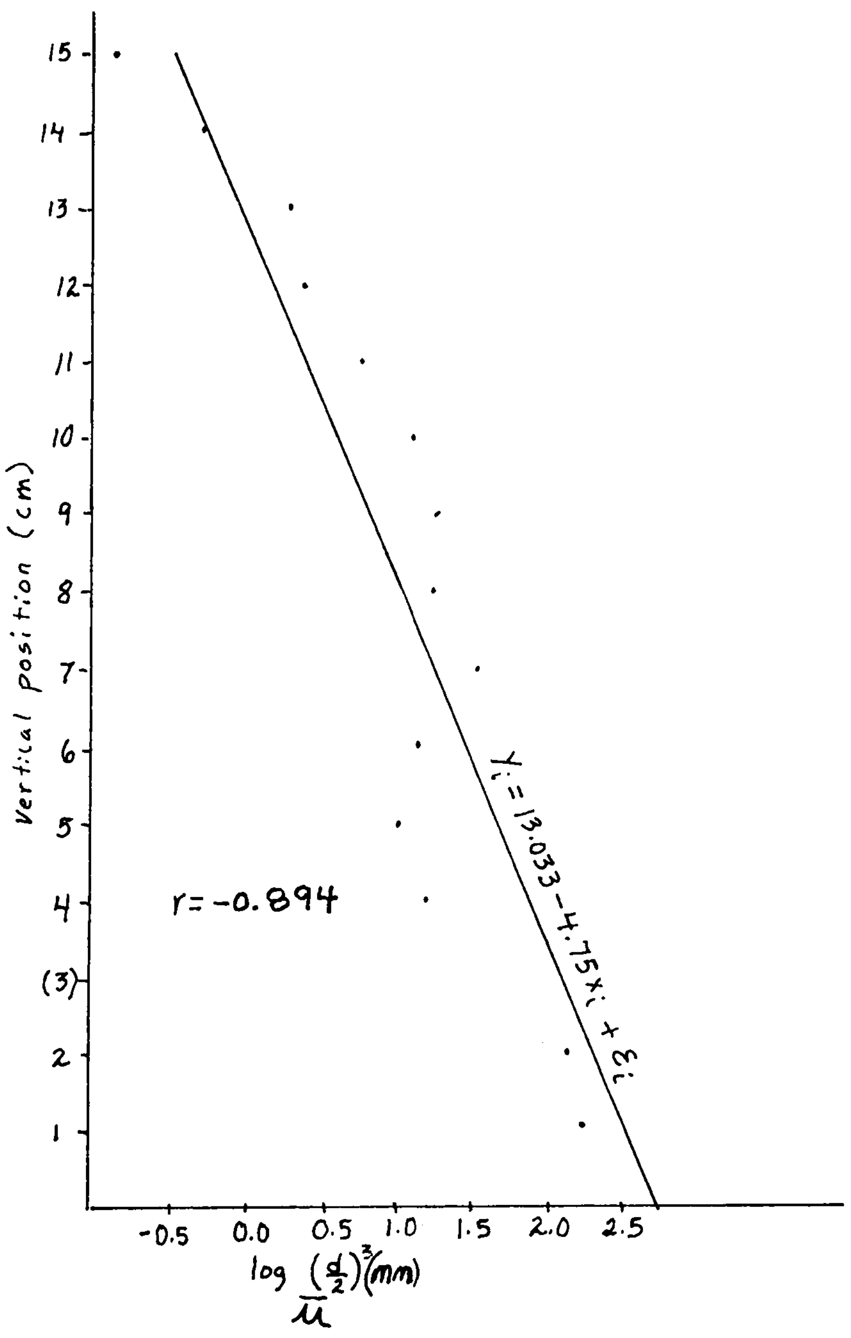

Figure 2-7. Regression on the row means of the normally graded layer of Slab A.

between vertical position and grain size in inversely graded intervals and a negative correlation is expected in normally graded intervals. Figures 2-8 and 2-9 show a similar relation in the plot of the values of D/10 for each row.

These results indicate that from the standpoint of the total population, a simple linear relationship between vertical position and height is capable of explaining approximately 15% and 16% of the variance in the grain sizes of the normal and inverse layers, respectively. The ANOVA model explains some of the total population variance, but it leaves a great deal unaccounted for. What factors other than simple vertical position might affect the grain size distribution?

In the preliminary conditions, density and shape were assumed for simplicity to be isotropic. It is probable that they contribute a good deal to grain size variance in graded beds. Disc-shaped clasts will tend to have an "out of place" association with smaller, more spherical clasts and smaller, denser particles will be found with larger, lighter particles. However, it may be that even with these factors taken into account, the variance still will not fit an ANOVA model comfortably.

An examination of the row means for the normal layer (Figure 2-7) shows several central centimeters where an approximately constant mean grain size is held. What this may physically indicate is that the sedimentation-sorting device was not discriminating different grain sizes very well when these grains were deposited. It is not uncommon in the best "graded" beds for a massive or trendless interval to lie between well-graded intervals. Such massive intervals indicate rapid,

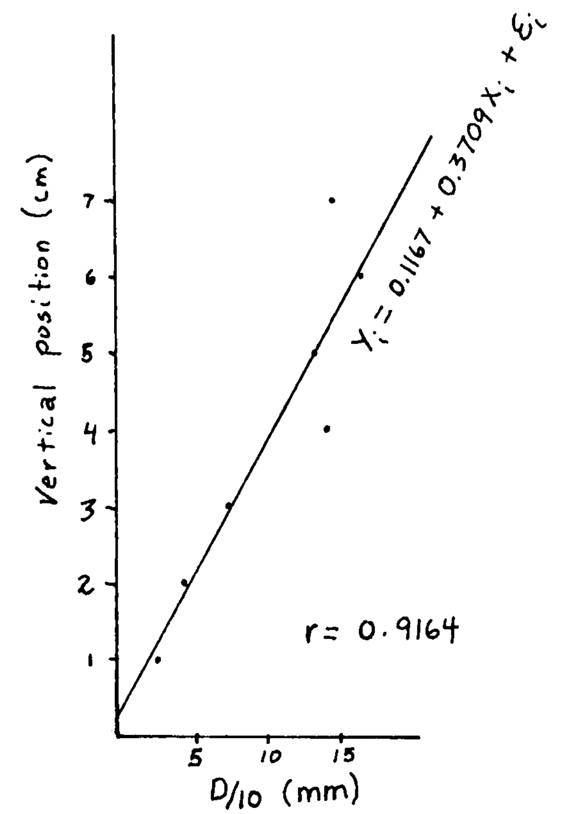

Figure 2-8. Regression on the D/10 row values of the inversely graded layer of Slab A.

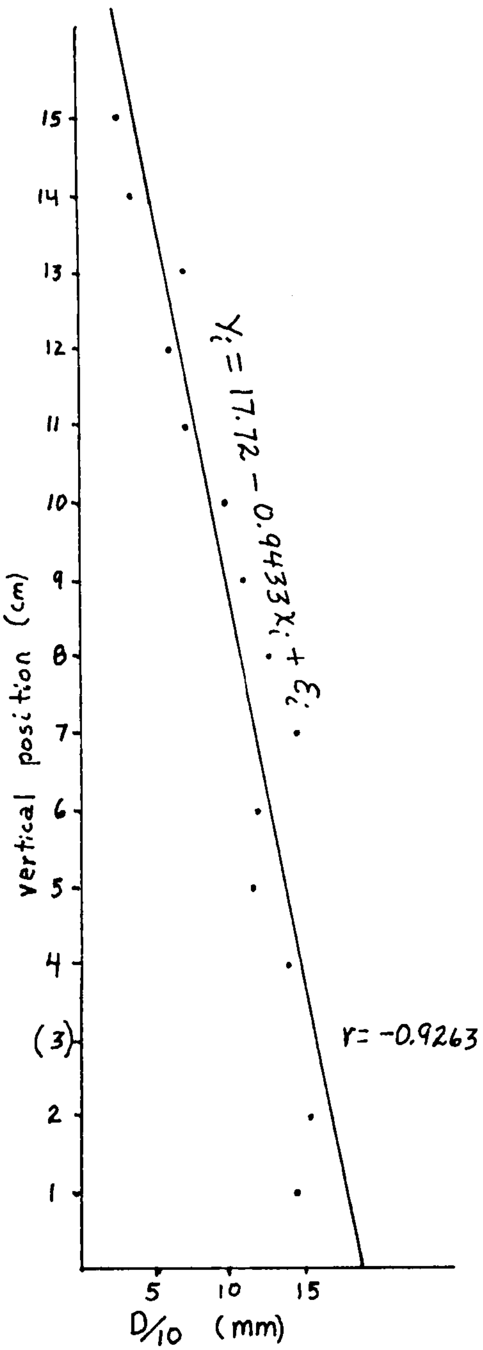

Figure 2-9. Regression on the D/10 row values of the normally graded layer of Slab A.

near chaotic dumping of material from the flow. There is no time available for size sorting to operate until the flow has reequilibrated to new physical conditions (Middleton and Hampton, 1973). For the inverse layer, the rapid increase in grain size, though regular and uninterrupted, is not linear; but, perhaps an exponential model would fit the data better.

Grading patterns may fall within an envelope of ideal types, as suggested by Scheidegger and Potter (1965). This envelope is shown in Figure 2-10. The relationship between height H, maximum clast size diameter d_{max}, and the modal class diameter d_m is given by

$$H = R(d_{max}^{2p+5} - d_m^{2p+5})$$

where R is some numerical constant. In the case of perfect linearity, $p = -2$. In the case where $p > -2$, the relationship between H and d_m plots as convex upward (roughly the case for the normal layer of A). In the case where $-2.5 < p < -2$, the curve is concave upward. The variable p is a function of the *initial* size distribution at the source of the sediments.

It might be speculated that for convex-upward curves (the most common in nature according to Scheidegger and Potter, 1965), the convexity is due to rapid deposition caused by decay of current competence and sorting ability. For concave-upward curves, the current may have been *capable* of transporting larger material, but none was available. On the basis of this speculation, one can recast the Scheidegger-Potter envelope as shown in Figure 2-11.

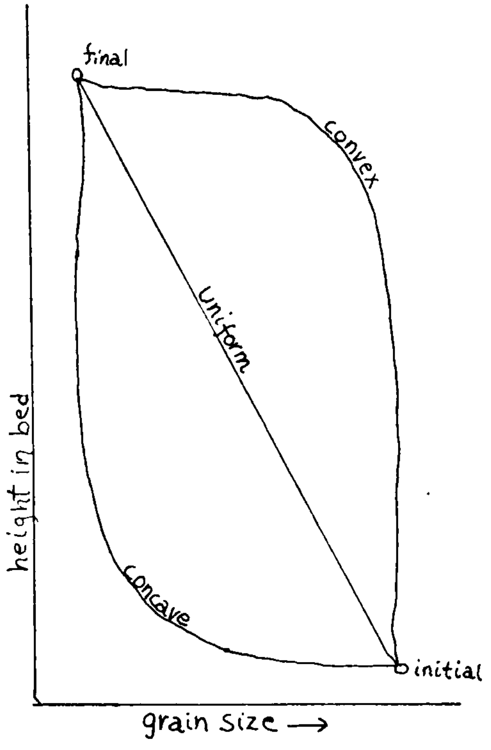

Figure 2-10. The Scheidegger-Potter (1965) envelope.

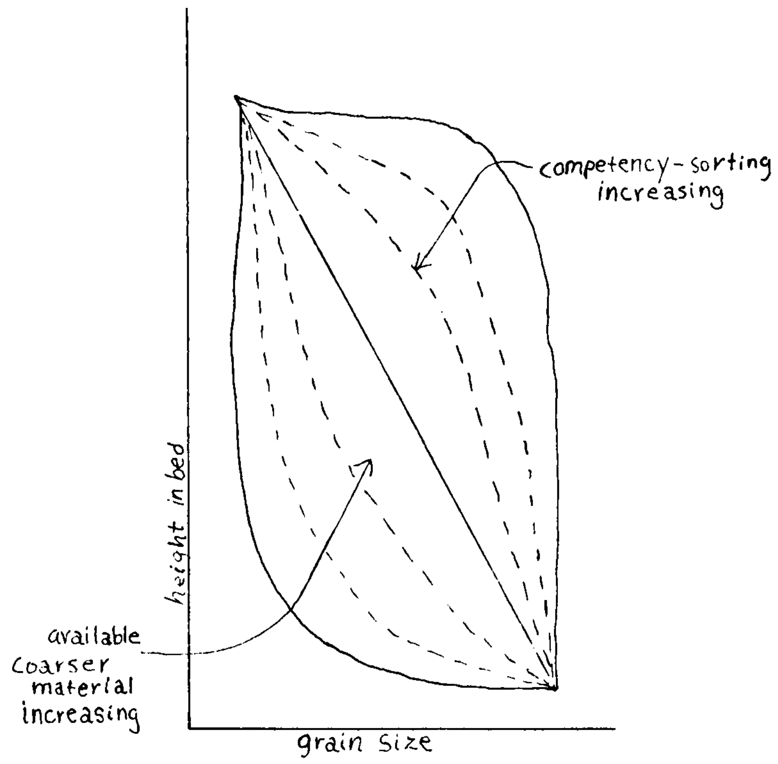

Figure 2-11. The Scheidegger-Potter (1965) envelope redrawn to reflect availability and competency relationships.

Summary and Clarification of Terminology

Grading does exist as an obvious feature of many coarse clastic beds though its definition and description may be far from obvious. It appears unlikely that a simple linear model is an effective way of describing grain size gradients in graded beds. However, the departures from linearity may actually be informative as to depositional process.

As we have seen both the row means and D/10 values show strong linear trends that do not reflect a basic underlying linear trend in the total population. Thus, while they perhaps provide good graphical displays of the most obvious grading patterns, they must be cautiously applied with the understanding that they tell little concerning the total population.

In the bed descriptions that follow in Chapter 3, it is, of course, the general appearance of a bed that is used in the identification of its grading type. It is, then, quite important to qualify the denotation of the terms of this description on the basis of the foregoing discussion.

"Distribution grading" is a term that will be applied only to clast-supported beds in which observed grading appears to occur for most of the obvious (roughly equivalent to D/50) clasts of the population. No claim is made as to whether the entire population is significantly graded or whether the style of its variation is linear. Hence, the usage of the term in this work differs from its definition in the literature. The author would suspect that what is called "distribution" graded in this work denotes exactly the same set of objects as those picked out by any other "looser" usage of the concept. The difference is that no inferences are made with respect to the total clast distribution on the basis of this term. "Coarse-fraction" grading is the term used for matrix-supported beds in which a relatively constant mean is observed for the finer constituents (matrix) but in which either the mean μ_i or the frequency of the coarser grains shows a vertical trend.

Synthesis of Descriptive Properties and Their Implications

The following discussion introduces transport and support mechanisms that are considered important in emplacing deep water, coarse clastic sediments. Three major types of processes possibly responsible for the properties just described are discussed and expected "ideal" deposits of each of the three types are characterized. It is important to notice that these processes are not mutually exclusive since in the actual rock record we may find deposits whose properties result from the interactions of several processes.

Fluid Turbulence

In fluid turbulence, clasts are supported by the upward component of turbulence within a flow. The deposit that has classically been interpreted to result from transport of sand and finer material by lower density turbidity currents is the complete turbidite (Bouma, 1962). Figure 2-12 shows the complete turbidite and its associated hydrodynamic interpretation.

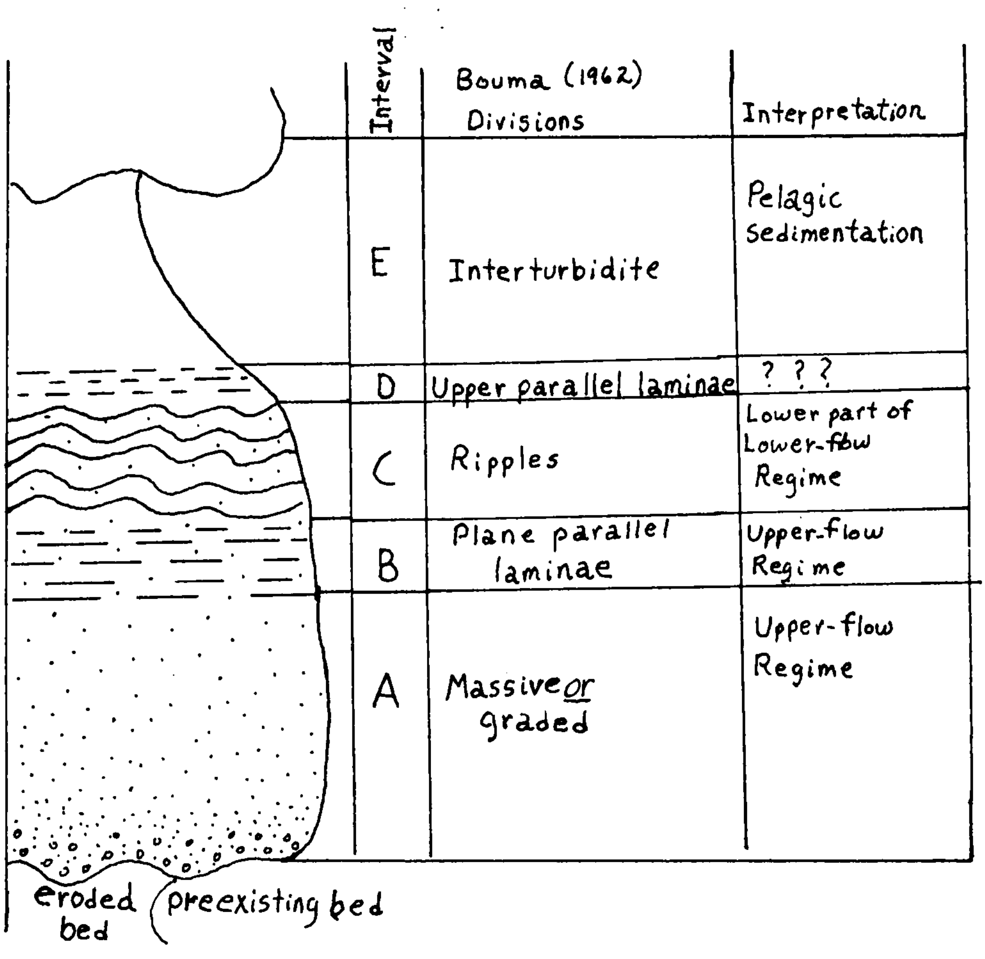

Figure 2-12. The complete turbidite, its divisions, and its interpretation. Drawing after Middleton and Hampton (1973).

Ideally, a turbidity current may be an almost perfect natural sorting device. The deposits at one time and each successive time interval thereafter represent the selection of the largest extremes of the size distribution of the turbulent cloud. The mechanism remains unchanged, the "daughter" distributions changing only in size and variance (sorting) parameters. Deposits thus generated will show well developed distribution grading. This process results in a progressive decrease in the variance of the distribution of sizes in the cloud of moving particles as the coarsest extremes of that set are progressively removed. It should be noted that this sorting mechanism is a *stochastic* device and not a deterministic one: hence, even for an "ideal" flow, there is an expected randomness in the sorting mechanism and the resultant deposit (Bardsley, 1978).

As the current moves into the basin, its head is an effective agent of erosion. The underlying bed is scoured and the suite of sole-marks so typical of flysch deposits is formed (Dzulynski and Walton, 1965). Rapid sedimentation from the body of the flow preserves these erosive features. Tractional features such as cross lamination develop as the current wanes. Suspension fallout of the fine fraction dominates final turbidite deposition. Fine hemipelagic or pelagic sediment accumulates slowly, after deposition from the current ceases.

For a classical, dilute turbulent flow, we would thus expect the following features in a deposit: eroded base with sole marks--normal distribution grading--lower flow regime tractional features--suspension deposit pelites. However, there are three complicating factors that will alter these expected deposits.

First, if the current is concentrated with sediment ("high density" flows), the sorting mechanism will not be as effective and coarse-fraction grading may develop. The flow is too choked with sediment for good size-sorting (e.g., distribution grading) to take place (Middleton and Hampton, 1973). Second, if current competence decays rapidly (perhaps caused by a gradient change), the current may dump most of its sediment as a result of equilibration to changed flow velocity and competence. The resulting deposit is a structureless bed without textural trends and tractional features. Faint laminations may result if there is time for the development of size segregation, possibly in response to continued shear from the overlying flow. Third, very coarse material will tend to be dropped into structureless (disorganized) beds. A slight change in competence of the flow may result in the sudden loss of its coarsest fraction. It should not surprise us then if lower flow regime tractional features are not present along with these very coarse-grained beds. In other words, the absence of tractional features in coarse conglomerates does not necessarily imply that they were supported by some mechanism other than fluid turbulence. What it does perhaps imply is extremely rapid deposition.

Grain Interaction

Another way in which grains in a flow can be supported is by dispersive pressure (Bagnold, 1954). For cohesionless grains on a slope, movement occurs when gravity shear exceeds the frictional resistance of the grains. As the body of grains moves it dilates since the grains receive an upward supportive force component from mutual collisions. This dispersive pressure acts to keep grains from settling out of the flow.

Deposition occurs when the force of gravity no longer is sufficient to drive the sediment movement forward (e.g., at a change in slope). The bed simply "freezes"--many grains are deposited simultaneously (Middleton and Hampton, 1973). Deposits of this type of grain support mechanism may exhibit two important characteristics: imbrication and inverse grading.

Imbrication. Imbrication of clast long axes parallel to flow can be seen to develop in a system in which there is grain-to-grain interaction (Rees, 1968). If we assume for simplicity a dispersion of elastic, ellipsoidal particles in motion, collision between two particles results in a force that is normal to the tangential plane passing through the point of contact. This collision produces on the clasts a rotational couple if the collisions do not occur on a principal axis. There will be no couple if the collision occurs on a principal axis; hence, this will be the statistically most stable configuration. In order to achieve this configuration, overlapping layers of clasts must be tilted at some angle to the direction of flow (i.e., dip up current) since collision along a principal axis is not possible otherwise. Figure 2-13 should make this clear. We may expect that the long axis will be parallel to flow, as less momentum is transferred by the glancing collisions of grains whose long axes are parallel to flow.

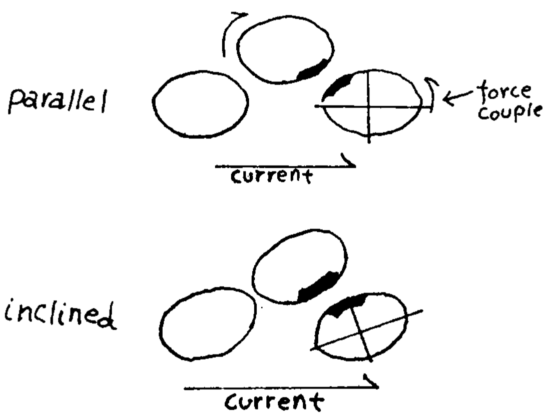

Figure 2-13. The cause of imbrication in a current. When clasts are parallel to flow, collisions cannot occur on a principal axis. When they are inclined, collisions occur on principal axes. This is the most stable position since there is no resulting force couple on the clasts following collision.

Inverse grading. The origin of inverse grading has been explained by two mechanisms: grain dispersive pressure (Bagnold, 1954) and the kinetic sieve hypothesis (Middleton, 1970). Bagnold thought dispersive pressure in grain dispersions caused larger grains to migrate upward to regions of lower shear. Middleton proposed instead a kinetic sieve mechanism for inverse grading in which smaller grains tend to fall in between larger ones and displace the larger particles upward. The analogy he uses is a box of sand or popcorn: Shake the box and the smaller grains fall down between the larger ones. Sallenger (1979) conducted experiments with sand-sized materials suggesting that Bagnold's dispersive pressure hypothesis is the most important factor in the inverse grading of particles. He notes, however, that the kinetic sieve of Middleton's hypothesis may also be operative in some flows--especially those in which there is a wide range of clast sizes.

Debris Flow

In contrast to the preceding two types of flow, in debris flows grains are supported by a fluid that has cohesion. Unlike Newtonian fluids (e.g., water), such flows exhibit strength. They do not flow until internal shear stress exceeds their yield strength. Their behavior is, from a rheological point of view, similar to that of a plastic solid (or Bingham plastic in Hampton's terminology, 1975--a plastic which exhibits strength and whose viscosity is constant once flow begins). Support of the clasts in a debris flow depends on this property of strength. Buoyancy also provides some support. Since the fluid phase of a debris flow is a clay-water mix, it is denser than water and is capable of supplying an upward buoyant force to the clasts within the flow. It is thought by some (Hampton, 1975; van Olphen, 1963) that the strength of the fluid is derived from the network of clay particles bound by attractions explainable by the electric double layer theory. The amount of clay needed to provide this strength can be surprisingly low, as low as 9 weight percent (Curry, 1966; Hampton, 1972). Large boulders may be carried by a flow containing only a few weight percent of clay (given that water content is low also). The highly concentrated, viscous nature of these flows inhibits turbulence. Laminar flow, then, is thought to be of most importance. Fisher (1971) lists features of mudflow deposits that he thinks indicate laminar flow. For a more theoretical treatment of the development of laminar flow in debris flows, see Bagnold (1954) and Johnson (1970).

The deposits left by such a flow are typically rather chaotic in appearance and have been mistaken for tillites in the past (Ackerman, 1951; Crowell, 1957). Since deposition is by "freezing" there is no opportunity for grain-by-grain sedimentation or sorting of clasts. Large clasts rest unsupported in a finer matrix and sorting is poor. There may be alignment of clasts parallel to bedding as a result of laminar flow (Fisher, 1971; Lindsay, 1966, 1968). Also, as a result of laminar flow, transport involves far fewer grain collisions than in turbulent flow or grain flow. There is consequently less breakage of clasts, and relatively fragile features or clasts can be rafted along in the flow and preserved in the deposit (Johnson, 1970).

Summary of Flow Mechanisms and Their Deposits

Figure 2-14 summarizes the expected deposits for each of the three end-member transport mechanisms in subaqueous gravity flows. It is important to emphasize that in many--if not most--cases, deposits may bear features of more than one process. However, as the next chapter will show, most deposits tend toward either the debris flow or turbulent ends of the spectrum. Grain flow features usually occur in patches or small portions of beds that mostly contain features of turbulent flow.

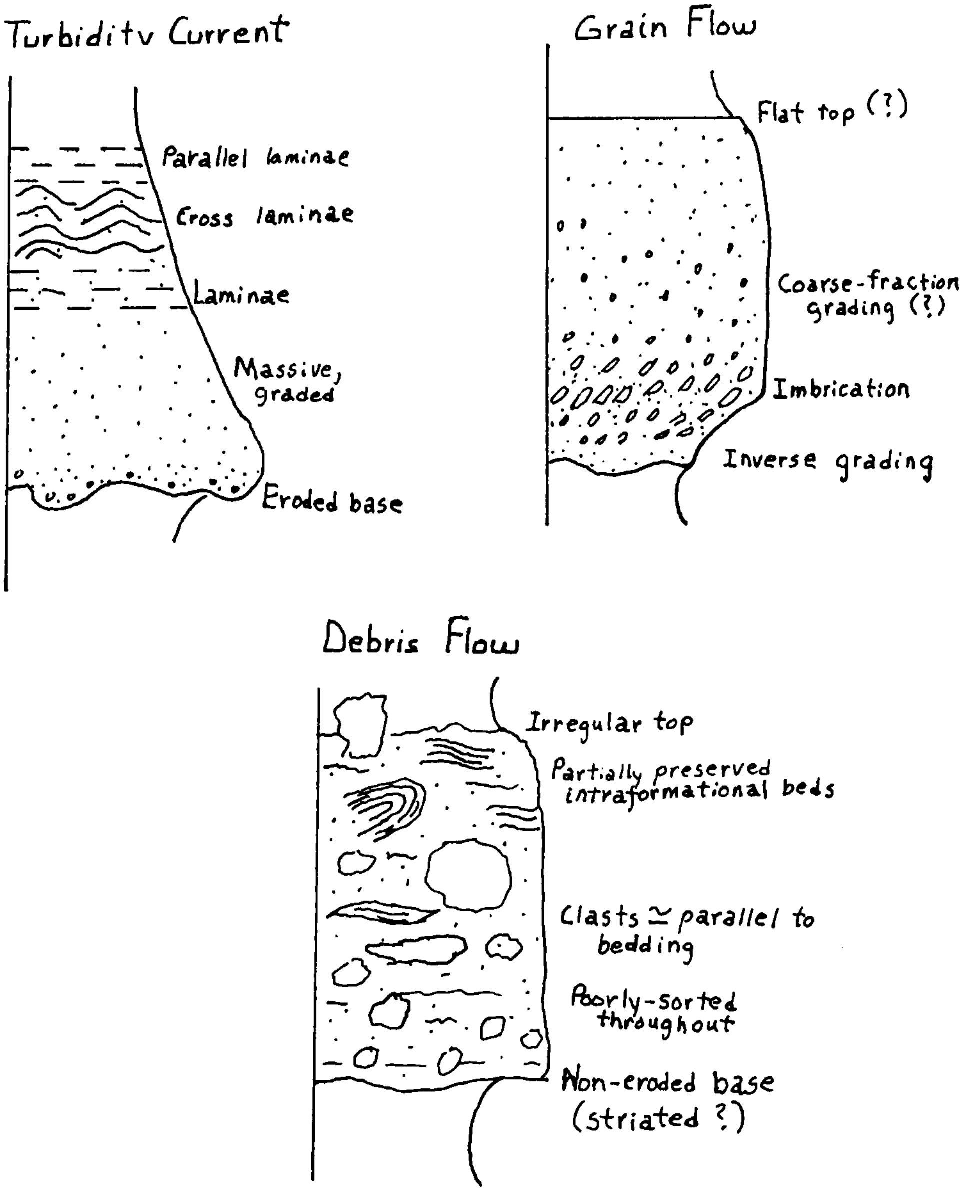

Figure 2-14. Summary of deposits from ideal end members of three kinds of transport mechanism.

CHAPTER 3

COARSE CLASTIC LITHOTYPES

Introduction

In the previous chapter, certain properties of coarse clastic sediments were introduced and defined. In this chapter these properties are used to classify beds into families whose members bear close resemblance to each other. In the following discussion, these families are termed "lithotypes" in contrast to the term "facies" as it is similarly used by other workers (e.g., Aalto, 1976; Walker, 1978; Walker and Mutti, 1973). The writer prefers not to use the term "facies" as it is more properly applied to the rock record of a specific area characterized by distinctive physical, chemical, and biological parameters--i.e., the sedimentary product of a sedimentary environment in which several beds representing several lithotypes may be deposited.

Initially, the coarse clastic sediments of the study are divided into 5 descriptive lithotypes, equivalent to those of Walker (1978): classical turbidites, massive sandstones, pebbly sandstones, clast-supported conglomerates, and matrix-supported beds. This scheme is adopted because there are relatively few lithotypes distinguished, and consequently, a reasonably nonarbitrary assignment of a given bed to an appropriate category can be made. The system is not unequivocal in the use of a single parameter for discriminating categories, and two of the proposed lithotypes have a mixed genetic-clast size definition (turbidites and matrix-supported beds); but, in general, most beds are for all practical purposes placed within a given lithotype on the basis of clast size. Subsequent discussion of deep water sediment classifications will outline the problems with this (and other) classifications, and a new approach to the problems of coarse clastic classification will be proposed based on factor analysis (Chapter 5).

Herein, the deposits studied are reviewed and placed in one of the five categories. While these categories are somewhat suspect as general descriptive categories, they enable us to interpret the paleoenvironments of the study area; hence, their use is justified.

Classical Turbidites

Introduction

The suite of characteristics and the hydrodynamic interpretation of turbidity currents and their deposits are so well-known and generally established, both in field observation and experimentally, that I will not dwell at length upon them. Interested readers are directed to Chapter 2 or to the large mass of literature that has accumulated concerning them. (See Walker, 1978, for a helpful bibliography of some of these works.) A typical, complete turbidite was shown earlier in Figure 2-11 (p. 40).

Examples in the Study Area

All outcrops studied have examples of turbidites. At SHDC and AFC, the examples were few, and probably most of them might better be classed as massive sandstones (though such a distinction is somewhat arbitrary) in light of the very proximal suite of deposits contained in those outcrops. Several well developed turbidites occur at USHDS among the otherwise massive sands of that outcrop and become increasingly abundant higher in that section. At the Lucy Creek outcrops (LLCD and ULCD), rather thin-bedded turbidites, mostly A(D) or (D) beds, dominate the sequence above and below the slump-debris flow deposits. There are a few thicker, more lenticular bodies of sandstone at LLCD (proximal, channel facies turbidites?). But, again, they are A(D) beds; only the scale is larger.

The best examples of turbidites occur in the LSHDS outcrop. There, a variety of turbidite types are exposed. Approximately 600 separate turbidite beds were recognized in this outcrop. Few are complete ABC(D) turbidites, more are AC(D) or A(D) varieties, and still more are various types of base-absent sequences. Although the bedding surfaces of units are not usually well exposed, flutes, grooves, loading features, and other bed-plane properties were observed. Amalgamation of the coarser divisions of some beds was inferred on the basis of thin shale partings and interrupted grading sequences.

Description

Table 3-1 shows the types of turbidites observed in the sequence, the number of beds of a given type, the numerical percent, the mean thickness, and the percent of the stratigraphic section encompassed by the sum of the members of a given type. Because it is often difficult

Table 3-1. Data on turbidite beds of LSHDS

Type	Number	Numerical %	Mean Thickness (cm)	Thickness % of Outcrop
A	18	3.1	20.13	4.26
ABC(D)	4	0.7	39.25	1.85
AC(D)	54	9.4	33.96	31.57
A(D)	85	14.7	26.6	26.6
B(D)	1	0.1	58.0	0.68
C(D)	50	8.7	12.84	7.55
(D)	365	63.3	9.0	38.65

to distinguish the D, E, and interturbidite intervals in fine material, the author has taken Walker's (1967) suggestion that these intervals be designated (D). The beds labeled simply "A" in the table were measured from units in which amalgamation had occurred in the coarse to medium sand of the A division(s) of the bed.

The numerical percent of (D) is somewhat misleading in its dominance. The percent of the stratigraphic section encompassed by the various turbidite types gives a different picture. Beds beginning with the A division dominate the greatest proportion of the total thickness of the outcrop. This indicates that the outcrop is relatively proximal in location with respect to the source area of the turbidity currents that emplaced the sequence.

Other features of this outcrop are summarized in Table 3-2. Comparison of these features with those determined to result from deposition by turbulence discloses close agreement. Hydrodynamically, it is reasonable to infer that the beds of this outcrop were deposited by turbidity currents.

Table 3-2. Features of the turbidite beds at LSHDS

Feature	Observation
Bed thickness	Mean thickness: sandy beds approximately 0.25 m Mean thickness: (D) beds approximately 0.09 m.
Outcrop scale bed geometry	Tabular. Thickness varies only slightly along exposure.
Bedding contacts	Sharp, well-defined bases with typical sole marks. Transitions within beds from division to division may be sharp or gradational. Upper contact with overlying bed has usually been scoured; hence is sharp.
Texture and grading	Grading: almost always distribution (normal); rare coarse fraction. No inverse grading observed. Some beds show a massive rather than a graded A interval--usually occurs in thicker beds.
Convolute laminations	Rare.
Amalgamation	Unequivocal amalgamation is difficult to determine (18 observations); 52 less certain observations in finer material. More common lower in section.
Grain size	Typically not greater than medium sand; a few units have coarse sand or scattered granules at their bases.
Sorting	Fair to good at any given vertical interval. Some massive A divisions are only moderately sorted.

Massive Sandstone Lithotype

Introduction

The designation "massive sandstone" has been used both as a term descriptive of a given particular bed and as a term that is applied to a family of beds characterized as texturally massive in the particular sense of the term (Walker and Mutti, 1973). While such an equivocal usage is generally not desirable, the overlapping denotation here is actually illuminating: massive sandstones (particular sense) do tend to occur in packages with other massive sandstones.

In a particular sense, these beds might be assigned to the Bouma A interval; but, in the extended usage of the term, a distinction should be made between beds contained in bedding sequences that are essentially AAAAA . . . from standard proximal turbidite A divisions. While there is a strong descriptive similarity in the A intervals of turbidites with *some* massive sandstones, one cannot on this basis assign to all massive sands a label that is tied to a very particular genetic mechanism (fluid turbulence). It may be that neither the mechanics nor the depositional environment are the same for massive sandstones and turbidites. It is well, then, at least at this stage, to avoid the Bouma (1962) notation in describing massive sandstones.

Examples in the Study Area

In the study area USHDS provides the best examples of massive sandstones. They also occur at AFC and SHDC but are fewer in number and do not constitute as well-defined a facies of massive sandstones as those at USHDS. The following discussion is based on the deposits at USHDS.

General Characterization of the Outcrop USHDS

USHDS is characterized by thick, massive sandstone, fine-pebble conglomerate (pebbly sandstone, in Walker's 1978 terminology), a few turbidite beds, and some slump or debris flow deposits. Pelitic intervals are rare and the sand-shale ratio for the outcrop is quite high (>10). Of the 70 beds recognized in the outcrop (50 m of exposed section), 36 can be conveniently placed in the category of massive sandstone.

Description of the Massive Sandstone Beds

General bedding characteristics. The sands at USHDS are generally thick, tabular to highly lenticular bodies. Maximum observed thickness is 5.2 m for one exceptionally thick (though probably amalgamated) bed. Mean bed thickness is 97.7 cm.

The lenticularity of some of these beds is suggested by the thickness changes of beds 6-9. Their combined thickness drops from a maximum of 262 cm to 190 cm (a change of almost 30%) laterally over 12 m. Some of the smaller beds exhibit obvious channel geometry at the scale of the outcrop. Some beds pinch out completely over short lateral distances (e.g., beds 17, 18). A larger scale exposure might have disclosed broad lenticularity for even the apparently tabular beds of the outcrop (Ricci-Luchi, 1975; Cas, 1979).

Sedimentary structures. The beds generally lack a well-developed suite of sedimentary structures, though there may be a few features that are poorly developed or that show good development in certain small parts of the bed.

Grading of several kinds is observed in these beds but is not well developed in most. Typically, the basal and uppermost portions of a bed show grading, while the middle portion is texturally homogeneous. Some beds contain patches of grading internally or contain interrupted graded sequences that probably indicate the amalgamation of successive flows.

Coarse-fraction grading in scattered granule-sized material (especially coarse-frequency grading) is observed; a few beds have an inversely graded interval at their base. Well-developed distribution grading is most commonly found only in the uppermost few centimeters of these beds where the entire grain size distribution appears to decrease rapidly in size.

Figure 3-1 shows the upward tally, upward transition probability matrix, and a diagram of the likely path of textural transitions *within* given beds. The upward transition probability matrix is derived from the tally matrix by summing the rows and dividing each cell tally of a given row by its row sum. Although the number of entries is extremely low, there does appear to be a preferred vertical sequence of types: inverse--coarse-fraction or massive--normal distribution grading. Occasionally, an entire bed that might be otherwise regarded as distribution graded has a middle, texturally homogeneous section. It is not clear whether such a unit should be described as distribution--

$$
\begin{array}{c} \\ IN \\ CF \\ M \\ D \end{array}
\begin{array}{c}
\begin{array}{cccc} IN & CF & M & D \end{array} \\
\left[\begin{array}{cccc}
\text{--} & 1 & 3 & \text{--} \\
\text{--} & \text{--} & 2 & 3 \\
\text{--} & \text{--} & \text{--} & 9 \\
\text{--} & \text{--} & \text{--} & ? \\
 & & (?) &
\end{array}\right] n_{ij}
\end{array}
$$

$$
\begin{array}{c} \\ IN \\ CF \\ M \\ D \end{array}
\begin{array}{c}
\begin{array}{cccc} IN & CF & M & D \end{array} \\
\left[\begin{array}{cccc}
0.00 & 0.25 & 0.75 & 0.00 \\
0.00 & 0.00 & 0.40 & 0.60 \\
0.00 & 0.00 & 0.00 & 1.00 \\
0.00 & 0.00 & 0.00 & ? \\
 & & (?) &
\end{array}\right] p_{ij}
\end{array}
$$

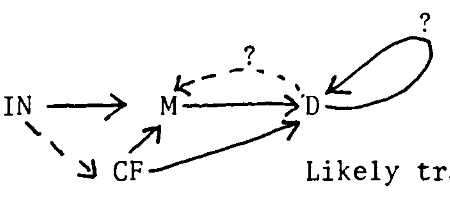

Likely transition

Figure 3-1. Tally matrix (n_{ij}), probability matrix (p_{ij}), and likely transition diagram for within bed textural transitions in the massive sandstones at USHDS. IN represents inverse grading; CF, coarse-fraction grading; M, massive texture; and D, distribution grading. The solid lines in the likely transition diagram show the most probable one-step transitions. The dotted lines show less likely transitions.

massive--distribution graded or whether it should be simply described as exhibiting "poorly developed" distribution grading. Perhaps a distinction should be made in these cases between basal distribution grading and final-state distribution grading. The author has indicated this uncertainty with a dotted arrow in the likely-transition diagram.

Stratification, especially thin laminations, is not uncommon in these beds. Thicker (10-20 cm) strata occur in the AFC outcrop but no stratification on this scale was observed at USHDS. Lamination at USHDS is more evident toward the tops of beds than toward their bases and is also faintly expressed in otherwise massive portions of beds. Maximum lateral continuity of the laminae appears to be less than 30 or 40 cm.

Cross bedding and cross lamination were not observed in any of the 36 beds classified as massive sandstones.

Sole marks were not very commonly observed. This is perhaps due more to the poor exposure of basal surfaces of beds than to an actual dearth of these erosional features. Some beds do contain grooves and flutes. In general, both lower and upper bedding contacts are sharp, though some of the upper contacts with thin scale partings that separate consecutive beds are rapidly gradational.

A few beds contain outsized mudstone clasts at various levels in the bed. Occasionally, these clasts serve as apparent traps for fine pebbles or coarse sand. The pebbles may have simply adhered to the sticky surface of the mudstone. The presence of these clasts indicates that during part of its transport history, the transporting flow was capable of eroding underlying mudstone beds.

Features of this lithotype are shown in Figure 3-2.

Mode of Transport and Deposition

The transport and deposition of massive sandstones have been objects of study for some time (Cas, 1979; Chipping, 1972; Link, 1975; Stauffer, 1967). Their similarities with proximal turbidites (A interval) have led some investigators to dismiss for all practical purposes any transport mechanism other than fluid turbulence (Link, 1975). However, the suite of features associated with these beds makes an explanation of their formation by fluid turbulence alone very questionable. Allen (1970) and, later, Cas (1979) proposed that the A interval of the Bouma sequence be subdivided into:

1. an inversely graded lower division (a_1)
2. a nongraded (or coarse-fraction graded) middle division (a_2)
3. an upper, distribution graded interval (a_3).

Such a suggestion seems to fit the upward transition values for beds of this study and implies the importance of nonturbulent transport and depositional mechanisms.

Inverse grading suggests the operation of a grain flow mechanism. Massive texture in relatively nonviscous flows may be the result of several factors. In a concentrated flow, both turbulence and grain collisions may act to suspend particles up in the flow. Deposition of material as a result of waning velocity will tend to be rapid and may produce an under-consolidated, water-rich deposit (Middleton, 1970). Continued movement in the upper part of the bed acts to shear this

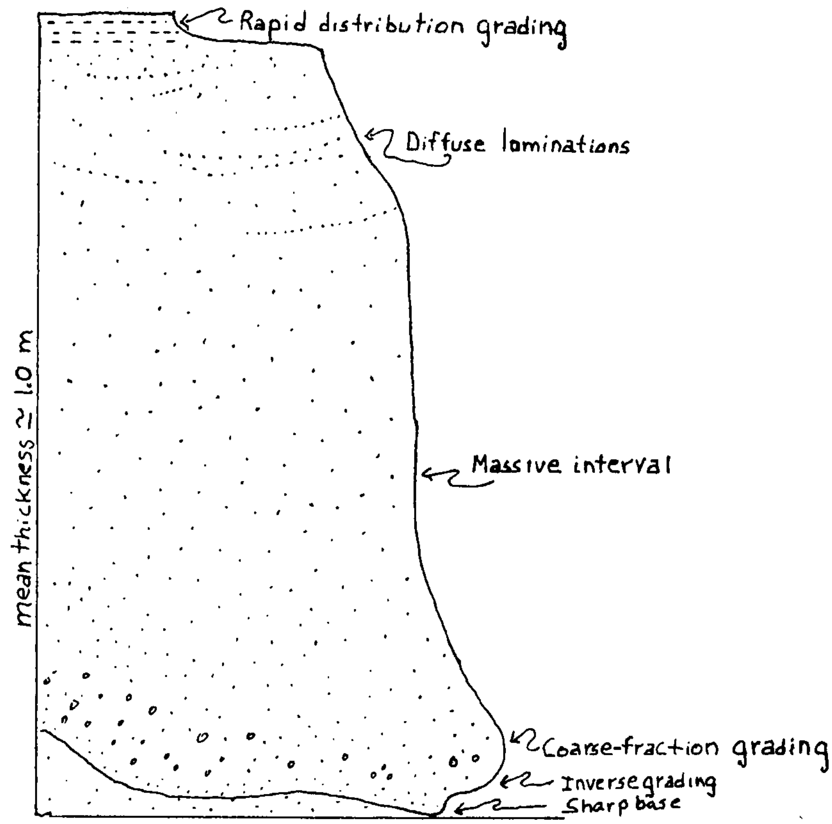

Figure 3-2. Composite diagram of several features of the massive sandstones at USHDS.

"quick" bed and produces a massive layer lacking tractional features (Allen, 1970). The diffuse parallel laminations observed in several of the beds result from this current shearing of the bed during and perhaps for a short time after its deposition (Stauffer, 1967). The exact mechanism that operates to segregate coarser grains from finer grains, while perhaps related to this continued shear, has not as yet been satisfactorily explained.

Coarse-fraction grading is generally thought to arise as a result of deposition from highly-concentrated suspensions that inhibit distribution grading of grains (Middleton and Hampton, 1973). Coarse-fraction grading that passes into a massive division may indicate that crude size sorting had begun during the flow of a concentrated dispersion. Rapid deposition freezes this fabric in place without further improving the sorting. Consequently, either crude coarse-fraction grading is displayed throughout the bed or is displayed more strongly toward the base, depending upon the degree of sorting achieved during transport.

Bona fide distribution grading is usually thought to result as decreasingly smaller grain sizes are deposited layer by layer from a suspension that is dilute enought to permit the unimpeded segregation of grain sizes and densities in the flow (Middleton, 1970). The grain support mechanism in these dilute flows is probably fluid turbulence. This state and process can be regarded as an "absorbing Markov state" (Icaacson and Madsen, 1976), as a dilute, waning current will not physically be able to make an upward-transition to upper-flow regime conditions. The thin veneer of distribution graded sediments on the tops of several of these beds represents a textural "trap," physically reflecting the last stages of deposition.

Conclusions

The massive sandstone beds were probably deposited by large, sediment-charged flows. Grain-dispersive pressure was probably important in the transport of beds that show inverse, coarse-fraction, or massive textures. Fluid turbulence probably played a reduced role in these flows--at least during the last stages of transport of the bulk of the bed. The massive texture is perhaps attributable in part to a massive, ungraded pattern of deposition as well as to shearing and dewatering during and after deposition. Distribution grading (final state) indicates the dominance of fully turbulent flow in the dilute suspension that accompanied the main flow.

Pebbly Sandstone Lithotype

Introduction

The pebbly sandstone lithotype is distinguished on the basis of clast size and abundance from some massive sandstones and turbidites on the one hand and some fine conglomerates on the other. It appears that the only difference between pebbly sandstones and some conglomerates is in the smaller size of their coarsest particles; the distinction of pebbly sandstone from some massive sandstones is likewise somewhat arbitrary. The term is applied in this work to beds in which particles of granule to pebble size either composed a distinct clast-supported interval or constituted the volumetrically most important (>50%) clasts in coarse-fraction grading.

Examples in the Study Area

Pebbly sandstones occur at USHDS, SHDC, and AFC. The outcrop at AFC illustrates several features of pebbly sandstones so beds from it have been chosen to illustrate this lithotype.

Description

The pebbly sandstone beds at AFC occur interbedded with coarser conglomerates and massive sandstones. Twenty-three beds are classified within the pebbly sandstone lithotype. Maximum observed thickness is 85 cm. Mean thickness is 33 cm. The shape of the beds is generally a rather well-defined channel form (highly lenticular). For example, bed AFC-6 is 30 cm in maximum thickness and pinches out completely within one meter to either side of this maximum. Most of the other beds appear to pinch and swell laterally, and the outcrop appears in places to have been built up vertically by intervals which were laterally the result of coalescing of many individual flows (see, also, Walker, 1978).

Bases and tops of beds are sharp and the top usually appears to have been eroded by the current that deposited the overlying bed. The basal surfaces of beds are not well exposed, but the channel geometry and deep incision into underlying beds indicate an erosive emplacement for most beds of this lithotype. Large sole markings, while not observed at this outcrop, are commonly reported in the literature for this lithotype (Walker, 1978).

Internally, most beds are normally distribution graded, at least in their lower portions. Some have small basal inversely graded intervals; four appear to be coarse-fraction graded; and, five are not noticeably graded at all. Imbrication was not too common but was observed. Stratification was observed in two beds. In general, sorting is rather good (±1 phi unit). The sandy matrix appears to be relatively clean and free of excessive clay content. Induration is very pronounced. Figure 3-3 summarizes some features of this lithotype.

Mode of Transport and Deposition

As with massive sandstones, a variety of processes probably contributed in differing degrees to the formation of the pebbly sandstone beds. The channel geometry, rather clean, clay-free matrix, and common distribution grading indicate that fluid turbulence, with its sorting of clasts and erosive action, was probably the main process responsible in the transport of the sediments. Late stage concentration of material during waning of the flow may have given rise in some beds to grain collisions and support by dispersive pressure. The inverse grading and imbrication exhibited by some beds seem to support this hypothesis. Detailed petrographic work on clay content would be necessary to assess the role of matrix strength and buoyancy. However, the debris flow mechanism is not thought to have been of major importance in the transport of these sediments.

Discussion

The category of pebbly sandstone is a particularly artificial one. Deposits of this type appear to involve no unique mechanisms of flow.

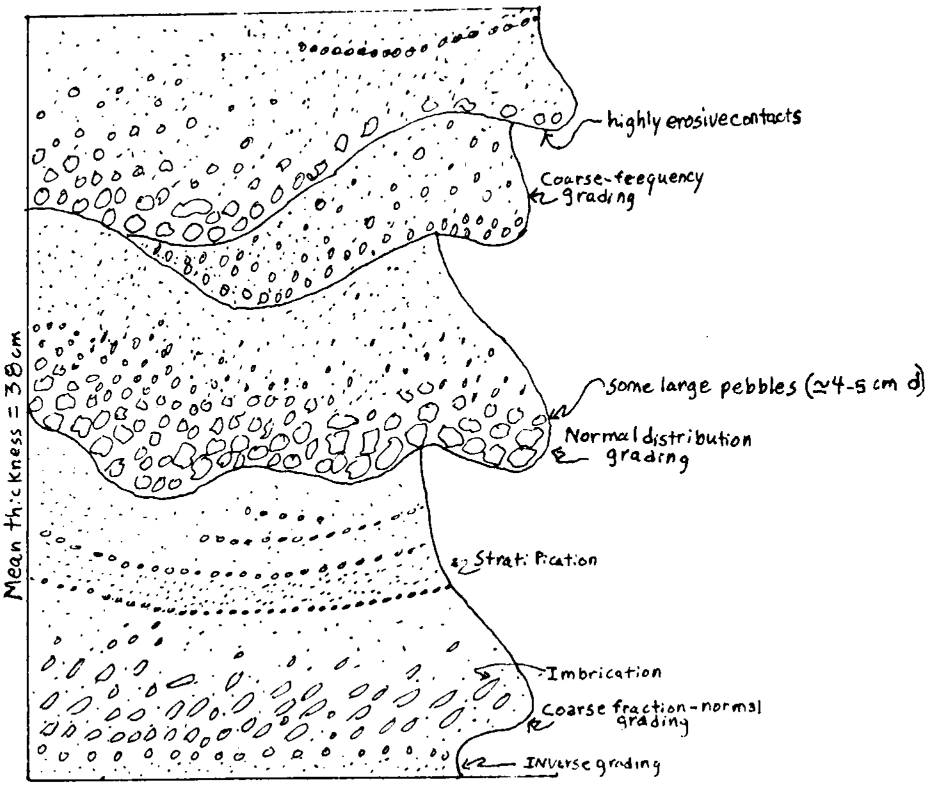

Figure 3-3. Typical assemblage of pebbly sandstones.

Their distinction from conglomerates appears to be solely based upon clast size. They could, then, with the specification of grain size, be placed mainly in the fine conglomerate category (or massive sandstone class if the coarse particles are rarer).

The role they play in Walker's system (1978) is as a transitional type between conglomerate and massive sandstone in his proximal-to-distal reconstruction of a basin of deposition. In order to make it appear that this category is ontologically distinct, Walker denies that beds of the pebbly sandstone family can show inverse grading or imbrication. However, it is obvious from the above discussion of their features that they can show imbrication and inverse grading.

Clast-Supported Conglomerates

Introduction

Probably the most spectacular and prominent deposits in the study area are the conglomerates. The sheer size of the clasts, thicknesses of the beds, and their sedimentary features, however, create problems in the description and choice of parameters of quantitative evaluation. It is probably because of this complexity that conglomerate studies have lagged so far behind other areas of sedimentology. Walker's work (1970, 1975, 1977, 1978) on resedimented conglomerates has been both foundational and seminal. While probably not adequate in every respect, it is primarily his terminology and methods that will be used in this study.

Definition

Following Walker and Mutti (1973) and Walker (1978), the term "conglomerate" is applied to beds containing cobble or larger sized clasts. Though this violates standard nomenclature (Wentworth, 1922; Pettijohn, 1975) by excluding pebble and granule sized material, this nominal distinction need not cause any confusion for the purposes of this study, and so the author simply accepts Walker's definition.

One problem not addressed by Walker concerns the parameter of clast size upon which a bed is classified as a conglomerate. Is it D/10, the mean, or the maximum that has to be in the cobble size range before a bed is classified as a conglomerate? Very few "conglomerates" contain cobble-sized material from bottom to top, so it appears that the mean need not be within the cobble-size range. Yet, there should be more than one clast in the cobble-size class, so simple maximum size would probably not be appropriate as the definitional parameter. D/10 would perhaps be better, though one anomalously large clast might raise D/10 to cobble-sized range. Some sort of simple frequency or abundance criterion is implied in classifying a bed as a conglomerate (see, for example, Folk, 1974).

Since confusion is the rule in conglomerate classification, the author has adopted a simple practice in the field for the labeling of beds as conglomerates. First, and foremost, the beds must be clast-supported, not matrix-supported. Second, cobble-sized clasts must dominate in at least some portion of the bed (volumetrically, not numerically): in normally graded conglomerates, this level is at the base; in inversely graded conglomerates, this level may be above the base. By "dominate" I mean that the face of the rock is taken up by cobble-sized clasts to at least 50% of its area (the clast-supported criterion, of course, actually almost insures this in such large sized clasts). This definition is admittedly arbitrary and pedantic, but it is both loose enough to include all important beds as conglomerates and strict enough to exclude beds in which, for example, only a few scattered cobbles were observed.

Occurrences in the Study Area

Conglomerates appear at SHDC and AFC. At AFC, 10 conglomerates are interbedded throughout the outcrop with massive sandstones, diamictites, and pebbly sandstones. They exhibit no apparent vertical segregation or sequential regularity. At SHDC, the conglomerates constitute roughly 10 beds near the base of the outcrop. The upper part of the section is composed mainly of massive sandstones. Due to lateral changes in thickness as well as poor exposure, it is difficult to say whether some beds are laterally equivalent with other beds. Either deposits of different flows appear at similar or equal stratigraphic positions or the deposits of one flow thicken and thin radically along exposure. The latter could occur when a major flow in a submarine "braided" channel environment left deposits simultaneously in several channels disconnected in the plane of the outcrop. Because of the above uncertainty in the continuity of these beds, the author has separated obviously distinct channel deposits in describing the section even though they may have originated from the "same" flow.

As well as problems of lateral correlation, there is considerable difficulty vertically at both AFC and SHDC. In most cases, the bases of conglomerates are fairly well-defined (±5 cm). The tops are less clear, as many conglomerates fine upward into material that may have been amalgamated from several flows. The thickness of the actual conglomerates are consequently difficult to ascertain.

Descriptions

Diagrams showing several possible conglomerate types are shown in Figure 3-4. A summary table of the descriptive features of the conglomerate beds at both outcrops is shown in Table 3-3.

The ten beds at SHDC have a mean thickness of 1.8 m. The thickest bed observed (amalgamated?) was 3.5 m thick. At AFC, mean thickness is 0.54 m and maximal thickness is 1.3 m. In all cases, the thicknesses of the beds vary laterally, and most beds have a lenticular shape. The beds at AFC are not as well exposed laterally as the beds at SHDC but appear to be less persistent. Some AFC beds pinch out laterally in a distance within a few meters of their maximum vertical thickness.

The conglomerates show clast size gradients laterally as well as vertically. Some beds at SHDC are not even classifiable as conglomerates except in a certain lateral location along their exposure. Such variation seems roughly correlated with bed thickness changes. In general, the larger clasts are located at thicker portions of the bed. This variation is not surprising because it is not expected that a channelized flow would or could operate with the same hydrodynamic efficiency in shallower parts of a channel as in deeper parts.

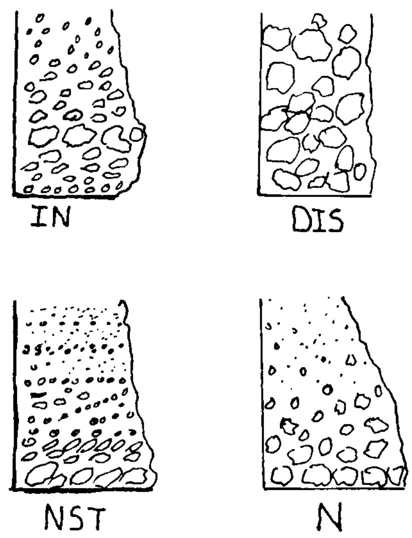

Figure 3-4. Conglomerate types. In this sketch, IN represents inverse-to-normally graded conglomerates; DIS, disorganized conglomerate; NST, normally graded-stratified conglomerate; N, normally graded conglomerate. Drawings after Walker (1975).

Table 3-3. Summary of features of conglomerates at AFC and SHDC

Bed Number	Thickness (m)	D max (cm)	D/10 cm	Grading	Stratification	Imbrication	Bed Geometry	Erosive
SHDC-I	Base not exposed	27.0	18.1	disorganized	no	no	lenticular	?
SHDC-II	1.1	12.5	7.5	normal	no	no	lenticular	yes
SHDC-III	1.5	37.0	20.3	normal/disorganized	no	no	lenticular	yes
SHDC-IV	3.5	65.0	31.0	disorganized	no	no	lenticular	yes
SHDC-V	1.3	19.0	11.9	inverse-to-normal	yes	yes	lenticular	yes
SHDC-VI	2.0	32.0	16.5	inverse-to-normal	crude	no	lenticular	yes
SHDC-VII	1.0	12.0	7.2	normal	yes	yes	lenticular	yes
SHDC-VIII	1.5	12.0	7.8	normal	yes	no	lenticular	yes
SHDC-IX	1.2	23.0	13.9	disorganized	no	no	lenticular	yes
SHDC-X	2.5	16.0	12.8	inverse-to-normal	yes	yes (?)	lenticular	yes
AFC-1	0.45	9.0	6.3	inverse-to-normal	crude	yes (?)	lenticular	yes
AFC-3	0.85	6.5	4.9	massive-to-normal	crude	?	lenticular	yes
AFC-28	0.30	9.0	5.7	normal	no	yes	lenticular	yes
AFC-29	0.81	6.5	4.2	normal	no	no	lenticular	yes
AFC-35	0.18	8.5	5.3	massive-to-normal	no	no	lenticular	yes
AFC-39	0.35	8.0	4.8	normal	no	yes	lenticular	yes
AFC-51	1.05	12.0	5.9	normal	no	no	lenticular	yes
AFC-54	0.25	8.0	3.7	disorganized	no	no	lenticular	yes
AFC-59	0.35	9.0	6.1	normal	no	yes	lenticular	yes
AFC-60	1.30	13.0	6.6	disorganized/normal	no	no	lenticular	yes

What is more surprising is the lateral variation in internal structures. There is some suggestion in the SHDC beds that disorganized conglomerates tend to occur at the thicker parts of the bed and more organized styles of textural trends to occur in the thinner portions.

Walker (1975, 1977) has observed a vertical sequence of beds of disorganized--inverse-to-normally graded--normally graded (and stratified) conglomerate. He has suggested that each step in the sequence represents a diminishing competence ("energy") of the transport mechanism of successive currents. The assumption is that in a recessional (e.g., channel filling) suite of beds, upward vertical transitions between beds may be used as a clue to lateral transitions within beds since upward transitions in such a recessional regime represent at the same time successively more "distal" lateral environments. Thus, even though we cannot usually trace out a single bed laterally and observe property transitions in this dimension, the upward transitions between beds with diverse properties give a (stochastic) picture of what the lateral changes within beds may be like as the sediments are deposited relatively further from source.

In an effort to test this hypothesis, the SHDC outcrop was divided into 28 vertical traverses, normal to bedding. Although only a small number of separate or "different" flows may be represented here, the lateral variation mentioned above justifies upward transition studies at multiple locations. The upward tally matrix, upward transition probability matrix, and a likely upward transition diagram are shown in Figure 3-5.

	DIS	IN	NST	N	NON
DIS	7	5	6	8	7
IN	1	0	4	4	2
NST	0	0	3	5	4
N	0	1	2	7	5
NON	1	3	6	7	23

n_{ij}

	DIS	IN	NST	N	NON
DIS	0.21	0.15	0.18	0.24	0.21
IN	0.09	0.00	0.36	0.36	0.18
	0.00	0.00	0.25	0.42	0.33
N	0.00	0.07	0.13	0.47	0.33
NON	0.03	0.07	0.15	0.18	0.58

p_{ij}

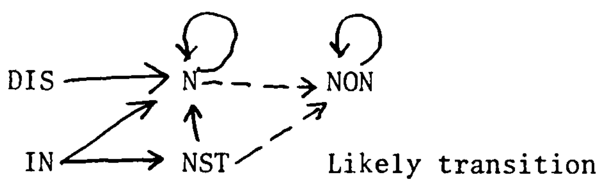

Figure 3-5. Lithotype transitions in the SHDC beds. Shown are the tally matrix (n_{ij}), probability matrix (p_{ij}), and likely transition diagram. DIS represents disorganized conglomerate; IN, inverse-to-normally graded conglomerate; NST, normally graded conglomerate; and NON, nonconglomeratic lithotypes such as massive sandstones or pebbly sandstones. The solid lines in the transition diagram represent the most likely transitions; the broken lines represent less likely transitions.

There is obviously a great deal of uncertainty in the system and the transitions can hardly be offered as a strong confirmation of Walker's claims, though they do seem to tend toward the transitions that he proposes. It should be noted, however, that Walker places the normally graded conglomerates before the normally graded-stratified conglomerates in his ideal sequence. My data indicate that the placement is more of an alternative between the two rather than a precedence of one over the other. Further, the placement of disorganized is almost randomly divided between all entries. This seems to suggest that Walker's placement of this type of conglomerate is questionable (at least on the limited data contained in this study).

Mode of Transport and Deposition

It is now thought that the primary supporting mechanisms for clast-supported conglomerates during most of their transport history is fluid turbulence (Stanley and Bertrand, 1979). Late stage modifications due to clast concentration (grain dispersive pressure) lead to other features such as imbrication and inverse grading. Deposition of large vertical intervals may be rapid early on at changes in gradient. A large flow might be expected to dump large clasts in structureless beds in more proximal positions. Farther down slope, clast concentration and dispersive pressure would act to imbricate and reverse the grading of the clasts. Continued depletion of the flow and rapid waning of velocity might give rise to normally graded or structureless beds (depending upon rapidity of deposition). The nonpreferential nature of the upward transitions from disorganized beds may simply indicate that a large flow is capable of interrupting an otherwise preferred sequence of conglomerate types.

The outcrop at AFC, somewhat ignored in the preceding discussion, is less interesting than SHDC because all upward transitions with the exception of two normal transitions are transitions to nonconglomeratic lithotypes (pebbly sandstones and massive sands). As can be seen from Table 3-3 (p. 74), the outcrop is of "distal" conglomerates and is dominated by normally graded beds. The excellent small scale channeling, normal distribution grading, and good sorting indicate deposition from fully turbulent flows.

Matrix-Supported Beds

Introduction

This suite of beds is interesting both from a sedimentological and classificational point of view. A strict understanding of the term "matrix" as the relatively smaller grains in a rock would include a large number of beds in this category. What is actually intended by the term "matrix" in Walker's (1978) classification, however, is just as much interpretive as descriptive. Matrix support does not mean just an observed field property but a hypothetical transport mechanism that operated to support the clasts as the sediment moved down into the basin. The two components of this mechanism are taken to be finite yield strength of the matrix and buoyancy resulting from its relative density (see Chapter 2). The problem of assigning beds to this category, then, is that one is assigning them to a genetic class.

Occurrences in the Study Area

Beds that belong to this class are found at all outcrops in the study area. Particularly prominent, thick, poorly sorted, conglomeratic-to-silty sandstones or mudstones (diamictites) occur at AFC, LLCD, and ULCD. At the Lucy Creek outcrops, these beds also contain large chunks of distorted, partially preserved beds of turbidites and other lithologies. Some beds at SHDC, LSHDS, and USHDS are likewise interpreted to be debris flows or slumps. Since the beds of this class are so diverse and widely spread in all study locales, beds from all six outcrops will be used in characterizing this class.

General Descriptions

Two descriptive end members exist in this group of beds: slumps and diamictites. Between these two end members, there appears to be a spectrum of gradations. Some beds contain well preserved, though contorted, intraformational beds. Other beds contain almost completely disaggregated beds that might more properly be described as clasts rather than as partially preserved beds.

Particular Description

In the particular descriptions which follow, a continuum of descriptive types from slumps to diamictites will be examined. First the descriptive end members are discussed. The gradations between them then will be studied.

Slumped bed: USHDS-69. This unit is 150 to 175 cm thick and is composed of at least 6 separate beds of sandstone, shale, and granule sandstone. The structure of the bed is essentially a recumbent fold with some minor contortions. It rests nonerosively on a friable, muddy, fine sandstone bed.

The internal beds still retain their individual identities even though they are overturned in part and no longer display bedding parallel to general outcrop bedding. There is a strong parallelism of internal bedding planes one with another. All indications, then, are that these internal beds deformed and moved as a unit. The scale of the movement must not have been great since the internal beds are individually so well preserved and relatively undisturbed with respect to each other.

Diamictites at AFC. At AFC, at least four major diamictite beds crop out. They are interbedded with conglomerates, massive sandstone, and pebbly sandstone. The thickest is almost 5 m thick and contains large dispersed clasts of various rock types. Usually, these relatively larger clasts do not touch each other. One discoidal clast of greywacke sandstone over 70 cm in diameter lies near the top of the bed in a position approximately parallel to bedding. In other diamictites, large chunks of shale and sandstone beds, presumably also derived from within the basin, lie roughly parallel to overall outcrop bedding.

A summary of features of the four major diamictites at AFC is shown in Table 3-4.

It should be noted, finally, that these diamictites are or appear to be compositionally distinct from the conglomerates of the outcrop. The conglomerates lack the greywacke sandstone and shale clasts that

Table 3-4. Summary of the features of the diamictite beds at AFC

Bed Number	Thickness (cm)	D max (cm)	D/10 (cm)	Imbrication	Stratification	Grading	Erosional Features	Clast Supported	Bed Geometry
4	500	70	18.3	no	no	no	no	no	lenticular
9	60	8	4.9	no	no	no	no	no	lenticular
27	210	21	6.2	no	no	no	no	no	lenticular
48	400	15	5.7	no	no	no	no	no	lenticular

appear in the diamictites. This point will become important later when we turn to questions of transport mechanism. The preservation of what were apparently poorly indurated, deformable sediment bodies indicates a rather gentle mode of transport, a gentleness unlikely under the conditions of fully turbulent flow.

Transitional deposits. Between the two well-defined end members are a range of beds that exhibit properties transitional between the essentially nonsedimentary fabric and inferred processes of deposition of slump-type units to the complete homogeneity of the diamictites. I will describe some deposits that illustrate some of these transitional beds.

1. ULCD: This outcrop contains one large (approximately 5 m thick) bed that in part is very similar to the slumped beds described earlier. It has enough interfingering diamictite, however, so that characterizing it simply as a slump is misleading.

The bed rests sharply on thin (5-10 cm) beds of alternating sand and shale (turbidites). Its overall form is apparently irregular to lenticular in shape, and the entire unit pinches out about 40 m east of its point of maximal thickness. The western end of the bed is covered. There is no evidence of erosion of the underlying beds even though the basal contact is relatively sharp. The unit is capped by an erosive, channeling, medium-grained sandstone.

Within the unit, preserved beds similar to the underlying beds can be seen, though they are complexly folded and some are pulled apart.

Sole marks are visible on the upturned bases of some of these internal beds. These remnant beds are not laterally continuous but float in the ubiquitous, poorly sorted, clay-rich matrix. This matrix also contains discoidal cobbles and boulders of sandstones, presumably derived from within the basin itself, as well as very faintly preserved ghosts of shale, siltstone, and sandstone beds, now almost homogenized beyond recognition.

Toward the west end of the exposure, the diamictite interfingers with huge (approximately 4 × 4 m) blocks of relatively undeformed turbidites. When this feature was described by King and Ferguson (1960), they assumed that the diamictite had plowed into these turbidites and that the turbidites were essentially in place (see Figure 3-6). Close examination of these blocks show them to be completely surrounded by the diamictite. Given the common association of partially preserved beds in this larger bed, it seems a bit more plausible that these enormous blocks were transported at least a short distance within the flow itself. It may be that they slid or slumped into the flow and did not move a great deal. However, it is worthwhile noting that these blocks do not touch the base of the bed but are supported within the sandy-silty matrix. We must presume, consequently, a substantial strength for the flow, a strength that could have been capable of supporting these blocks during actual movement.

2. LLCD: The outcrop at LLCD is very similar to ULCD but represents a further homogenization of remnant beds and in many places has a very similar texture to that of the diamictites at AFC. The unit is

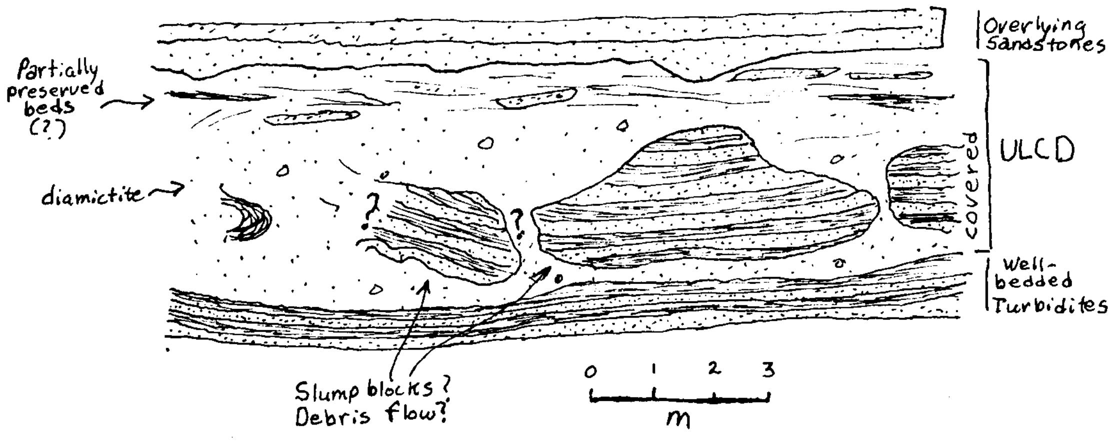

Figure 3-6. ULCD. The relationships are far from clear. It appears that the large blocks of turbidites are actually *within* the debris flow. A channeling sandstone caps this bed.

approximately 2 to 3 m thick and again rests nonerosively upon finer-bedded material. It appears to terminate laterally in a rather blunt, rounded mass rather than by progressive thinning. The bed is capped by an erosive sandstone unit with well-developed channel geometry. In one section within the bed (LLCD), remnant sand beds are still well preserved and can be traced for short distances laterally (see Figure 3-7). Apparently, they were rafted-slumped along in the main body of the flow without extensive disaggregation. However, in general, the shreds of former beds are present on a much smaller scale. For example, ragged, distorted fragments of shale beds can still be seen in polished slab even in the more thoroughly mixed portions of the bed (Figure 3-8).

This unit fits descriptively between LLCD and the diamictites at AFC. Some portions have the completely homogenized appearance of the AFC diamictites; other portions have relatively well-preserved bed remnants. A continuum of descriptive types, thus, seems to be exhibited in one and the same bed and supports the gradation from diamictites on the one hand to slumps on the other.

3. SHDC-5: This bed does not fit well in the spectrum presented thus far. The bed is approximately 2.5 m thick but pinches out (or passes into disorganized, clast-supported conglomerate?) within 30 m of this maximum thickness. It contains many intraformational shale and sandstone clasts, as well as large limestone clasts (up to almost 1 m in diameter), and smaller clasts of various other rock types. The matrix supported fabric is not nearly as pronounced as that supporting the

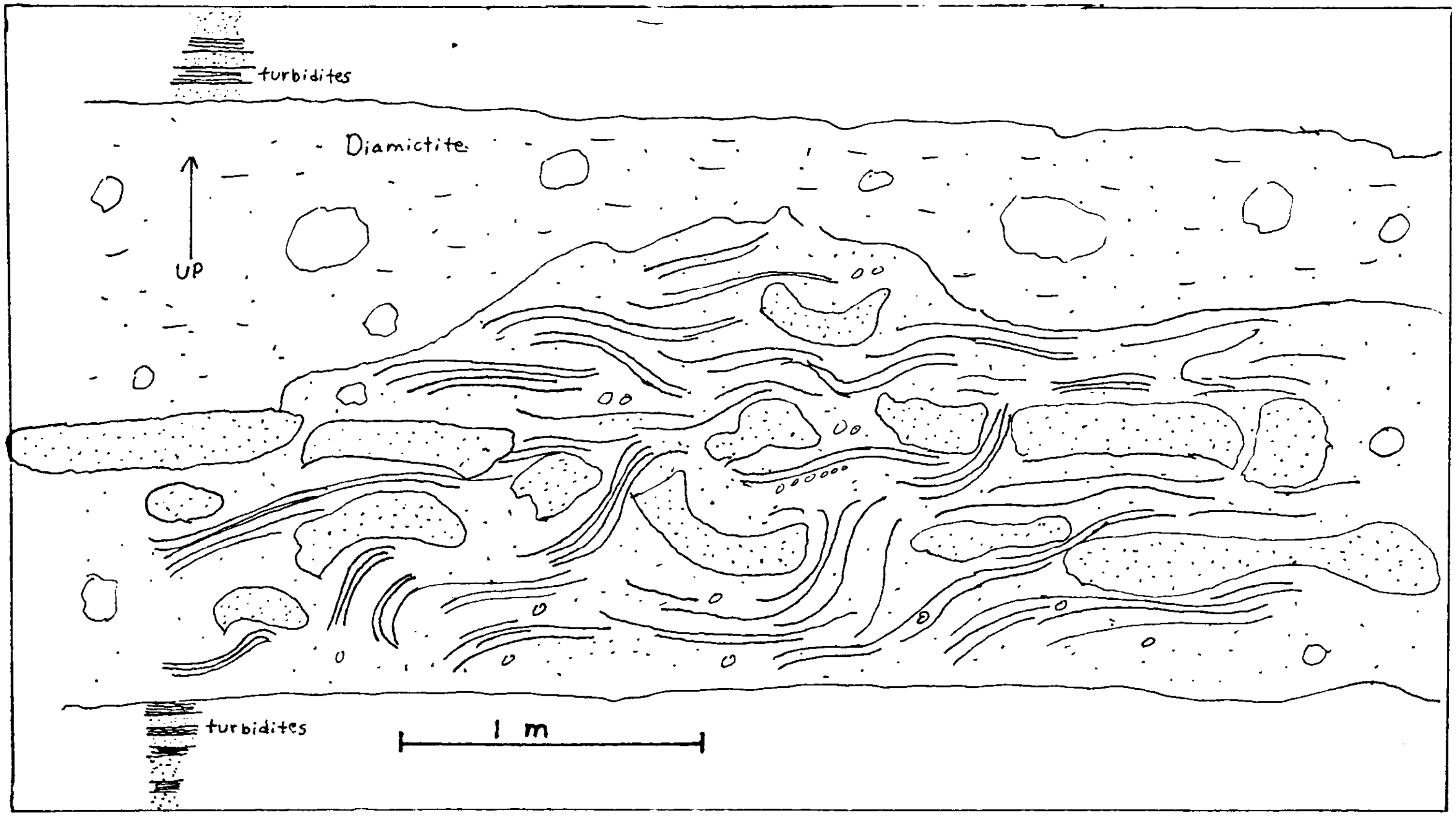

Figure 3-7. Sand body geometry at LLCD. The large beds of sandstone and shale are in a silty-sand "matrix." More homogenized diamictite lies above and is so labeled. Turbidites are found at the top and bottom of this bed.

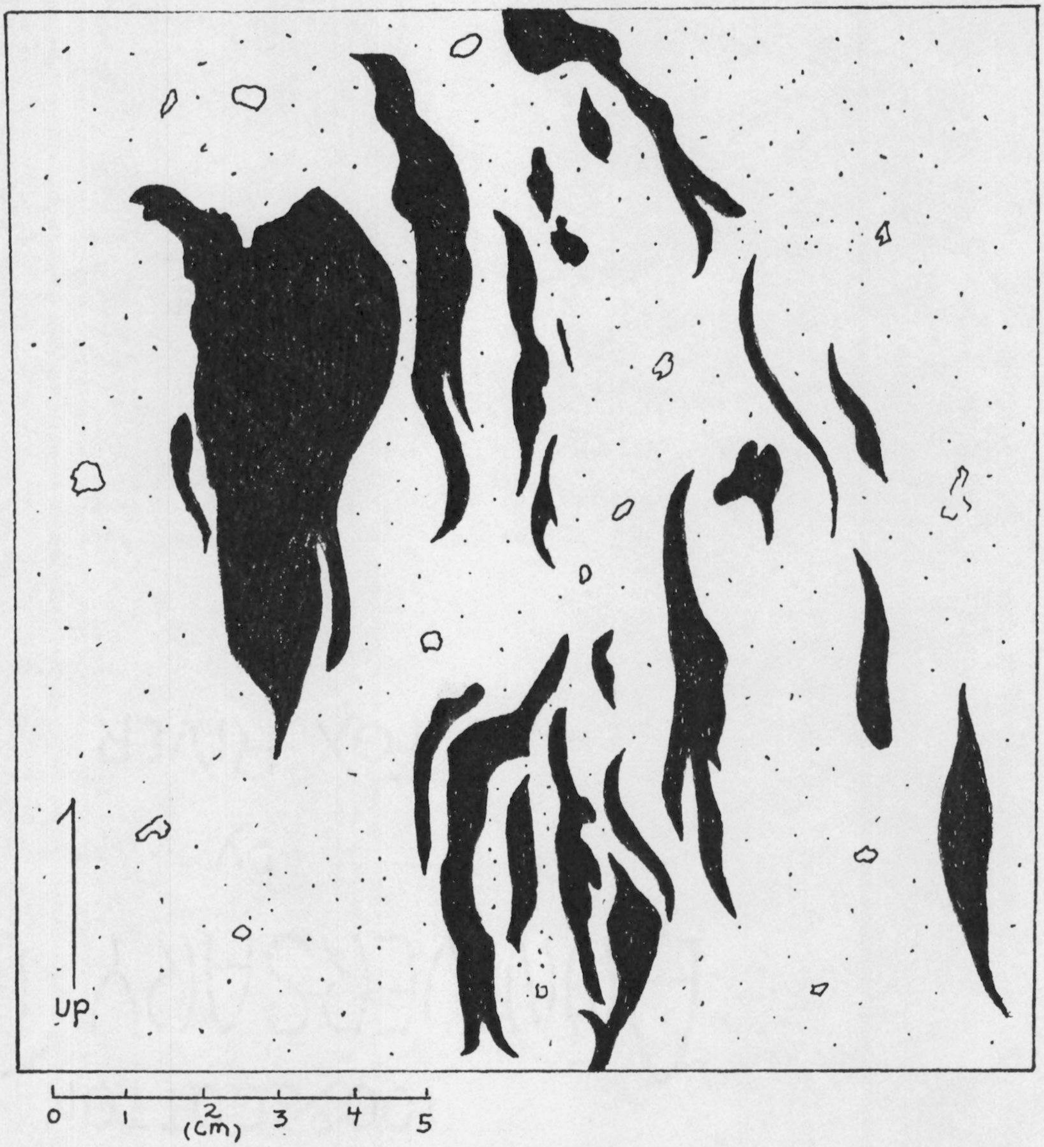

Figure 3-8. Remnant shale clasts at LLCD. Drawing taken directly to scale from a polished section. The shale clasts (black areas) are contained in a silty-sand matrix. The peculiar orientation of the clasts is puzzling. Perhaps, a slow, viscous circulation at the snout of a debris flow gave rise to this orientation.

boulders in diamictite, and in many cases, the clasts seem to touch other.

The bed rests smoothly upon and is almost amalgamated to a large conglomerate bed. There is no evidence of grading or other common fabric elements within the bed. However, there is a well-developed parallelism of very large shale clasts with each other and (in general) with overall outcrop bedding. Unlike a slump deposit, these clasts display an apparent ordered parallel fabric throughout much of the bed that would not have come about through rotation of the clasts solely under the influence of gravity. This fabric must have been derived from the action of some other mechanism that acted on the clasts individually. The competence of this mechanism must have been great. At one place where the bed is little more than one meter thick, a limestone clast 75 cm in diameter is supported near the top of the bed. There apparently was little opportunity for size sorting of material during or after movement.

4. LSHDS-B-168: As we have seen previously in this chapter (p. 55), the outcrop LSHDS is dominated by and mainly explicable in terms of the turbidity current mechanism. However, there are some beds in this outcrop that are so very different in character from the standard turbidite bed that it is difficult to believe they can be entirely accounted for by the same mechanism.

B-168, for example, though only 8 cm thick contains discs of well-indurated sandstone up to 12 cm in diameter parallel to bedding. While these discs are very similar in density, induration, and overall appearance to the associated turbidite beds of the outcrop, the bed itself is very dissimilar. The discs as well as dispersed granules and coarse sand are set in a very poorly sorted, less dense, extremely friable, clay-rich matrix. The base of the bed appears smooth and rests upon apparently noneroded shales. Amalgamated to this bed is a very well-sorted, standard C(D) turbidite bed.

While it is possible that this bed is not an amalgam but an AC(D) sequence, classification of the coarse part of this bed under the label A violates all expectations, theoretical as well as practical, about the coarse division deposited by fluid turbulence. A comparison of this bed with the A division of B-170 (a *bona fide* turbidite) emphasizes this difference (Table 3-5). If fluid turbulence is called upon to explain the set of properties which this bed has, properties at essential odds to those of standard turbidites, then it loses any explanatory or predictive force it might have. One, of course, expects a range of variation in one property or the other as simple "error" of the process. But, a consistently contradictory set of properties seems to indicate the action of some other process. In light of this, it would seem best not to describe such beds as this one as A intervals deposited by turbidity flows. Certainly, from the standpoint of pure description, they bear little resemblance to the standard A divisions of turbidites.

As a qualification on this last statement, it should be noted that the differences between turbidites and the beds of this category are not always so drastic and some gradations can be seen in the field between the two. However, it seems reasonable to assume that while turbulence

Table 3-5. Comparison of LSHDS-B-168 with LSHDS-B-170

LSHDS-B-168	LSHDS-B-170
very poorly sorted	well sorted
D max = 12 cm	D max = sand
less dense	dense
nongraded	graded
nonerosive	erosive
8 cm thick	26 cm thick
poorly indurated	well indurated
clay-rich	clay-poor

may have played some role in transporting these beds, some other mechanism(s) must also have been operative.

Mode of Transport and Deposition

There are several facts to consider before attempting to interpret these deposits genetically. First, it is of critical importance that a single descriptive spectrum not blind us to the possibility of multiple processes operative in the transport of the sediment. Second, the flows that deposited these units had enormous competence (large clast size) but at the same time most appear to have been surprisingly nonturbulent internally (nonerosive emplacement and the preservation of fragments of obviously soft, deformable intraformational beds). In associated conglomerates with similar sized clasts, there are no traces of partially preserved beds. Since we have interpreted the conglomerates to have been transported mainly by fluid turbulence, the role of turbulence as a support mechanism for the matrix-supported beds must have been considerably reduced. Major turbulence would have destroyed the beds preserved in these units. Third, in many of the beds, the clasts and intraformational beds are parallel or subparallel to outcrop bedding. Such a fabric would not likely arise in turbulent flows; it may perhaps indicate a much more viscous laminar type of flow (Fisher, 1971). Fourth, there is a problem as to how a homogenized diamictite can be present in one part of a bed while chunks of preserved beds are present in another part: What process could possibly homogenize some beds completely and leave adjacent beds only slightly deformed?

The author does not think that there would be any argument about assigning beds such as USHDS-69 to a slump mechanism of formation. The lack of evidences of flow and the good preservation and internal parallelism of bedding planes indicate a relatively sudden down-slope slump along a few planes of shear. There was little, if any, movement of internal points relative to each other as would be necessary in a flow (innumerable shear planes) and the deposit gives all indications of having rotated and deformed as a unit. Slumping is the most likely mechanism for production of these features.

The classical and long-accepted view as to the origin of pebbly mudstone (diamictite) was given by Crowell (1957). He argued that conditions favorable for the formation of pebbly mudstone occur when gravel is deposited on a soft substrate of mud. The instability due to density differences between the two layers results in the sinking and loading of gravel into the mud. If the slope angle is steep enough, this deforming mass moves downward. The final deposit is a homogenized pebbly mudstone.

This well-argued position provides a phenomenology of flow but does not specify a mechanism of support and transport. As we have seen, evidence of fluid turbulence and grain dispersive pressure are rare in deposits of this kind. It is more reasonable to assume that the debris flow mechanism was the major transport mechanism operative in the emplacement of these beds. The obvious competence of the flows and their strength in supporting clasts upward in their body after deposition indicates a relatively dense sediment with considerable plastic yield strength and buoyant force. Lindsay (1966) thinks that turbulence may be operative in part of the history of some of these flows. This may be correct for the very homogenized beds at AFC but seems unlikely in the deposits at LLCD.

Crowell's (1957) model presents the picture of a sudden, "instantaneous" event. A model such as his seems quite adequate for explaining the AFC diamictites and beds such as LSHDS-B-168, and perhaps SHDC-5. But, what of the Lucy Creek beds?

In order to explain these beds, a considerable adjustment of perspective must be made. In thinking of turbidites, conglomerates, and most deep ocean density deposits, the imaginative picture that we have is of a process which abruptly starts, operates for a short period of time, and then is over. However, the author believes that the Lucy Creek outcrops may represent deposits from a mix of processes that may have operated almost as a steady state over a relatively long period of time.

Stanley (1974) describes two separate, though interfingering, facies of deposits in a modern deep-sea channel. A pebbly mud deposit (homogenized diamictite) occupies the axial position of the channel. To either side of this, slumped beds of intraformational turbidites make up a jumble of large fragments along the sides of the channel. Stanley thinks that these facies are the result of two distinct types of processes: debris flow in the central pebbly mud deposits and slumping in the marginal deposits. The slumping and sliding of large blocks onto the poorly consolidated pebbly mud is thought to initiate debris flows that move as extremely viscous, laminar masses down the channel.

The deposits at Lucy Creek certainly bear a descriptive similarity to the deposits described by Stanley. His model makes sense of the fact that there can be a spectrum from completely homogenized diamictite to ghostly remnant beds to quite well-preserved beds in one and the same deposit. The homogenized material originated much further up channel; the remnant beds slumped into the flow a lesser distance up channel; and, the well-preserved beds may have been the last additions to the flow before movement ceased. Consequently, we cannot think of such flows as the result of down slope movement of a given original mass of sediment; rather, they are perhaps best conceptualized as flows which moved down the channel, being augmented continually by the addition of fresh material by slumping along their margins. The flows may have alternately moved and come to rest depending upon the "push" of new pebbly mud originating further up channel. In this manner, such flows may have achieved near steady-state conditions: the pebbly mud that moved into final depositional sites being continuously replaced by the generation of more sediment further up channel. The notion of a precise spatial and temporal beginning and ending for such flows may be misleading. They may be better modeled as a near steady-state system of sediment production and deposition. In this way, they may be quite different from other subaqueous deposits both as to physical transport process as well as temporal and spatial dimensions.

CHAPTER 4

FACIES PACKAGES AND THEIR ENVIRONMENTAL SIGNIFICANCE

Introduction

In the following discussion, the author briefly presents the salient features of the environmental model used to interpret the deposits of the study area. The environmental settings and development of the outcrops are interpreted on the basis of two types of regularity defined in the stratigraphic sequence. One type is an associational regularity in which a given lithotype is found preferentially with similar lithotypes or with lithotypes that taken together constitute an environment of deposition. Closely related to associational regularity (and often necessary for its full interpretation) is regularity defined on the changes in lithotypes and beds stratigraphically--i.e., sequential regularity. There are two important types of sequential regularity: lithologic and thickness regularity. These regular changes may be unidirectional or cyclic, depending upon the particular facies of deposition and the scale of the investigation. For example, at the very broadest scale of sequential change (basin level), the changes are probably noncyclic, evolutionary changes controlled by large scale tectonic events. Imposed upon this grand scale evolutionary spectrum, however, there may be many repetitive or cyclic styles of regularity that represent continual and repeated adjustment of a limited number of environmental options over space and time. At any scale, the sequential patterning (lithologic packages) and associational changes in lithotypes provide important information about the environment of deposition of the particular sequence under investigation and its development through time.

The Submarine Fan Model

The submarine fan model has been quite well characterized both as to expected sedimentological features (Ricci-Luchi, 1975; Walker, 1978; Walker and Mutti, 1973) and as to its general physiographic features (Normark, 1970; Normark, 1978; Selley, 1979). The author will briefly summarize the salient features of submarine fan morphology and deposits. The following discussion is primarily based upon, Walker (1978) and Normark (1978) to which the interested reader is referred for more complete details.

Morphologically, submarine fans may be divided into three major divisions: upper, middle, and lower fan (see Figure 4-1). Each of these divisions is characterized by typical associational suites of lithotypes (Figure 4-2).

The upper fan is characterized typically by one main valley that may have a single active thalweg channel continuous with the feeder canyon or a braided system of channels. The channels are flanked by well-developed levees that result from continual spill-over and overbank deposition. Deposits typical in this fan division are conglomerates or coarser sand in the channels (if such coarse material is available to the basin), and levees that consist of finer, alternating sand and shale

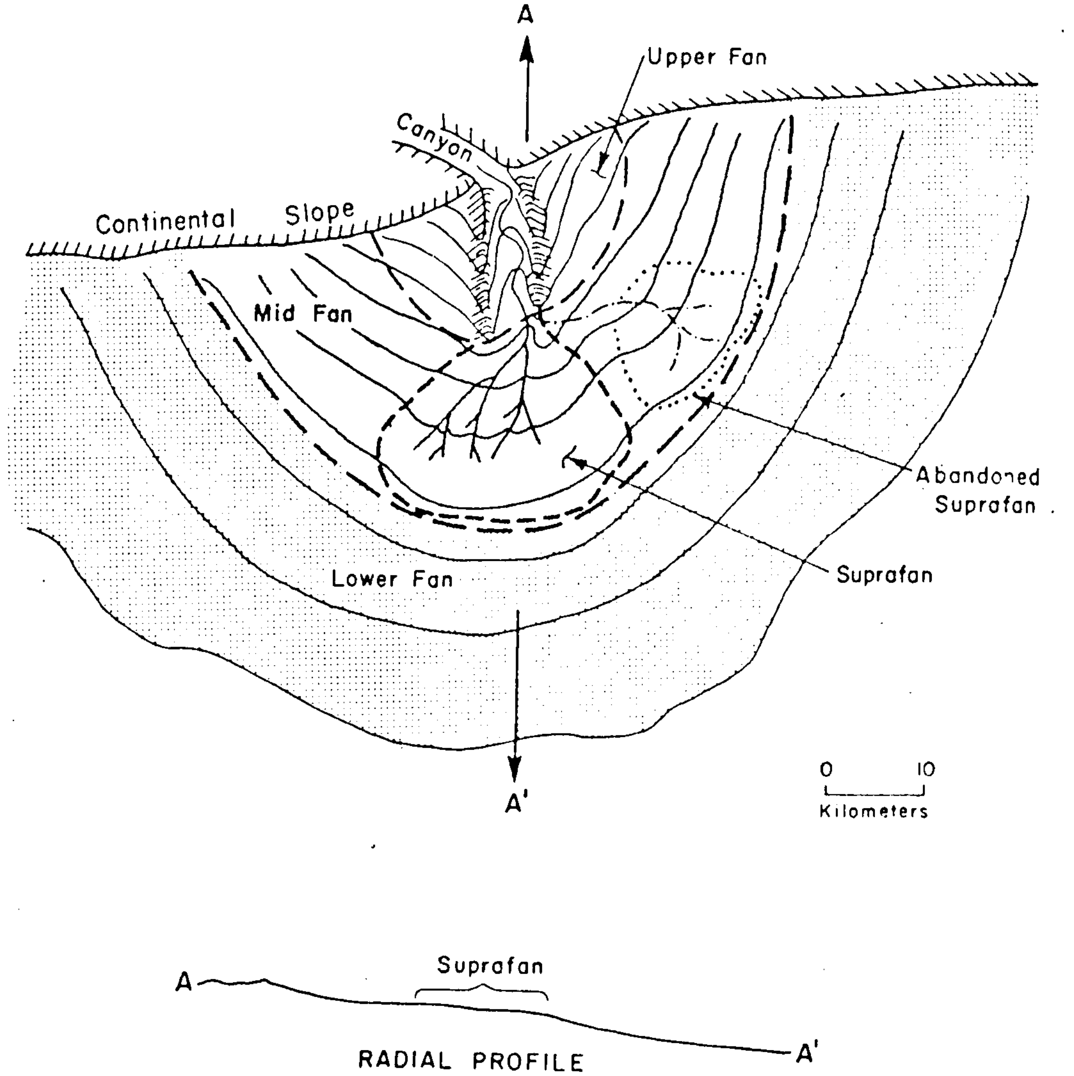

Figure 4-1. Physiographic model of submarine fans. Sketch taken from Normark (1978).

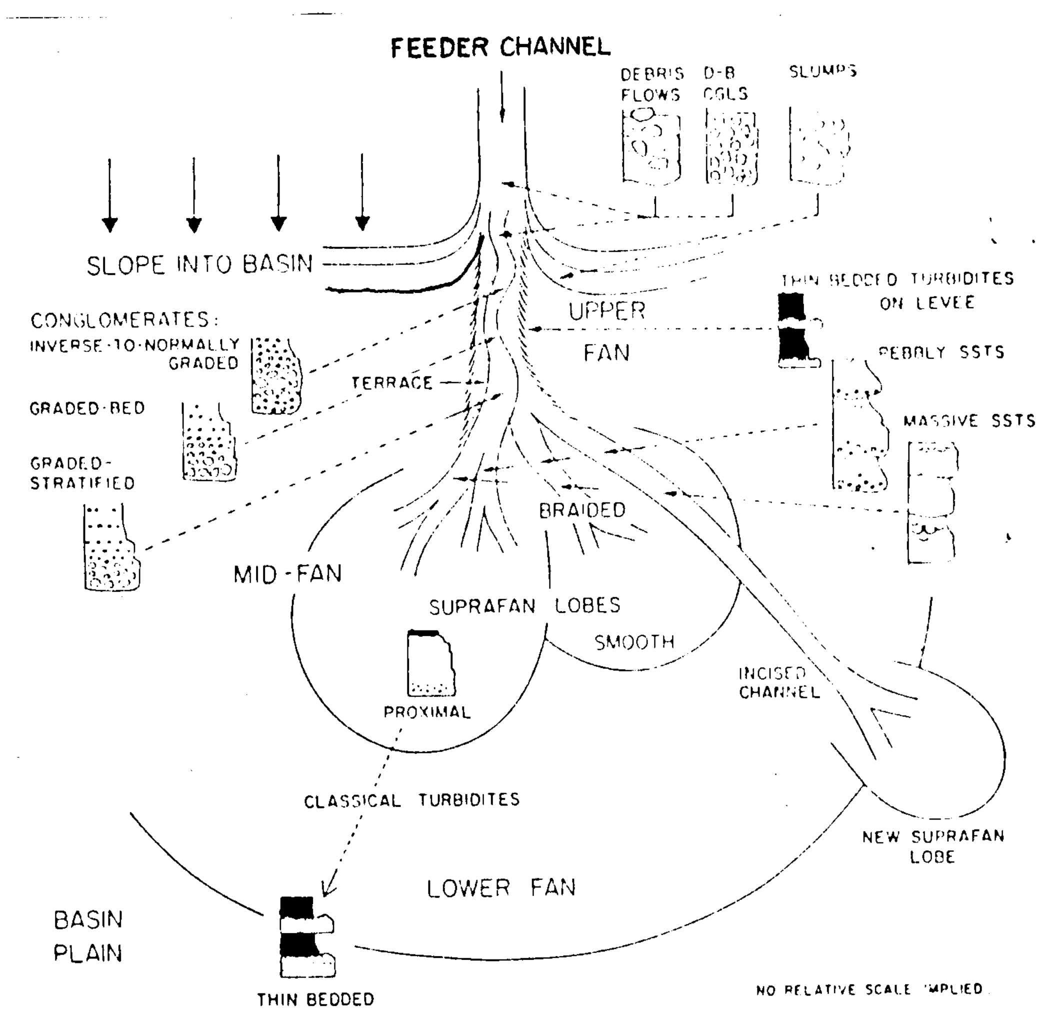

Figure 4-2. Expected deposits in a submarine fan depositional environment. D-B denotes disorganized-bed conglomerates. Sketch taken from Walker (1978).

which can be confused with distal turbidites if their association with channelized, coarse sediments is not observed (Nelson et al., 1974). One complication in this picture is that a channel may cut downward and outward across the fan as a result of a locally increased gradient and avulsion from another major channel in the system (see Figure 4-2). In this case, conglomeratic channel deposits may abruptly incise much thinner, finer "distal" turbidites and produce apparently anomalous associations of "inner fan" deposits along with "outer fan" deposits.

The associational regularities in upper fans are lenticular channel-fill conglomerates and other coarser clastic sediments. Finer levee deposits occur on either side of these coarse deposits. Slumped deposits may occur as the channel(s) migrate and undercut the valley walls. Large scale debris flow deposits may also occur in this very proximal environment. Sequential regularity observed in aggradation of the fan should exhibit coarser channel-fill deposits capped by finer, thinner massive sands and classical turbidites. A rapid rise in sea level may lead to only very fine suspended sediment being deposited on top of the inner fan channel--as is the case in several modern fans following the post-Pleistocene rise in sea level (Normark, 1974; Walker, 1978).

The middle fan is recognized morphologically as a distinct depositional, convex-upward bulge (Normark, 1978). The region is commonly called the suprafan and consists of lobate sediment bodies that shift in location in much the same manner as delta lobes. The inner suprafan is characterized by slightly or unleveed distributary channels that braid and coalesce into laterally extensive coarse clastic deposits. The deposits left in these shallow channels may include finer conglomerates, pebbly sandstones, and massive sandstones. More distal areas of the suprafan are characterized by classical proximal turbidites which may or may not be characterized by obvious thinning-upward packages of beds. The repetitive thinning-upward packages of coarse clastics on the suprafan are thought to represent the filling and abandonment of shallow channels (Walker, 1978). Trendless sections of finer, thinner-bedded material may represent interchannel deposits. The abandonment of a suprafan lobe due to channel switching breaching (avulsion) in the upper fan results in a lobe sealed by very fine suspension-fallout sediments or fine overbank sediments from an actively developing lobe. A hypothetical vertical and plan view of the results of suprafan lobe switching is shown in Figure 4-3.

The associational regularities in the middle fan are, from proximal to more distal regions, coalesced pebbly to massive sandstone in lenticular, shallow channels and classical proximal turbidites interspersed with finer, thinner overbank deposits of finer sandstones and shales. Sequential regularities include fining- and thinning-upward sequences of channel-fill and channel-abandonment turbidites. Thicker mudstone may drape a coarse clastic sequence following lobe abandonment.

The lower fan is areally the most extensive of any of the physiographic divisions of the fan and passes gradationally into basin plain sediments (hemipelagic and pelagic shales). The relief is extremely low, and laterally continuous, tabular, fine-grained (distal)

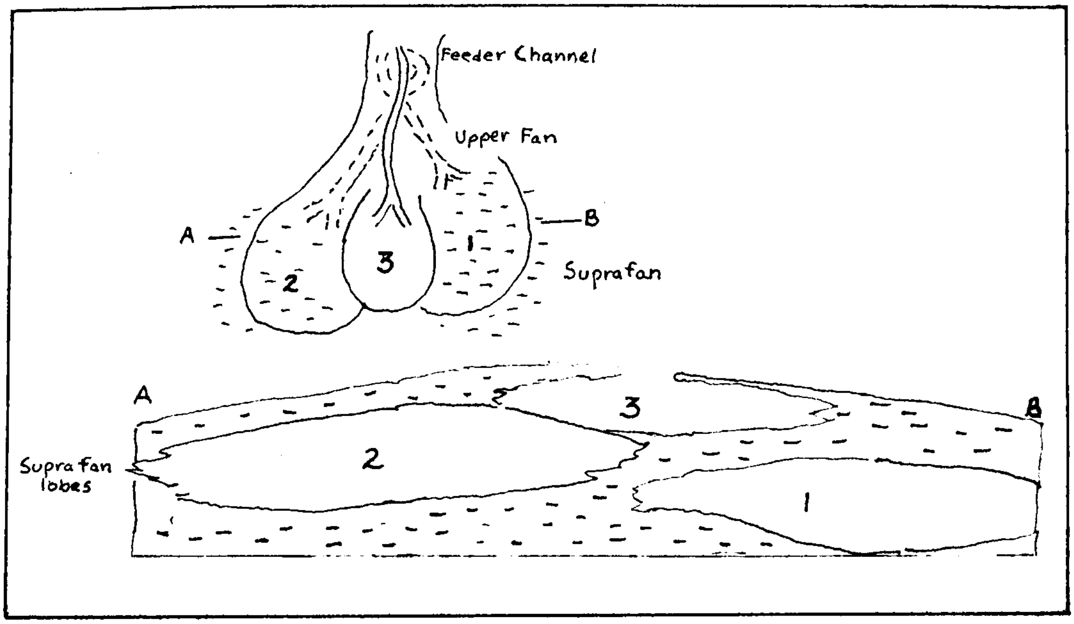

Figure 4-3. Vertical and plan view of a prograding middle fan system. The vertical profile is the result of lobe switching from positions 1, to 2, to 3. Abandoned lobes are draped by a shale blanket upon cessation of active lobe sedimentation. Drawing is after Walker (1978).

turbidites are the dominant and typically monotonous deposit. Sequential regularities in a prograding fan system are repetitive coarsening- and thickening-upward cycles.

The associational and sequential regularities associated with a prograding fan system are summarized in Figure 4-4.

Interpretations of Deposits in the Study Area

SHDC

The lithotype associations within this outcrop (associational regularity) are clast-supported conglomerates, pebbly sandstones, massive sandstones, slump or debris flow deposits, and base-present turbidites. The entire body of this otherwise very coarse outcrop rests abruptly upon very fine siltstone and shale of the Blockhouse Formation. These silt beds are graded and monotonously interbedded with the shales, so they are thought to represent relatively distal turbidites (Shanmugam, 1978).

To test for any lithologic regularity an informal Markov test was performed for the upward transition tally matrix of lithotypes found in this outcrop. The test is "informal" because there are few entries in the transition matrix. There is no precise agreement as to the number necessary. Lumsden (1971) thinks 10 times the number of cells; Krumbein and Graybill (1965) suggest that 5 tallies are needed per observation (e.g., cell) for the application of the chi-square statistic. In either case, the matrix is insufficient from a formal sense (i.e., we cannot extend the deductions to unsampled populations).

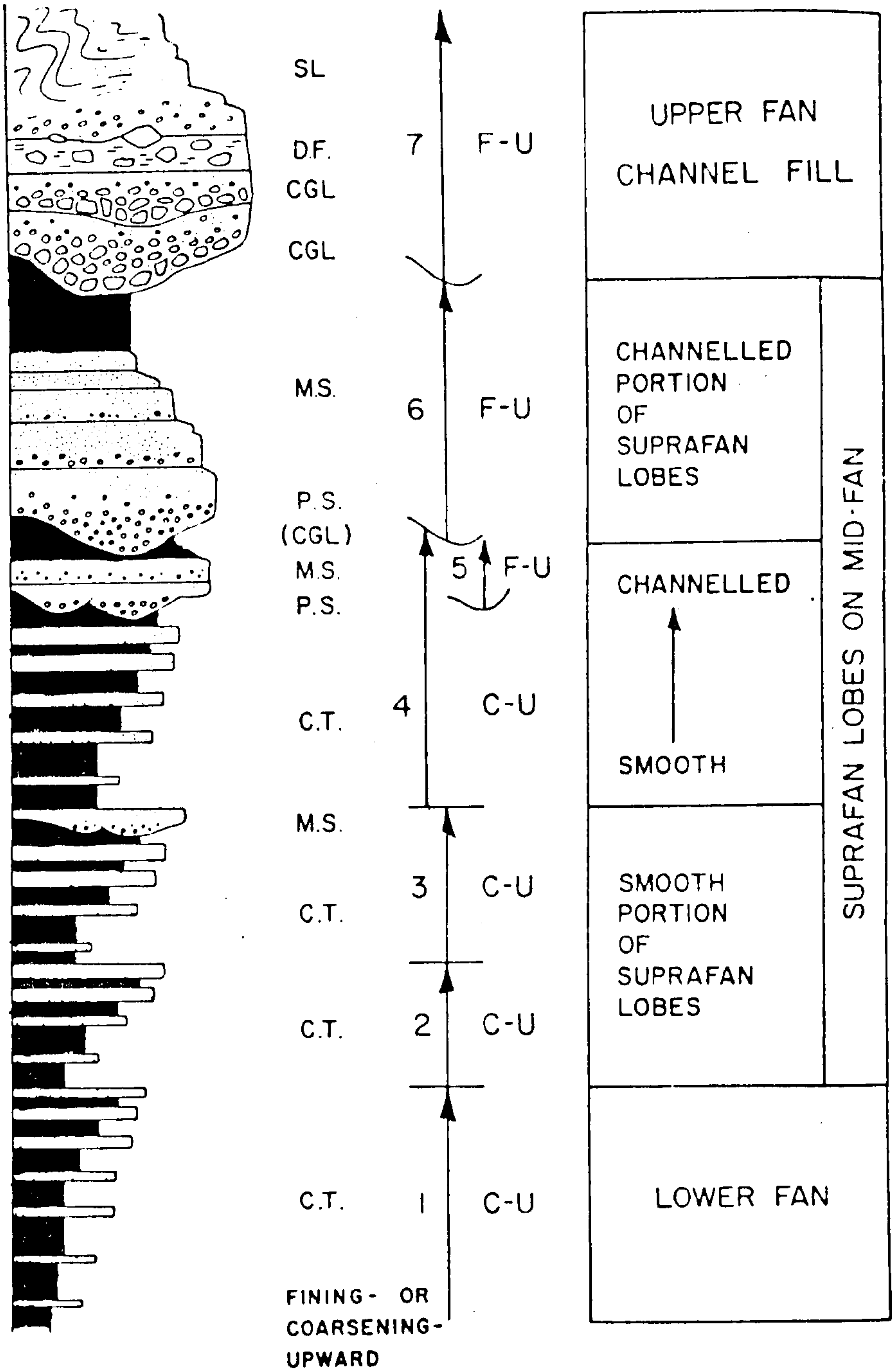

Figure 4-4. A stratigraphic sequence developed during fan progradation. There are seven packages of sequential regularities in grain size and bed thickness in this hypothetical reconstruction. C-U represents thickening- and coarsening-upward; F-U, fining- and thinning-upward; C.T., classical turbidites; M.S., massive sandstones; P.S., pebbly sandstones; CGL, conglomerate; D.F., debris flows, SL, slumps. Sketch taken from Walker (1978).

The hypothesis tested is that the sequence has the Markov property--the transitions are not random. Rather, each state "remembers" to some calculable degree (probability) the state immediately preceding it. Stated alternatively, a given event determines (stochastically) the state the sequence achieves at the next tick of the Markovian clock--i.e., the next bed (Howard, 1971). The null hypothesis tested is that the sequence is a purely random succession in which one lithotype is just as likely to occur as any other.

The test involves constructing an independent random tally matrix by multiplying row (n_i) and column (n_j) sums of the original tally matrix (n_{ij}) and dividing by the total number of entires (n). Thus, the entry e_{ij} in a given cell in the random matrix is:

$$e_{ij} = n_i n_j / n \quad , \quad n = \sum n_i = \sum n_j \ .$$

where n_i is the row sum of the original tally matrix, n_j is the column sum of that same matrix, and n is the total number of observations (i.e., the sum of all the row sums or column sums).

The following statistic is used to test for the Markov property:

$$\sum_{ij} \frac{(n_{ij} - e_{ij})^2}{e_{ij}}$$

where n_{ij} is the tally in a given cell in the original tally matrix (Collins, 1976; Schwarzacher, 1975). The statistic has a chi-square distribution with $(s - 1)^2$ degrees of freedom, where s is the number of states in the matrix (number of rows or columns). The tally matrix, random matrix, and value of the sum are shown in Figure 4-5. Since the sum exceeds the tabulated value of chi square for the α chosen, the null hypothesis of independent random events is rejected and the upward sequence shown in the likely transition diagram of Figure 4-5 is suggested as a reasonable upward lithotype transition diagram.

As the upward lithotype transition diagram shows, the directionality of this chain is toward finer, nonconglomeratic lithotypes or toward more "distal" lithotypes. It is likely then that the sequence represents a suite in which channel-filling "pushes" vertically on the lithotype succession, which "responds" by depositing more laterally "distal" deposits upward in the sequence.

This inference is corroborated by maximum thickness and maximum clast size variation upward through the outcrop (Figure 4-6). As the figure shows, the sequence exhibits strong thinning- and fining-upward tendencies and progressively more distal lithotypes.

The author interprets this outcrop as an incised fan channel in distal lower or lower-mid fan turbidities (see Figure 4-2, p. 98). The thinning and fining upward sequence so well exemplified by this outcrop may represent the subsequent filling of this incised channel. The incision of channels out on the mid or outer fan lobe is thought to indicate either a rapid lowering of sea level (with subsequent fan progradation) or a profoundly increased supply of sediment or perhaps a combination of the two (Walker, 1978). The increased supply of sediments probably points to increased tectonic activity with perhaps increased source area relief.

n_{ij}

	DIS	IN	NST	N	NON
DIS	7	5	6	8	7
IN	1	0	4	4	2
NST	0	0	3	5	4
N	0	1	2	7	5
NON	1	3	6	7	23

e_{ij}

	DIS	IN	NST	N	NON
DIS	2.68	2.68	6.24	9.22	12.19
IN	0.89	0.89	2.08	3.07	4.06
NST	0.97	0.97	2.27	3.35	4.43
N	1.22	1.22	2.84	4.19	5.54
NON	3.24	3.24	7.57	11.17	14.77

$$\sum_{ij} \frac{(n_{ij} - e_{ij})^2}{e_{ij}} = 29.81 \text{ , } 16 \text{ d.f.}$$

$$\chi^2_{(.95)}16 = 26.30$$

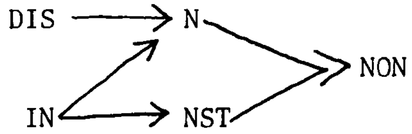

Likely transition

Figure 4.5. Tally matrix (n_{ij}), random matrix (e_{ij}), statistics, and likely transition diagram for SHDC lithotypes. The label DIS represents disorganized conglomerates; IN, inverse-to-normally graded conglomerates; NST, normally graded-stratified conglomerates; N, normally graded conglomerates; NON, nonconglomeratic lithotypes, primarily pebbly sandstones and massive sandstones.

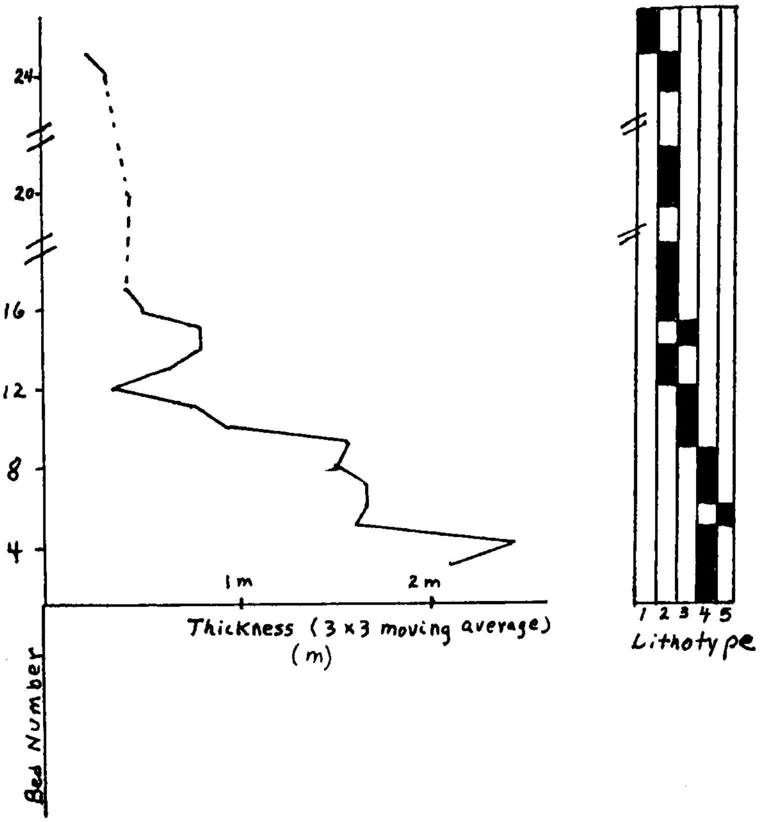

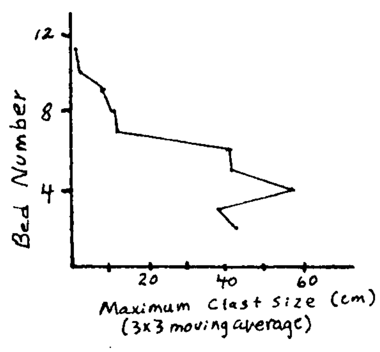

Figure 4-6. Thickness, lithotype, and clast size profile for SHDC. Bed thickness not computed for beds 29-33 which are finer silts and sands. Clast size is not computed for beds in sand-sized material. Lithotype identification is: 1 represents classical turbidites; 2, massive sandstones; 3, pebbly sandstones; 4, conglomerates; 5, matrix-supported beds.

AFC

The lithotype associations in this outcrop are conglomerates, pebbly sandstones, massive sandstones, and diamictites. Most beds are quite lenticular, and lateral coalescing of separate lenticular beds is especially characteristic of the pebbly sandstones of the outcrop.

There is no well developed sequential patterning in this outcrop. Neither bed thickness, clast size, nor lithotype succession appear to show any pronounced directionality. The outcrop itself rests on a sequence of finer, thinner-bedded sandstones and shales (turbidites). There are some thickening-upward sequences observable in this underlying material. The AFC outcrop itself apparently terminates upward rather abruptly (though this is not certain due to poor exposure) and is overlain by shale.

The evidence is not unequivocal, but the outcrop probably represents a channel fill on the mid to upper part of the suprafan. Its overall setting in a sequence of thickening-upward sandstones points to progradational development of a suprafan lobe. The incursion of coalesced, braided-channel material is not, then, a surprising or improbable upward development (see Figure 4-4, p. 103). Certainly, the associational pattern of relatively coarser material, as well as the highly lenticular though relatively shallow and unleveed channels, points toward a locale of deposition most likely situated in the inner suprafan location.

The suddenness of the deposition of coarse material in this outcrop without the development of the sequential features associated with gradual abandonment may indicate a sudden breach or switch in a feeder channel further up current from the beds of this outcrop. Relatively fine suspension-deposited material blankets the channel and caps it abruptly with shale.

USHDS

The lithotype associations for this outcrop are fine-pebbly sandstones, massive sandstones, classical turbidites, and slump-to-debris flow deposits. Beds are slightly to quite lenticular, and fine shale deposits are generally absent. The sequential association of lithotypes and a smoothed thickness curve (5 × 5 moving average) are shown in Figure 4-7. There seems to be an overall thickening- and coarsening-upward followed by an overall thinning- and fining-upward. The pebbly sandstone lithotype seems to be somewhat more important in the central portions of the sequence. Massive sandstones occur both above and below the pebbly sandstone interval. Turbidites become much more abundant toward the top of the section.

In light of these trends, the outcrop may represent a progradational upper fan lobe sequence followed by a recessional or gradual channel filling and abandonment suite. It is probable that smaller scale cycles are present in the outcrop, but their definition is difficult in deposits such as these where amalgamation and channeling obscure the thickness relationships.

Whether overall directional regularity is convincingly illustrated by this outcrop or not, the extreme top-absent character of the massive

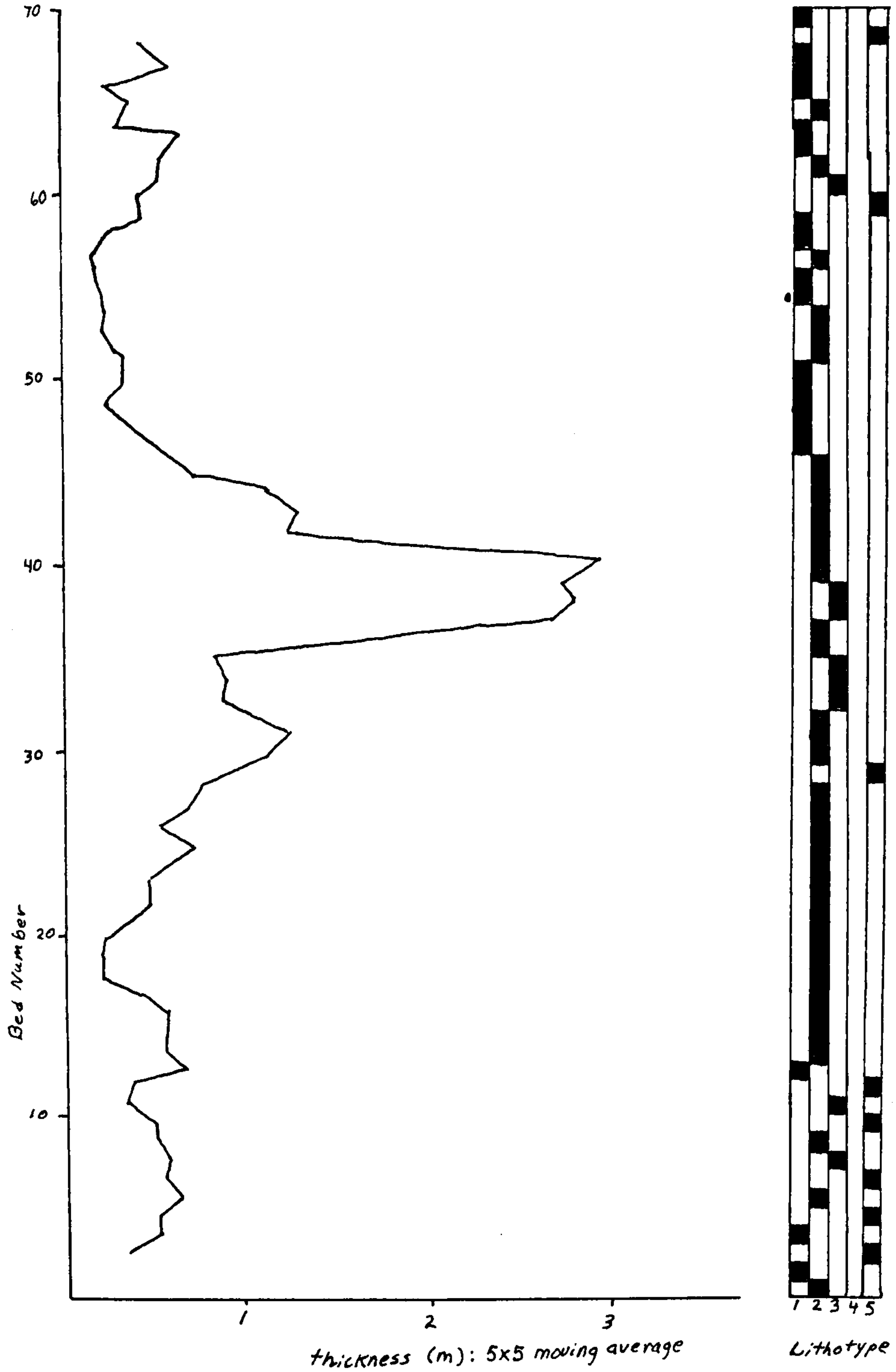

Figure 4-7. Thickness and lithotype profile for USHDS. Lithotype identification is: 1 represents classical turbidites; 2, massive sandstones; 3, pebbly sandstones; 4, conglomerates; 5, matrix-supported beds.

sandstones, the poorly sorted, relatively coarse clast size of some beds, and the lenticularity of the beds all indicate a fairly proximal, channelized upper mid-fan environment of deposition.

LLCD and ULCD

These two outcrops are puzzling. Their association is with thin-bedded turbidites and rare massive sandstone beds. The deposits themselves, however, contain boulder-sized material, slumped beds, and the homogeneous, poorly sorted muddy sand "diamictite." Associationally, then there is a perplexing juxtaposition of "proximal" with "distal" deposits.

Stratigraphically, the Lucy Creek outcrops are near the top of the preserved Middle Ordovician clastic section in this area (King and Ferguson, 1960). The remaining section--and much of the middle portion of the section beneath the Lucy Creek outcrops--is relatively monotonous "distal" turbidite deposits. The general picture, then, is of a relatively more distal regime than, for example, the regime that deposited the conglomerates at the base of the section (SHDC).

This "distality" may indicate a variety of things: lowered supply of sediment, rise in ocean level, switch in major fan distributaries, further subsidence of the basin. If the feeder channels that supplied sediment to the basin were cut off from their main sediment supply by, say, a relative rise in sea level, activity in them would be considerably reduced but perhaps not completely ended.

Stanley (1974) has described a modern channel cutoff from major sediment supply by the post-Pleistocene rise in sea level. Pebbly mud and slumped turbidite units, however, continue to be slowly transported by the debris flow mechanism down the channel in something of a steady-state process (see Chapter 3). Slumping of poorly consolidated material at the channel head supplies coarse sediment to the channel that may have been originally deposited by fluvial processes during a low stand (Stanely and Unrug, 1972).

It may be, then, that the lenticular beds at Lucy Creek are deposits in channels in which major transport by "energetic" processes (e.g., turbidity currents) was no longer occurring. The pebbly mudstone, intraformationally derived slumped deposits, and fine, distal turbidites indicate that the main sources of fresh, coarse material may have, for one reason or the other, been cut off from this area of the basin.

LSHDS

The associational lithotypes of this outcrop are nearly all turbidites. A few slump and possible fine-grained debris flow deposits make up the balance. The sequential regularities are not always pronounced, but there are some thinning-upward sequences in the outcrop. The thinning-upward sequences represent, perhaps, the filling of shallow middle fan channels and the (apparently) trendless or ambiguous sections may represent overbank deposition from some other closely adjacent channel. Prominent shale sequences both at the top of the section and at beds B-280-374 perhaps represent the abandonment of a particular depositional lobe and the dominance of fine, unchannelized deposits (see Figure 4-3, p. 101).

There is a marked packaging of turbidite types in this outcrop. The upward transition matrix was tested and found to exhibit the Markov property (Figure 4-8). (A different statistic was used to test the matrix since it has no 0 entries. It is chi-square distributed and the results are interpretable in exactly the same way in which Markov test results were interpreted earlier.) As the figure shows, the lithologies have a nonrandom sequential regularity. However, the fact that beds beginning with the A interval are associated typically with other beds beginning with the A interval is not unique in either type of thickness cycle that might be present. Such an association could occur in thickening as well as thinning up sequences. The matrix does not differentiate between these cases.

In Figure 4-9 a plot of beds LSHDS-A-59 to LSHDS B-20 is shown. While the cycles are not always strictly definable as to their beginning and ending, it is clear that the more pronounced cycles are developed as thinning-upward cycles. A thick bed induces on the sequence a strong likelihood that the next deposit will be relatively thinner. Such sequences are typically found on suprafan lobes as a result of channel filling (Ricci-Luchi, 1975).

Relationships among Outcrops

The question which invariably arises in the study of submarine fan deposits is whether the deposits represent more than one fan, more than one lobe, and so forth. To answer this question rigorously would involve

	A	C + B	D
A	92	17	44
C + B	13	14	17
D	51	18	288

n_{ij}

	A	C + B	D
A	0.59	0.11	0.30
C + B	0.28	0.30	0.41
D	0.14	0.05	0.81
p_j	0.28	0.09	0.63

p_{ij}

A D

C

$$-2 \log_e \lambda = 68.22 \text{ , 4 d.f.}$$

$$\chi^2_{(95)}(4) = 9.487$$

Figure 4-8. Tally matrix (n_{ij}), probability matrix (p_{ij}), statistics, and likely transition diagram for LSHDS turbidite types.

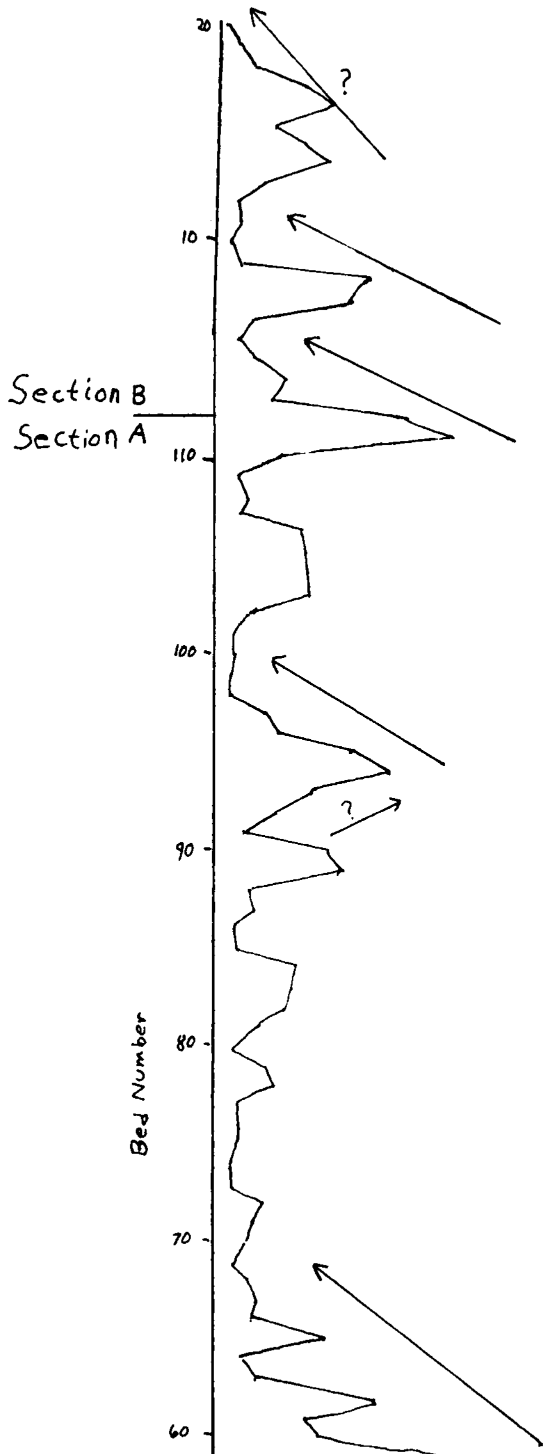

Figure 4-9. Plot of bed thickness against bed number: LSHDS-A-59 to LSHDS-B-20. The arrows indicate possible cycles in the sequence, primarily thinning-upward cycles.

detailed areal geology and careful study of paleocurrent dispersal patterns. This was not attempted in this study. A limited body of data, however, does suggest some likely relationships among the outcrops of the study area.

Paleocurrent information from LSHDS (ripple crests) indicates that currents originated in the southeast and flowed consistently toward the northwest with a mean current vector of 338.4° ($r = 0.9727$). The current rose and associated statistics are shown in Figure 4-10. Earlier reconnaissance work at SHDC used the orientation of pebbles in an imbricated bed to determine a trend in which the pebbles had a roughly southeast to northwest orientation. The conglomerates (SHDC) and the sands overlying them (LSHDS) then appear to have been deposited from a current moving from a south-southeast direction.

USHDS contains very limited paleocurrent information. Grooves on one bed and flutes on another indicate that the depositing current flowed toward the northeast (approximately 040°). The slumped bed (USHDS-69) slumped toward the southwest (227°). In light of the other directional data, it may be that this bed folded toward the axis of the channel (southwest current origin) rather than down general paleoslope. The interpretation of paleoslopes from slump fold orientations is problematic (Lajoie, 1972; Woodcock, 1976).

A study of one imbricated pebbly sandstone sample disclosed a mean vector orientation of 261° for pebble long axes (100 observations). The current rose and statistics are shown in Figure 4-11. The outcrop AFC differs compositionally from SHDC (Leible, 1975). It is richer in

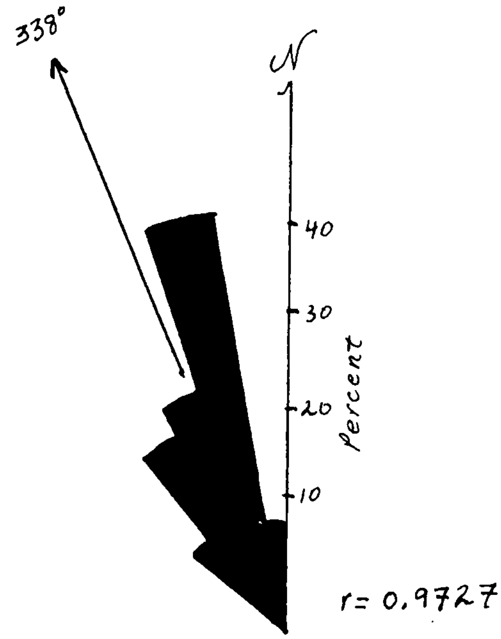

Figure 4-10. Current rose for LSHDS. Data measured on ripple crests. Grand current vector and index of dispersion (r) calculated by formulas in Rao and Sengupta (1972).

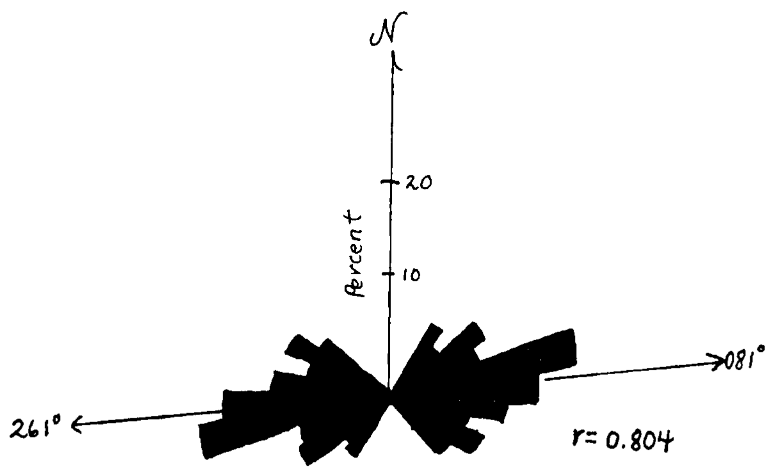

Figure 4-11. Pebble orientations from AFC. Mean orientation is 261°. Since the pebbles dip eastward, the current was probably from that direction.

quartz. In general, the deposits to the northeast of the study area become increasingly dominated by quartz (Kellberg and Grant, 1956).

Finally, 6 slump fold axes from Lucy Creek indicate a paleostrike of 060°.

Based on the available information, no definitive conclusions can be drawn about the number of fan systems in the area. However, the author tentatively suggests that SHDC, LSHDC, and USHDS are deposits from a single fan, with the directional divergence of USHDS paleocurrents being the result of deposition in a different lobe. A radial paleoccurent pattern is expected in submarine fan systems so the divergence certainly does not prove the existence of a different fan.

AFC may indeed be part of a different fan. The differences in paleocurrents and compositions would suggest that AFC sediments were derived from a different source and direction (different feeder channels?). However, again, composition may change through time in a single fan system.

LLCD and ULCD bear an unknown relationship to the other outcrops. They are "proximal" but if the interpretation of them (Chapter 3) is correct, they may represent abandoned channels in the upper mid fan or inner fan. Also, they may not even be part of a fan system but may be slumps off the slope itself. Their paleoorientation features suggest at least an agreement with SHDC-LSHDS paleoslope indication, but, stratigraphically, they are not equivalent. Whether they represent the same fan at a later time, a different fan, or a different base-of-slope environment cannot be determined from the present evidence.

Summary

The deposits in the study area are thought to represent various subdivisions of a submarine fan(s). The associational and sequential packaging of the outcrops suggests likely fan positions for the various outcrops.

On a broad scale, the incision of channels into "distal" deposits, the coarseness of clasts, the presence of thick units of disorganized conglomerate indicate initial greatly accelerated fan sediment supply (progradational regime). The gradual fining and thinning of beds upward, especially at SHDC-LSHDS, suggest a gradual maturing of the fan in the region and points to a recessional regime in this particular basinal locale.

CHAPTER 5

THE PROBLEMS OF COARSE CLASTIC CLASSIFICATION AND FACTOR ANALYSIS

Introduction

In the foregoing chapters, Walker's (1978) classification system has been used. It, like several other classification schemes (Mutti and Ricci-Luchi, 1972; Walker and Mutti, 1973; Aalto, 1975), uses clast size as the primary individuating property for the lithotypes ("facies") that are recognized. Lithotypes are then subdivided on the basis of the presence or absence of certain types of grading, stratification, and other features. Conceptual as well as practical problems arise, though, in comparing different rock types in the study area with the categories recognized in the several proposed models. These are treated below.

The Problems of Classification

The real value of lithotype classifications based on clast size is not so much in their descriptive adequacy but in the environmental significance of the individual categories. Beds with coarser clasts should ideally indicate a more proximal location than those with smaller clasts. Thus, clast-size based categories have a progressively more basinward significance with decreasing grain size. For example, conglomerates and matrix supported beds--pebbly sandstones--massive sandstones--classical turbidites represents the "ideal" proximal-distal transition among the categories of Walker's (1978) classification. Though somewhat simplified as a model of basin deposition, in a broad sense this progression is probably correct.

Associated with these beds are many properties (see Chapter 2) other than grain size. These properties are indicative of certain hydrodynamic processes operative in the emplacement of a particular bed. Some of the properties are particularly well exemplified in certain grain-sized material. To the above mentioned workers, this suggests an ideal model of basinward progression of clast size lithotypes with certain process (hence certain bed properties) inherent only in a particular type. Indeed, Walker (1975) postulates that the sequence inverse grading--normal grading--normal grading with stratification represents a basinward progression of features as well as clast sizes. The danger here is that the apparent connection between clast size and inferred depositional conditions is allowed to become normative and seems to rule out *a priori* the occurrence of diagnostic properties such as inverse grading or imbrication in lithotypes of several different clast sizes. For example, Walker and Mutti (1973) claim that inverse grading and imbrication cannot occur in material finer than cobble conglomerate, recognizing them only in their coarse "facies." They rule out the possibility that properties usually associated with coarse material can also be found in finer material, because it does not fit the idealized model of basinward progression. That is, descriptive lithotypes are force fitted into a genetic interpretation of proximality-distality. Ultimately, the misguided usage of the term "facies" for lithotypes probably also stems from this type of reasoning. Since certain lithotypes (and their inferred depositional processes) are considered to coincide with a certain range of distances from source, then, by the above it follows that their presence in a sequence automatically indicates a particular depositional site in a submarine-fan system--a particular sedimentary environment ("facies").

A major problem with the above approach is that many beds contain suites of properties that do not allow their practical or satisfying inclusion within established lithotypes. For example, USHDS-1 has inverse grading in medium-grained sand; AFC-43 shows imbrication in fine pebbles; AFC-12 has well-developed stratification in sand-sized material; LSHDS-B-168 appears to be a matrix-supported sandstone in an otherwise "distal" environment of classical turbidites. In none of these examples do the beds have the properties that they are "supposed" to have given their grain size. Thus, it is conceptually and empirically more appropriate to admit that similar physical mechanisms can operate within reason upon different sized materials. The common association of clast size and certain types of structures may stem from some underlying constraint that favors both rather than some quasi-causal connection between the two. For example, grain flow and thick matrix-supported beds are usually associated with steeper slopes (larger clasts being the result of a more proximal environment); fluid turbulence is usually the only mechanism operative on gentler terrains (smaller grain sizes being the result of a more distal environment). The real "causes" in this case are gradient and proximity to sediment source. Hydrodynamic mechanism and grain size are neither the cause of the other but are simply a reflection of a common association due to a common underlying control. It is thus not permissible to rigidly afix the properties of flows to a certain grain size.

While a classification of coarse-clastics based on grain size is certainly of undisputed merit in environmental reconstruction, it is probably not adequate for other usages. If the goal of classifying is the understanding and delineation of the factors that control the observed properties of the sediments, then perhaps another scheme or approach would be more direct and more adequate. The following analysis explores those factors that are reflected by some of the properties of the beds of the coarse clastic family.

Factor Analysis

The mathematical techniques of factor analysis were first proposed by the renowned statistician, Pearson (1901), and have been developed primarily by psychologists who were interested in certain underlying mental factors that might explain a broad range of human behavior. Geologists, for the most part, have not used this method of structuring data (but, see Imbrie and Purdy, 1962, and Joreskog et al., 1976) so that some comment on the principles and significance of the analysis is necessary. The details of this method are accessible in any of several standard references (for example, Harman, 1967; Joreskog et al., 1976; Rummel, 1970), of which Rummel's work is probably the best overall introduction and forms the basis for much of the following discussion.

General Principles

In geology, as well as other sciences, the data are often multivariate. Factor analysis relates observations and measurements on features to a few distinct patterns of occurrence. In terms of recognizing the underlying factors reflected by the bed properties of this study, there are two approaches.

One way is to look at variation among beds. Beds would thus be grouped on the basis of certain characteristics that best explain or account for their variance. This is known as Q-mode factor analysis. The second way of looking for regularity in the data is by examining the patterns of variation of the properties. For example, in the author's data, beds with greater thickness usually contain coarser clasts and tend not to be normally graded. There seems to be a regularity in these characteristics that picks out a particular pattern of variation in coarse clastic sediments. The type of factor analysis that discloses interrelationships between properties is known as R-mode analysis.

In the factor analysis performed for this study, five major kinds of regularity are revealed by R-mode analysis of 17 properties. Q-mode factor analysis of 99 beds reveals three underlying regularities that account for most of the information in the raw data.

In practice, there is more than one factor model. Each has advantages and disadvantages (see Rummel, 1970, for a discussion of these different styles of factoring). All these models, however, have some important general features in common which make them all methods of factor analysis. This commonality can be approached from two different (though actually identical) standpoints: a geometric approach and an algebraic approach.

Geometric approach. The geometric interpretation of factor analysis provides an intuitive access to its procedures. Let us consider, for example, three beds. Each bed can be thought of as defining a coordinate axis of a geometric space. The three beds (numbers 54, 55, and 56) define a three dimensional space, as shown in Figure 5-1. We can extend this construction analytically to any number of dimensions. For example, 99 beds are studied in this work; thus, for R-mode analysis 99 dimensions were required for the complete representation of the data. (Q-mode analysis would require 17 because there are 17 properties. The discussion that follows uses R-mode analysis as an example. However, Q-mode is understood in exactly the same way, though with properties substituted for beds, and beds for properties.)

In the space so defined, each property can be considered as a point whose location depends upon its value for each bed. In the figure, the author has shown the values of thickness and maximum grain size for each of the beds (a standardized coordinate system is, of course, necessary to plot these two properties whose parameters differ). Now, if we take each point and draw a line to it from the origin, as shown in the figure, we have a *vector* representation of the data. If we could pictorially represent the data (17 properties) for the 99 beds, then the 17 property vectors would define a vector space in the 99 dimensions of the data for R-mode analysis. The angle between any 2 of these vectors is a

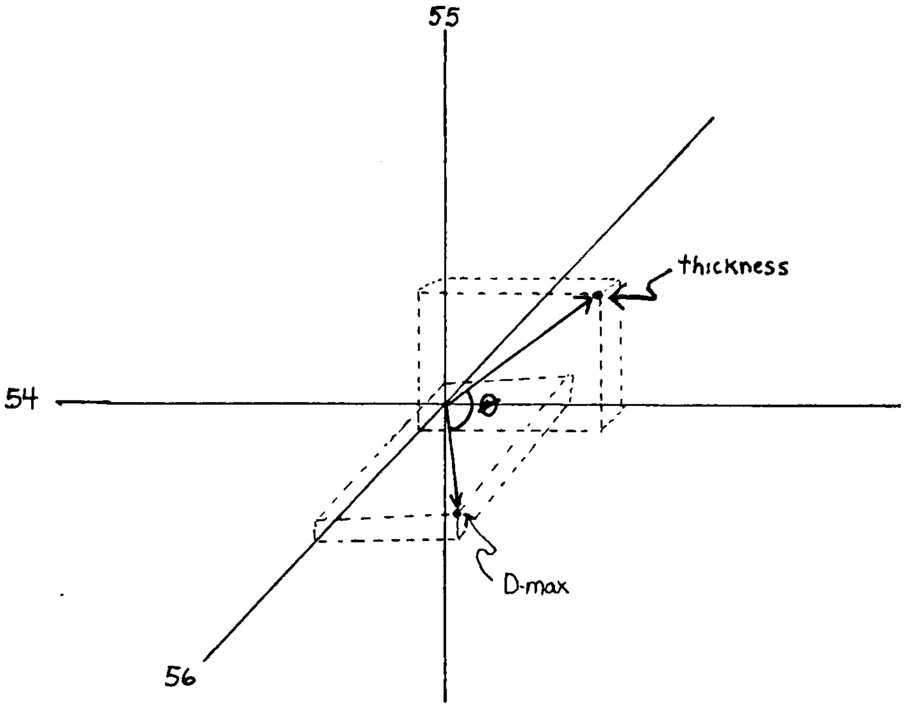

Figure 5.1. Properties plotted as vectors in the space defined by beds 54, 55, and 56. The angle measures the correlation between the two properties of thickness and Dmax.

measurement of the relationship between the two properties. This angular relationship turns out, with minor adjustment, to be nothing more than the correlation coefficient, r, which may be expressed as

$$r_{ij} = \cos \theta$$

where θ is the angle between the two vectors (see McCammon, 1969; Klovan, 1975). The properties with a low angular separation are highly correlated; those with angles of 90° are uncorrelated; and, those with obtuse separations are inversely correlated. At the extreme, an angle of 180° between the two vectors means that the two properties vary in a perfectly inverse fashion.

If we project the 17 property vectors in the 99 dimensional space, the configuration of vectors, then, will reflect the interrelationships (correlations) in the data. Characteristics that are highly correlated (low angular separations) will cluster close together; characteristics that are unrelated will be at right angles to each other; characteristics that are inversely related will have obtuse angular spacings (or negative r values). These clusters represent the underlying patterns within the data.

A factor is simply an axis that is projected through a cluster's center of gravity. The normal projections of each vector point onto the factor axes are called "loadings" and give the degree of involvement of a given variable in the particular cluster defined by the axis. They can be interpreted as correlation coefficients. The square of the loading multiplied by 100 equals the percent of the variation that a variable has in common with a common factor.

Algebraic approach. The bed properties treated in R-mode analysis can also be presented algebraically by:

$$X_1 = \alpha_{11}F_1 + \alpha_{12}F_2 + \ldots + \alpha_{1m}F_m$$

$$X_2 = \alpha_{21}F_2 + \alpha_{22}F_2 + \ldots + \alpha_{2m}F_m$$

$$\vdots \quad \vdots \qquad \vdots \qquad\qquad \vdots$$

$$X_n = \alpha_{n1}F_1 + \alpha_{n2}F_2 + \ldots + \alpha_{nm}F_m$$

where X_i are the variables (properties in R-mode--e.g., the set of thicknesses of all beds, the set of mean grain sizes of the beds, etc.), α is a loading that measures the degree to which each variable is explainable by a particular factor F_i. We assume that any property X_i is explainable by a linear combination of functions (which themselves may not necessarily be linear) that can be divided into several formal causes (common factors) and the "material" cause (the source of the uniqueness of the property). We also assume in all cases that the unique element is orthogonal (not correlated) to all common, formal factors and other unique factors. Thus the variable X_i may be expressed as

$$X_i = \underbrace{\alpha_{i1}F_1 + \alpha_{i2}F_2 + \ldots + \alpha_{ip}F_p}_{\text{COMMON FACTORS}} + \underbrace{\alpha_{iu}F_{iu}}_{\text{UNIQUE FACTOR}} .$$

In general we know the values for all X_i but do not know the parameters on the right-hand side of the equation. Factor analysis determines the unknown functions (F_{ij}) related to a common variance pattern of the properties (variables).

Data Analysis

This study treats 17 bed properties recognized in 99 coarse clastic beds of the study area. The specific procedures and methods of factor analysis and most of the tables associated with this analysis are contained in Appendix B. A list of abbreviations of the properties treated is also contained in this Appendix. The following discussion treats the choice of variables in the analyses (R-mode and Q-mode).

The beds chosen for analysis represent a cross section of coarse-clastic types. In Walker's (1978) terms these include 27 classical turbidites (or 28 if bed 97 is counted as a turbidite), 26 massive sandstone beds, 8 pebbly sandstone beds, 20 clast-supported conglomerates, and 17 matrix-supported or slumped beds (18 if bed 97 is counted with this group). Seventeen properties thought to be of most importance were considered for each bed. The properties chosen were numerical, dichotomous and ordinal. Bed thickness, D-max, D/10, and mean size of clasts are the numerical properties. In the case of turbidites, the mean is the estimate of the grain size from the graded or massive sand division. For the conglomerates, the mean is roughly D/50. Since there is such a great range of clast sizes, approximation does not materially affect the correlation coefficients derived from the figures. The dichotomous properties are: massiveness, normal distribution grading, coarse-fraction grading, inverse-to-normal grading, stratification, matrix support, lower flow regime features (e.g., ripple cross laminations, well-developed shale upper transition), and alignment of clasts (especially partially preserved beds parallel to bedding). Presence of the property was assigned a value of 1; absence was assigned a value of 0. Imbrication is also an important dichotomous property, but its ascertainment on the outcrop is so contingent upon the face exposed and on grain size that no definite meaning can be given to the failure to observe it. Consequently, it was omitted from the analysis. Ordinal properties are bed lenticularity, sorting, erosive evidences at the base of the bed, induration, and presence of previously formed and partially preserved beds *within* the bed in question (e.g., slumps and debris flows). The values 0, 1, and 2 were assigned to absence, some presence, and pronounced presence, respectively. For example, tabular beds received a 0 for lenticularity; beds receiving a 1 were those that showed thickness changes at the scale of the outcrop; beds receiving a 2 were those which have definite channel geometry and often pinched out entirely at the outcrop.

The assignment of dichotomous and ordinal values to properties always results in debatable assignments. It would not be likely that any two investigators would agree in every case. However, considering the large amount of data, questionable assignments in one category or the other probably do not have a great effect of the final results. Slight imprecision, rough assignments, and broad approximations lose weight in the final solution because it is *sets* of properties and *sets* of beds that are to be factored. The data as so scaled are contained in Appendix B.

Results of Analysis

R-mode: Graphical results of R-mode analysis are presented in Figures 5-2, 5-3, 5-4, and 5-5. Five factors were determined to account for the variation between properties. Examination of these graphical plots of loadings on their respective factor axes (rotated) suggests that the first factor is probably best thought of as a transport mechanism factor. On the negative axis are properties such as matrix-support, partially preserved beds, and other features normally associated with slumps or debris flows. The properties of sorting, erosiveness, and normal grading load highest (are most strongly correlated with) the positive end of this factor axis. These are all features which are best exhibited in deposits which are thought to result from the unimpeded movement of individual clasts in turbulent flows. Properties which are relatively indifferent to this factor are grain- and bed-size parameters, stratification, and inverse-to-normal grading. It is reasonable, then, to interpret the first factor as primarily a flow mechanism factor. For shorthand, this factor will be named for its positive pole as the "turbulence factor."

Factor two is easily interpretable as a dimensional factor: clast size parameters load especially heavily on it. Thickness, too, is strongly related to this factor. Most other properties are relatively

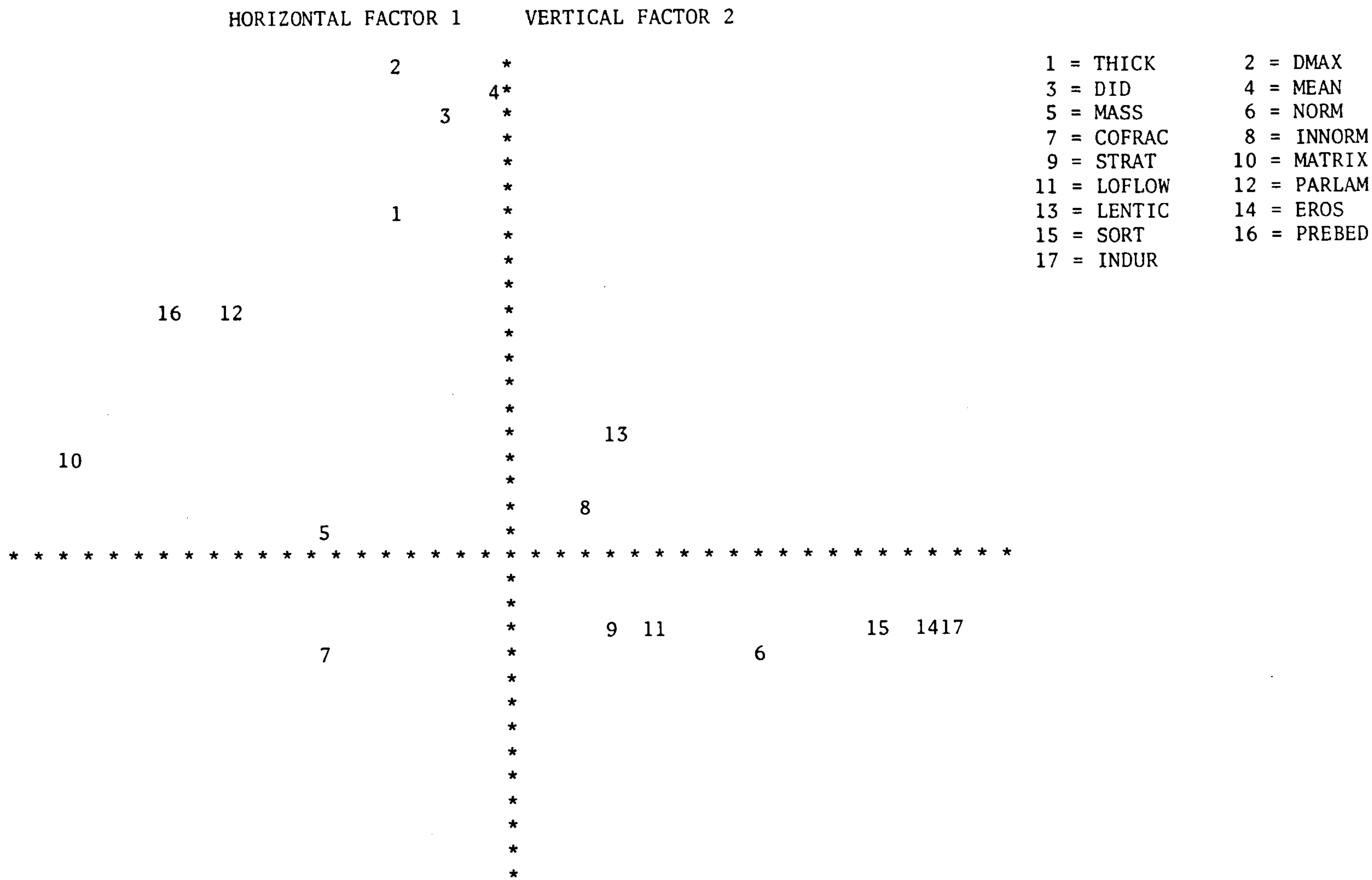

Figure 5-2. Factor loadings for factors 1 and 2 of the R-mode analysis.

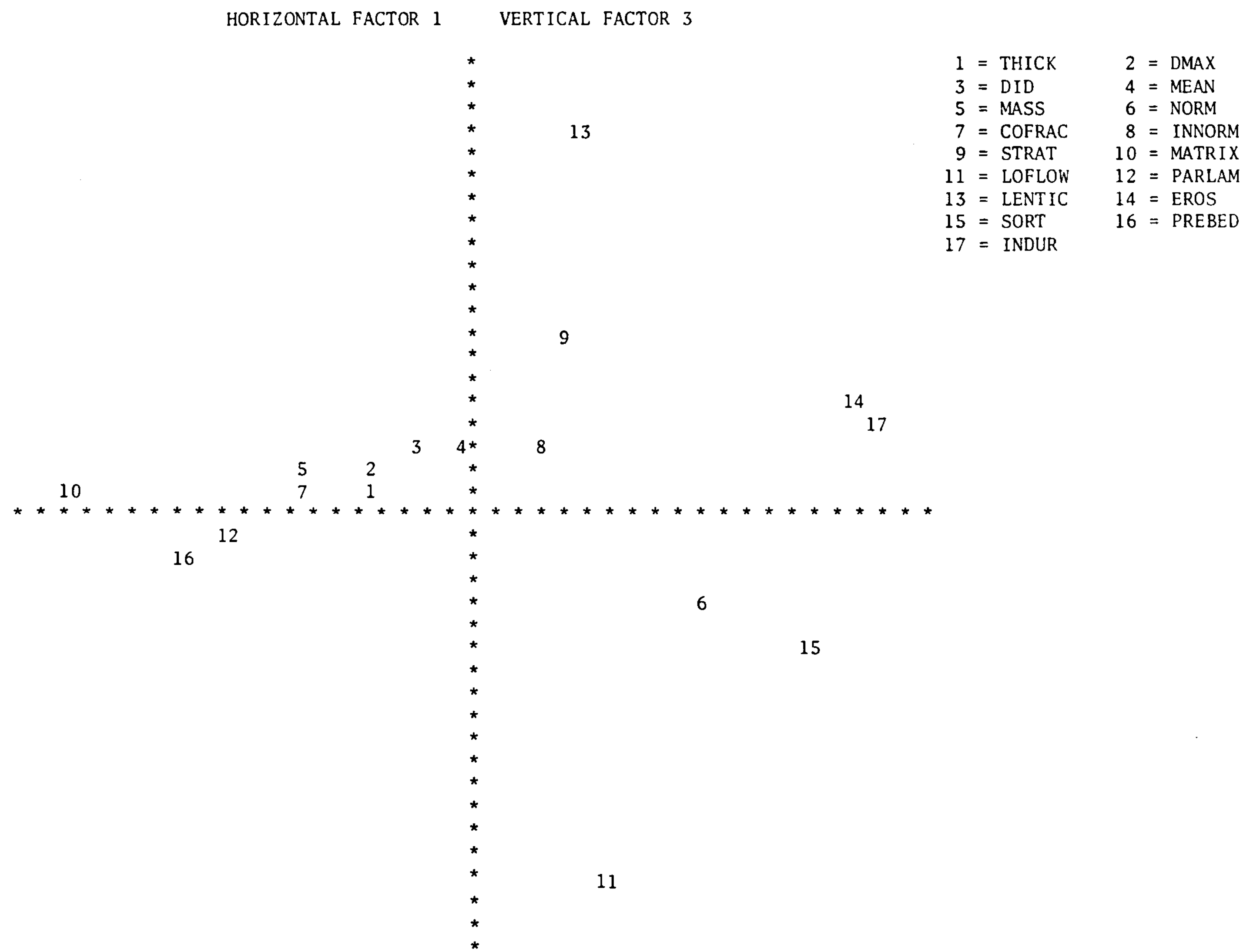

Figure 5-3. Factor loadings for factors 1 and 3 of the R-mode analysis.

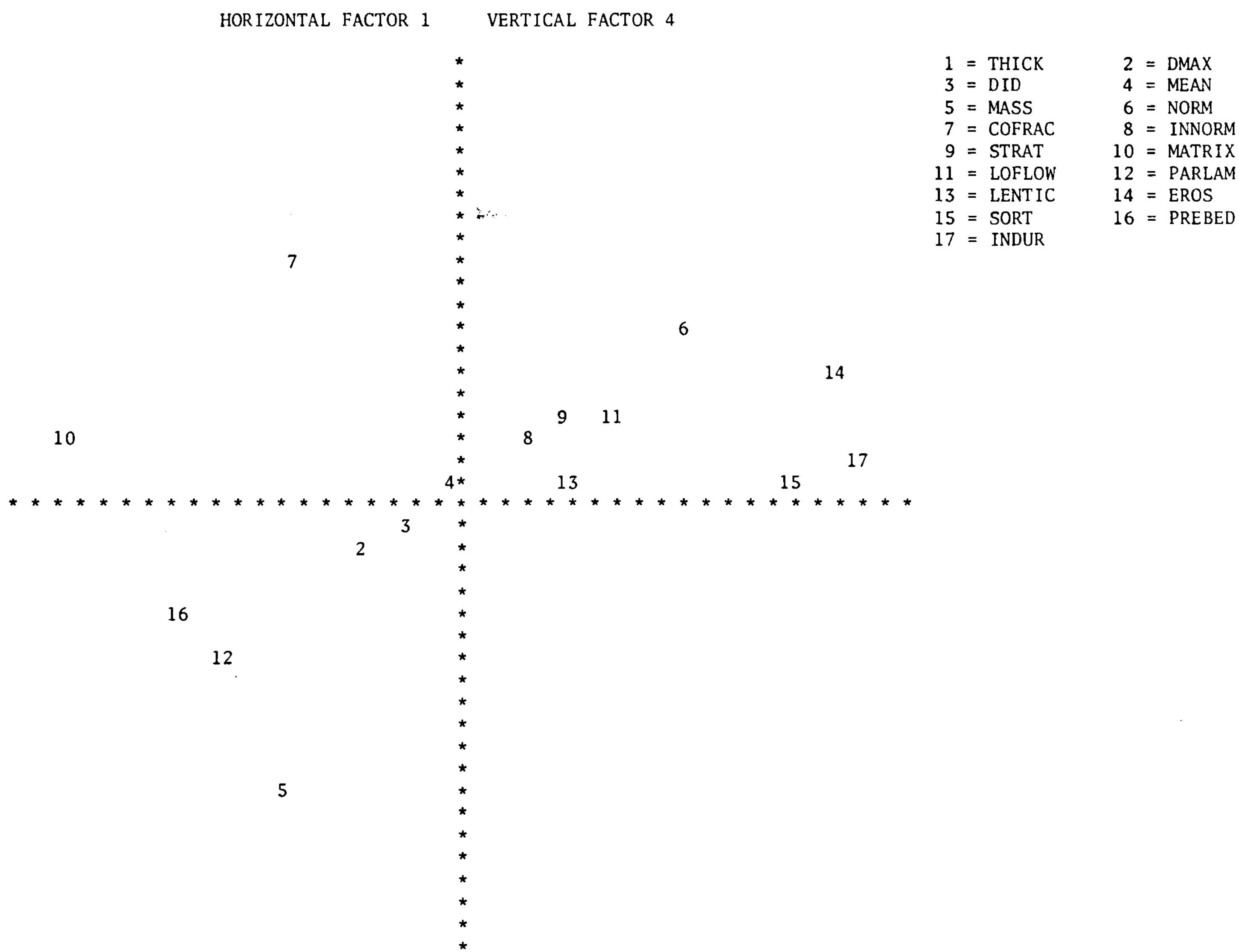

Figure 5.4. Factor loadings for factors 1 and 4 of the R-mode analysis.

HORIZONTAL FACTOR 1 VERTICAL FACTOR 5

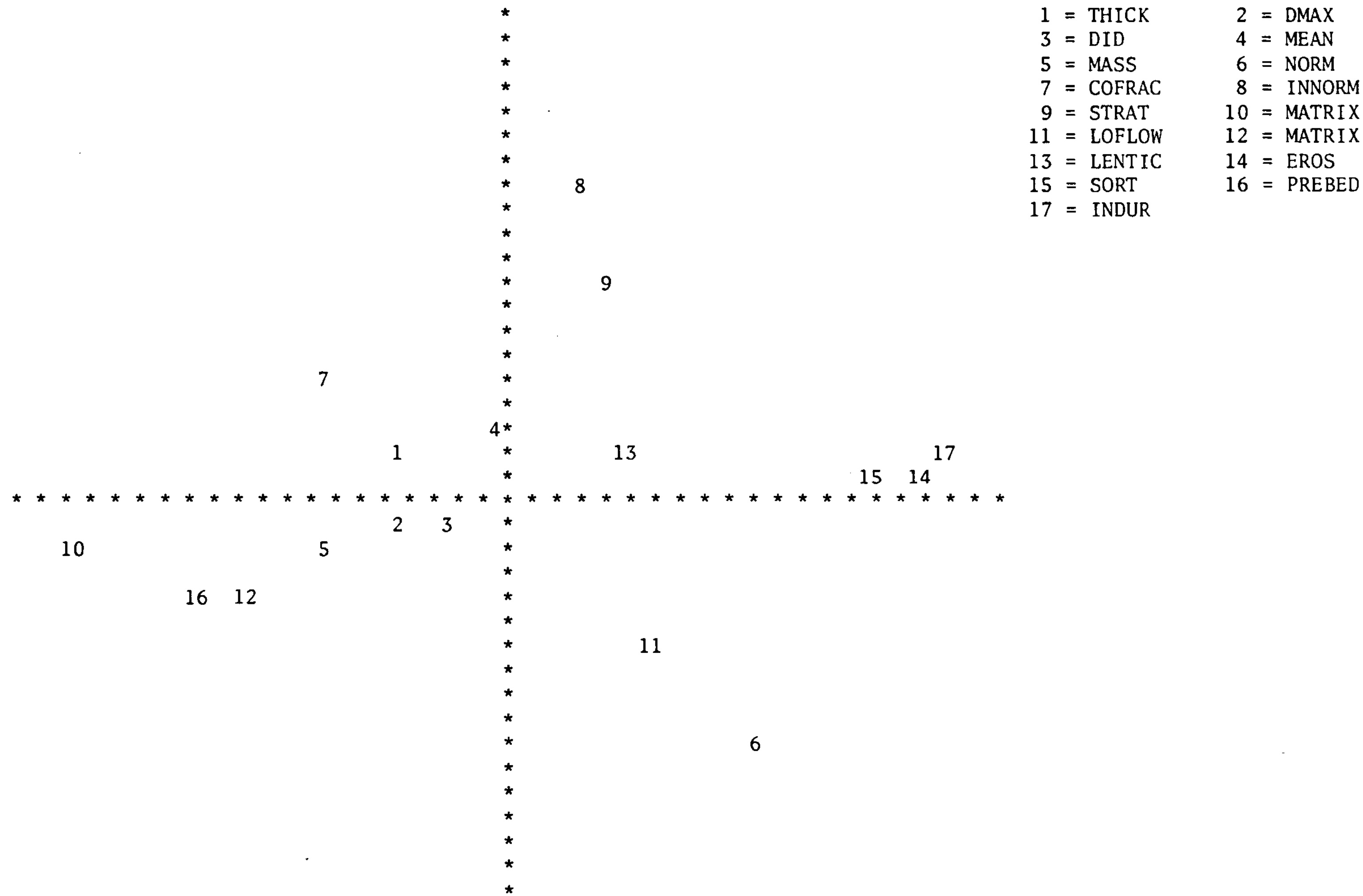

Factor 5-5. Factor loadings for factors 1 and 5 of the R-mode analysis.

indifferent to this factor. For example, normal grading can be exhibited either in coarse or in fine sediments; consequently, it is somewhat indifferent to a clast size factor. (It would be this factor that most traditional coarse clastic classification schemes would stress.) For short, factor two is called the "scale factor."

Factor three loads heaviest on lenticularity and negatively on low-flow regime features. If we consider that low-flow regime features are usually exhibited only in classical turbidites (i.e., more tabular bodies), then it appears that this factor is a reflection of the relative degree of channelization or lack thereof in coarse clastics. Observationally, it is a shape factor. It will be labeled the "bed shape factor." Environmentally, this factor might have significance as to proximal (=channelized, lenticular beds) versus distal (=tabular beds) identification.

Factor four is quite perplexing. Massive texture loads negatively and coarse-fraction grading positively on this factor. What the factor is measuring is not clear. Perhaps, it is related to rapidity of deposition and/or general grain dispersion which results in textural inhomogeneity in coarse-fraction versus massive beds. The author simply labels it as the "time-competency factor" with *no* implications other than those expressed in the loadings on this factor.

Factor five is loaded most heavily by inverse-to-normal grading, so the temptation is to simply call it the "grain flow factor." It should be noted, however, that coarse-fraction grading and stratification are also important positive loaders and low-flow regime features and normal grading are important negatively. It may be, then, that this factor measures (in some fashion) the variance in bed features imposed by concentrated as opposed to dilute suspensions. (If this is correct, does then stratification arise only or preferentially in concentrated dispersions? If so, then factor analysis may have uncovered an important fact concerning this puzzling feature.) Grain flow is one manifestation of physical process which is contingent upon concentration. But, concentration though a necessary condition for grain flow may not be a sufficient condition. Consequently, the author does not think that the variance structure of factor five can support the theoretical burden of being categorized as the grain flow factor *simpliciter*. Rather, for short, this factor is called the "clast concentration factor" with the realization that grain-flow features are probably strongly loaded onto it.

Significance of the R-mode analysis. As in any factor analysis the simple reduction of data to underlying factors is quite significant and some factor analyses terminate simply with this reduction. Indeed, it is significant that only five factors are needed to characterize most of the common variance of the bed properties. Instead of 17 independent variables whose relationships with each other are unknown, the factor analysis has produced 5 independent "variables" which are known to be uncorrelated with each other and which taken together provide an adequate summary of most of the information contained in the original 17. An important aim of scientific investigation, that of producing simpler analytic and interpretive structures, has thereby been accomplished.

What is more important in light of the present work, however, is that a characterization of beds in terms of clast size emphasizes only *one* of the factors--and not the most important one at that. Properties such as matrix support, grading style, bed shape, and erosiveness are *not* significantly loaded on (explained by) this factor. Their covariance with parametric measures is quite low. Consequently, the strong emphasis on clast size alone as the primary differentiating property is misleading. Many important properties of coarse clastic beds are not strongly related to the second factor. It would seem that a classification based upon properties of clast size is not optimal in its explanation of actual variance in the beds (surely, this is at the heart of what a classification should do).

Does this mean that earlier classifications should be abandoned? Certainly not--they have proven their utility in environmental interpretation. Restructured? Yes.

The author would suggest that in the case of Walker's (1978) classification, the category of matrix-supported beds be raised from that of being just one of five divisions to one of two fundamental end members in a coarse clastic dichotomy of matrix-supported as opposed to clast-supported beds (these are the best field properties for gaging the effects of factor one). *Then,* given this fundamental division, factor 2 (clast size, thickness) can be used to make subdivisions within these two general categories. Walker's divisions of pebbly-sandstone, massive sandstone, and clast-supported conglomerates would be obvious approximations to these clast-sized based subdivisions. Further refinements could be made on the basis of the other three factors.

Q-mode. The Q-mode analysis results are quite peculiar. Graphical plots of the three factors determined by this mode are shown in Figures 5-6 through 5-11. It is clear that the loadings on factors 2 and 3 are related to those on factor one by some regular quadratic relationship. This is odd since factors are defined to be unrelated.

Hill (1974) has shown algebraically how plots come about in which the loadings on one axis effectively fix the value for the other axes. They are primarily the result of very high correlations between variables (as was the case for the beds included in this analysis). The author will not summarize his very abstract and difficult arguments here. Conceptually, the results are interpretable in understandable terminology as a method of bed ordination.

Ecologists, archaeologists, philologists, and other assorted specialists have made use of these statistically odd plots in a very novel way (see Hill, 1974, for references to these various disciplines). A plot such as that found in the Q-mode results is used as ordinate, seriate, grade or otherwise rank objects as to their placement in some sort of order impressed upon them by some overriding cause (factor). For example, archaeologists have found that by carefully enumerating pottery types in graves, the oldest grave will appear at one end of a roughly horseshoe-shaped plot and the most recent grave will appear at

```
                      HORIZONTAL FACTOR 1     VERTICAL FACTOR 2

                                          *      26  44                                   1 = BED1      2 = BED3
                                          *46        273821                               3 = BED5      4 = BED7
                                          *            37                                 5 = BED9      6 = BED11
                                          *          30      20          50               7 = BED13     8 = BED15
                                          *                    40                         9 = BED17    10 = BED19
                                          *                      19     3                11 = BED21    12 = BED23
                                          *                                              13 = BED25    14 = BED27
                                          *                                              15 = BED29    16 = BED31
                                          *                            36                17 = BED33    18 = BED35
                                          *                                              19 = BED37    20 = BED39
                                          *                                              21 = BED41    22 = BED43
                                          *                                  18          23 = BED45    24 = BED47
                                          *                                    31        25 = BED49    26 = BED51
                                          *                                              27 = BED53    28 = BED55
                                          *                                    43        29 = BED57    30 = BED59
                                          *                                    41        31 = BED61    32 = BED59
                                          *                                    47        33 = BED65    34 = BED67
                                          *                                    1342      35 = BED69    36 = BED71
                                          *                                    4948      37 = BED73    38 = BED75
                                          *                                              39 = BED77    40 = BED79
* * * * * * * * * * * * * * * * * * * * * * * * * * * * * * * * * * * * * * * * * *      41 = BED81    42 = BED83
                                                                                         43 = BED85    44 = BED87
                                                                                         45 = BED89    46 = BED91
                                                                                         47 = BED93    48 = BED95
```

Figure 5-6. Factor loadings for factors 1 and 2 of the Q-mode analysis for odd-numbered beds.

```
HORIZONTAL FACTOR 1     VERTICAL FACTOR 3

                          *                                          1 = BED1      2 = BED3
                          *                                          3 = BED5      4 = BED7
                          *                                          5 = BED9      6 = BED11
                          *                                          7 = BED13     8 = BED15
                          *                               3          9 = BED17    10 = BED19
                          *                                         11 = BED21    12 = BED23
                          *                                         13 = BED25    14 = BED27
                          *                                         15 = BED29    16 = BED31
                          *                                         17 = BED33    18 = BED35
                          *                                         19 = BED37    20 = BED39
                          *                                         21 = BED41    22 = BED43
                          *                                         23 = BED45    24 = BED47
                          *                                         25 = BED49    26 = BED51
                          *                                         27 = BED53    28 = BED55
                          *                                   49    29 = BED57    30 = BED59
                          *                                         31 = BED61    32 = BED63
                          *                                         33 = BED65    34 = BED67
                          *                   2040      36  18      35 = BED69    36 = BED71
                          *      24  443837       19          4342  37 = BED73    38 = BED75
                          *  28  26  27  21                     48  39 = BED77    40 = BED79
* * * * * * * * * * * * * * * * * * * * * * * * * * * * * * * * * *  41 = BED81    42 = BED83
                      2935*34          30                       45  43 = BED85    44 = BED87
                      2522*46                                 4715  45 = BED89    46 = BED91
                          *                                   13    47 = BED93    48 = BED95
                          *                                         49 = BED97    50 = BED99
                          *
                          *                                2
                          *
                          *
```

Figure 5.7. Factor loadings for factors 1 and 3 of the Q-mode analysis for odd-numbered beds.

```
HORIZONTAL FACTOR 2     VERTICAL FACTOR 3
                  *                                   1 = BED1     2 = BED3
                  *                                   3 = BED5     4 = BED7
                  *                                   5 = BED9     6 = BED11
                  *                                   7 = BED13    8 = BED15
                  *                     3             9 = BED17   10 = BED19
                  *                                  11 = BED21   12 = BED23
                  *                                  13 = BED25   14 = BED27
                  *                                  15 = BED29   16 = BED31
                  *                                  17 = BED33   18 = BED35
                  *                                  19 = BED37   20 = BED39
                  *                                  21 = BED41   22 = BED43
                  *                                  23 = BED45   24 = BED47
                  *                                  25 = BED49   26 = BED51
                  *                                  27 = BED53   28 = BED55
                  * 49                               29 = BED57   30 = BED59
                  *                                  31 = BED61   32 = BED63
                  *                                  33 = BED65   34 = BED67
                  *        18   36    4020           35 = BED69   36 = BED71
                  *  42 4143 31          19   373844 37 = BED73   38 = BED75
                  * 48 6                        2726 39 = BED77   40 = BED79
* * * * * * * * * * * * * * * * * * * * * * * * * * 41 = BED81   42 = BED83
                  * 4539                   30        43 = BED85   44 = BED87
                  *  1547                     46     45 = BED89   46 = BED91
                  *  13                              47 = BED93   48 = BED95
                  *                                  49 = BED97   50 = BED99
                  *
                  *                        2
                  *
                  *
                  *
                  *
                  *
                  *
                  *
```

Figure 5-8. Factor loadings for factors 2 and 3 of the Q-mode analysis for odd-numbered beds.

```
HORIZONTAL FACTOR 1      VERTICAL FACTOR 2

                        *   463520                        1 = BED2      2 = BED4
                        *                                 3 = BED6      4 = BED8
                        *              1                  5 = BED10     6 = BED12
                        *                 23             24    7 = BED14     8 = BED16
                        *                                 9 = BED18    10 = BED20
                        *                       29       11 = BED22    12 = BED24
                        *                                13 = BED26    14 = BED28
                        *                         3631   15 = BED30    16 = BED32
                        *                         32  21 17 = BED34    18 = BED36
                        *                             27 19 = BED38    20 = BED40
                        *                              40 21 = BED42   22 = BED44
                        *                                23 = BED46    24 = BED48
                        *                                25 = BED50    26 = BED52
                        *                                27 = BED54    28 = BED56
                        *                                   43 29 = BED58    30 = BED60
                        *                                   4239 31 = BED62  32 = BED64
                        *                                   41 33 = BED66    34 = BED68
                        *                                     28 35 = BED70  36 = BED72
                        *                                     48 37 = BED74  38 = BED76
                        *                                   49 39 = BED78    40 = BED80
* * * * * * * * * * * * * * * * * * * * * * * * * * * * * * * * * 41 = BED82  42 = BED84
                        *                                43 = BED86    44 = BED88
                        *                                45 = BED90    46 = BED92
                        *                                47 = BED94    48 = BED96
                        *                                49 = BED98
                        *
                        *
                        *
                        *
                        *
```

Figure 5-9. Factor loadings for factors 1 and 2 of the Q-mode analysis for even-numbered beds.

HORIZONTAL FACTOR 1 VERTICAL FACTOR 3

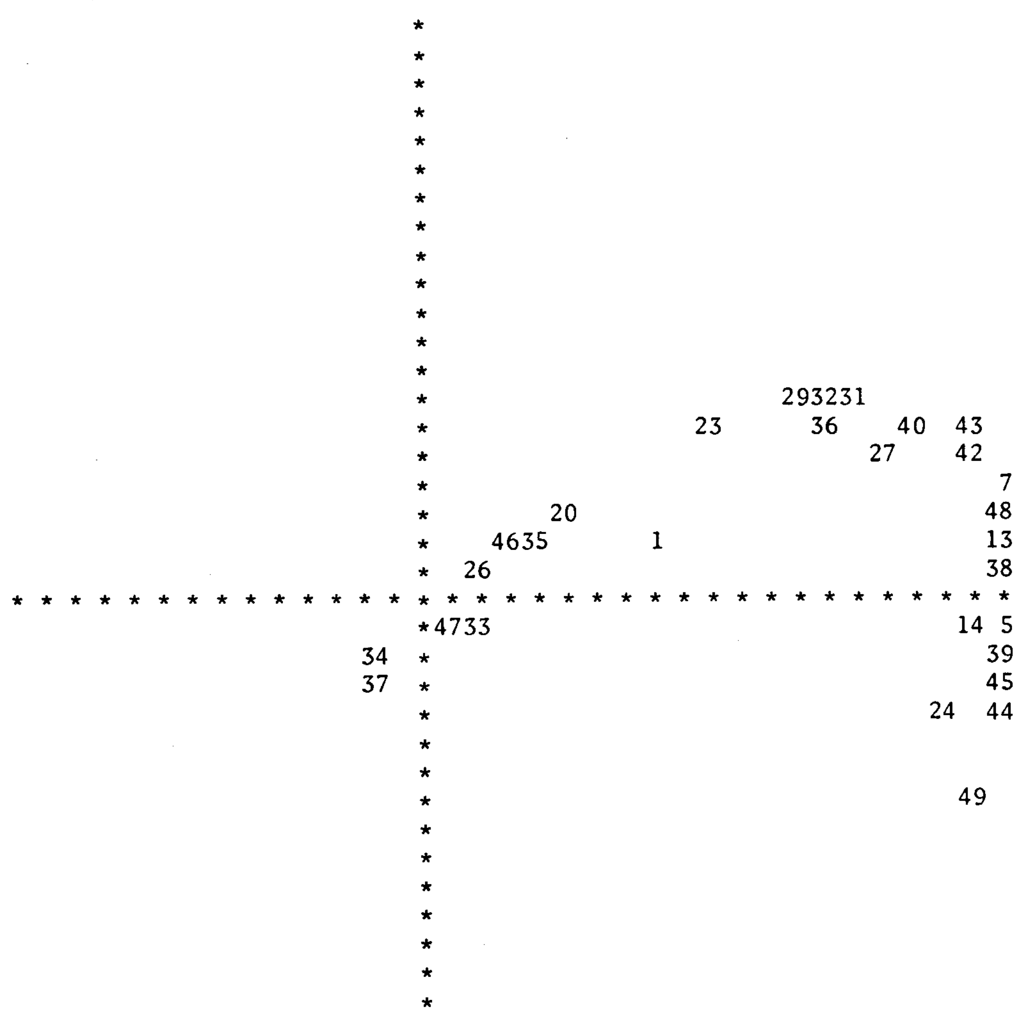

1	=	BED2	2	=	BED4
3	=	BED6	4	=	BED8
5	=	BED10	6	=	BED12
7	=	BED14	8	=	BED16
9	=	BED18	10	=	BED20
11	=	BED22	12	=	BED24
13	=	BED26	14	=	BED28
15	=	BED30	16	=	BED32
17	=	BED34	18	=	BED36
19	=	BED38	20	=	BED40
21	=	BED42	22	=	BED44
23	=	BED46	24	=	BED48
25	=	BED50	26	=	BED52
27	=	BED54	28	=	BED56
29	=	BED58	30	=	BED60
31	=	BED62	32	=	BED64
33	=	BED66	34	=	BED68
35	=	BED70	36	=	BED72
37	=	BED74	38	=	BED76
39	=	BED78	40	=	BED80
41	=	BED82	42	=	BED84
43	=	BED86	44	=	BED88
45	=	BED90	46	=	BED92
47	=	BED94	48	=	BED96
49	=	BED98			

Figure 5-10. Factor loadings for factors 1 and 3 of the Q-mode analysis for even-numbered beds.

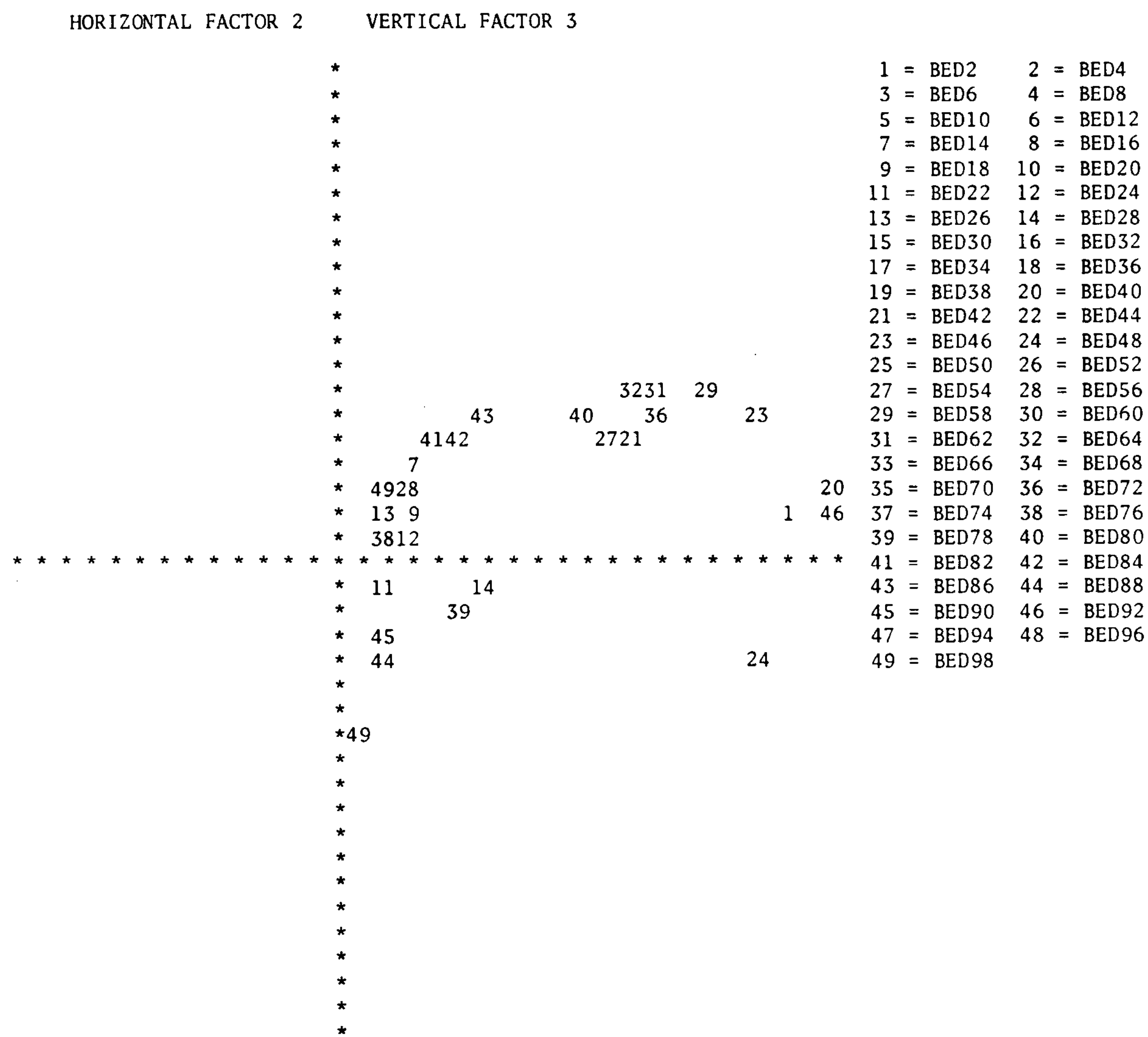

Figure 5-11. Factor loadings for factors 2 and 3 of the Q-mode analysis for even-numbered beds.

the other end. Ecologists notice that such curves define gradients from one type of environment to another (or gradations within a species in response to differing environments).

On the basis of Hill's (1974) algebraic interpretation of such plots and of these precedents of interpretation, the author believes that an objective ordination of coarse clastic beds has been achieved and that this order represents an overall "environmental" factor or constraint on the beds. The quadratic cloud of points has precisely the same order in plots of any of the axes against any other of the axes when read from one end of the "horseshoe" to the other end. Consequently, the interpretation is that this ordination represents the overwhelming influence of one underlying factor which in the case of these beds provides a stochastically rigorous gradient of beds from coarse beds to fine beds, from lenticular to tabular beds, from matrix-supported beds to clast-supported beds--in general, from "proximal" to "distal" environments of deposition.

Since so very many property variables are involved in this ordination, the ordination is not perfectly deterministic. Rather, it is probabilistic in that a given bed with a certain set of properties will usually be found along with other beds of the same type. "Mistakes" of ordination are made (apparently) in that massive sandstones are tangled up with turbidites. But, considering that these two are often quite similar, such a mistake is not surprising.

In Figure 5-12 the odd-numbered beds are plotted with Walker's (1978) classification substituted for bed number. There are several important points to be made concerning this diagram.

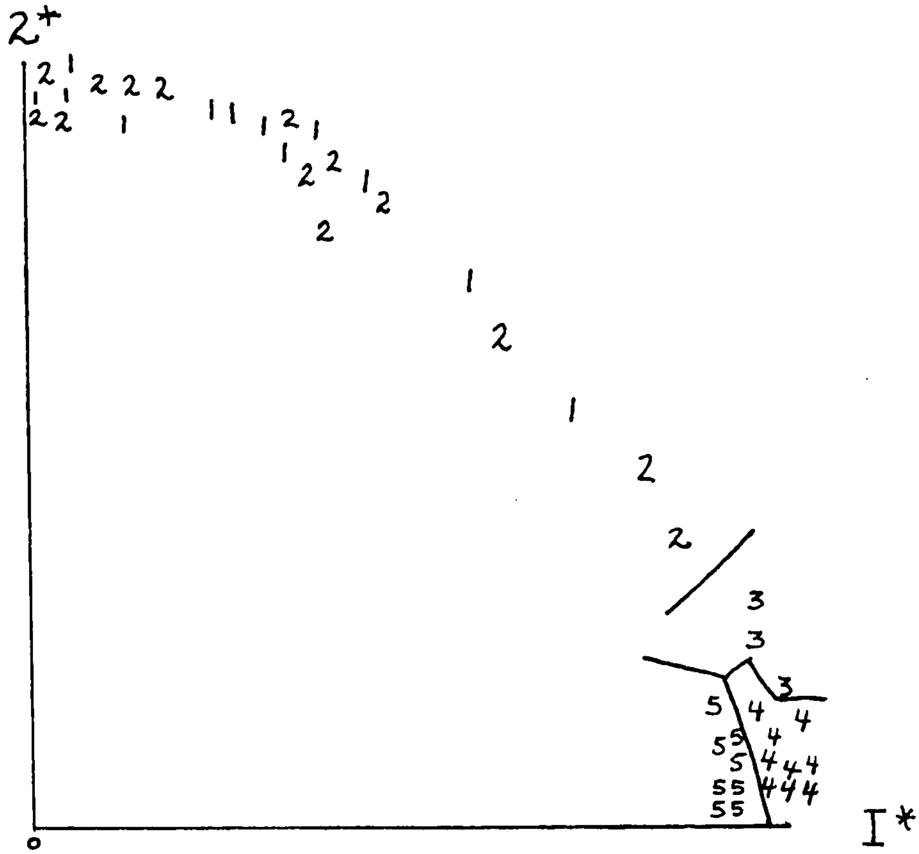

Figure 5-12. Plot of odd-numbered Q-mode beds with Walker's (1978) classification substituted for bed number. In this plot, the beds are plotted on the Varimax factor axes 1* and 2*. The lithotype identification is as follows: 1 represents classical turbidites; 2, massive sandstones; 3, pebbly sandstones; 4, conglomerates; and 5, matrix-supported beds.

First, Walker's classification is vindicated in certain ways by this ordination of beds--except in the case of massive sandstones versus turbidites. These are qualifications to this objectification of Walker's (1978) classification which will be discussed in the points below.

Second, there appears to be a spectrum rather than definite class limits. The clustering of data near the poles of the factor axes should not mislead the reader. This is due to a simple abundance of entries that were polarly ordinated. If, for example, many more massive sandstones and turbidites had been included, the cloud would have been denser in the middle regions. The fact that entries *do* fall in this middle region is what is important and indicates that these transitional values can and do exist. Consequently, on the basis of this particular study, no absolute boundaries can be drawn that would separate the beds into two polar subpopulations. The author has indicated some important clusters of beds with tentative "boundary" lines.

Third, pebbly sandstones appear rather obviously as *fine* conglomerates. The author's arguments (Chapter 3) concerning the superfluity of this category are supported.

Fourth, matrix-supported beds cluster to one side and conglomerates to the other in high loadings on factor one. This indicates an important (though perhaps gradational) difference in these two clans. However, contrary to Walker's classification *fine*-grained matrix supported beds are at this pole along with coarse-grained beds. The importance of matrix support, stressed in the R-mode results, is corroborated.

Fifth, the properties of the beds as so ordinated bear a statistical relationship to the ordination. Figure 5-13 shows a diagram of these relationships. This suggests an overall ordination of beds from statistically proximal environments to statistically distal environments. Consequently, ordination is a key to probable environmental constraints as well as a classificational device.

Summary: Relationship between R- and Q-mode Results

The R-mode analysis suggests that previous classifications of coarse clastics be modified to emphasize the action of factors other than simple parametric ones. It is thought that these modifications will give a more objective and comprehensive classification grouping of coarse clastic beds. The Q-mode ordination, indeed, shows that *fine* as well as coarse matrix-supported beds group together. Otherwise, the ordination primarily follows the grain size distinguished classes of Walker (1978). This indicates that the first and primary ordination step "found" matrix-supported beds first and grouped them together; then, it "found" the parametric properties of the remaining beds. The result is a plot which is a statistical picture of bed ordination from proximal to distal conditions, from mass-movement type flows to dilute turbulent suspensions. Consequently, the factor analysis has provided both a classificational refinement and an objective stochastic ordination of beds with respect to their relative basinal position.

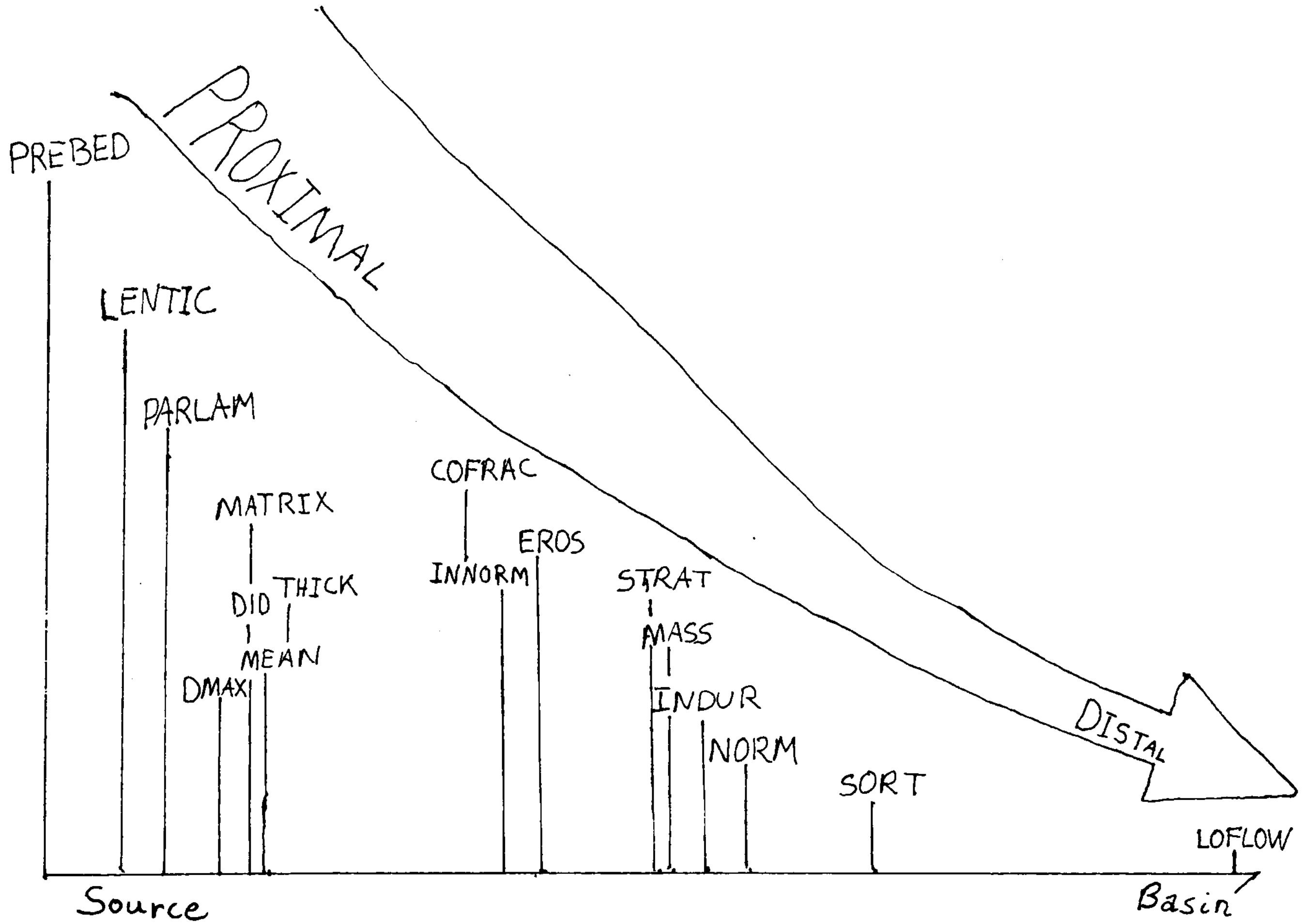

Figure 5-13. Ordination of properties. The horizontal scale is roughly representative of the mean of a particular property on the beds seriated in Q-mode analysis. The vertical scale is a graphical device, not an actual scale. The property abbreviations are explained in Table B-2 (p. 226).

CHAPTER 6

KOLMOGOROV ANALYSIS

Introduction

In Chapter 4 extensive use was made of Markov models of state transitions. The models were tallied on strictly observational properties: lithology and internal properties. From the standpoint of depositional events, however, the particular thicknesses of a sedimentary sequence and its individual beds are a result of the interplay between erosional as well as depositional processes. As Rivlina (1970) and later Hattori (1973) have suggested, an event Markov probability matrix for a sequence composed of sandstone and shale should appear with erosive state probabilities. Figure 6-1 shows the stable probability matrix for such an events Markov system as well as the likely matrix for a turbidite system. The entries in the stable matrix represent the stable probability vectors over a long sequence of events (Harbaugh and Bonham-Carter, 1970).

In a turbidite sequence such as that at LSHDS, sandstone deposition is followed by shale deposition from the suspended cloud of fine sediments brought in by the turbidity current as well as from the continual pelagic fallout contributed by the overlying water column. This nonerosive depositional event continues until another turbidity current enters the basin. (For simplicity bottom currents are ignored in this model.) In general, this incursion represents both an erosional and a depositional pair of events: shale is eroded and sand (or

	Dss	Ess	Dsh	Esh
Dss	SSd	SSe	SHd	SHe
Ess	SSd	SSe	SHd	SHe
Dsh	SSd	SSe	SHd	SHe
Esh	SSd	SSe	SHd	SHe

	Dss	Ess	Dsh	Esh
Dss	0	0	1.0	0
Ess	ρ_{21}	0	0	ρ_{24}
Dsh	0	0	0	1.0
Esh	ρ_{41}	ρ_{13}	0	0

Figure 6.1. Stable probability matrix and likely probability matrix for turbidite sedimentation. The stable probability matrix can be derived from a given probability matrix by powering the matrix until the values in a column approach a stable, unchanging value. The value in each cell of the stable probability matrix represents the actual percent of an event.

whatever sized particles are carried by the flow) is deposited. If the underlying shale bed is completely eroded, the sandstone bed beneath will also suffer erosion. Consequently, the number of *preserved* shale beds remaining in the sequence could be found in principle by subtracting the number of cases in which sandstone is eroded (SSe) from the total number of shale depositional events (SHd). The proportion of initially deposited shale beds left in the sequence would then be:

$$p_{sh} = (SHd - SSe)/SHd$$

(Hattori, 1973).

The problem with this equation is that, while formally correct, there is no empirical way to count missing shale beds. Amalgamation surfaces represent shale removal, but several shale beds may have been removed; the number is unknown. Is there any rigorous way in which this proportion can be estimated?

While it will probably remain impossible to point to a particular bedding plane and determine the amount of material that was once present between the underlying and overlying beds, a statistically valid apparatus for analyzing the amount of erosion in a sequence has been developed by Kolmogorov (1951). Essentially, Kolmogorov's theory provides a method by which a bed thickness distribution can be extended into the negative region of a frequency diagram, a region whose "negative" area supplies a statistical estimate of the amount of material eroded from a sequence of beds.

Theory

If a frequency percent plot could be made of the differences between the uneroded thicknesses of beds in a sequence and the amount removed from each by erosion, including the cases in which erosion was of greater magnitude than deposition (negative thickness), the resulting distribution could be described by some appropriate probability density f(x). This, of course, is not directly possible, and a frequency distribution plot of *actual* bed thicknesses (i.e., the cases in which the difference was positive) is terminated at the ordinate axis. The relation that this truncated distribution, f*(x), has to the total thickness distribution f(x) is:

$$f^*(x) = f(x)/p \qquad \text{when } f(x) > 0 \, ,$$

$$f^*(x) = 0 \qquad \text{when } f(x) \leq 0 \, ,$$

$$p = \int_0^\infty f(x)dx \, .$$

If, for example, f(x) is a normal Gaussian distribution, the relationship between f(x) and f*(x) may be seen graphically in Figure 6-2. For a sequence that has undergone any degree of erosion, the probability density f*(x) is always at higher ordinate values than f(x), since for any interval (a_i, a_{i+j}) in the region right of the ordinate

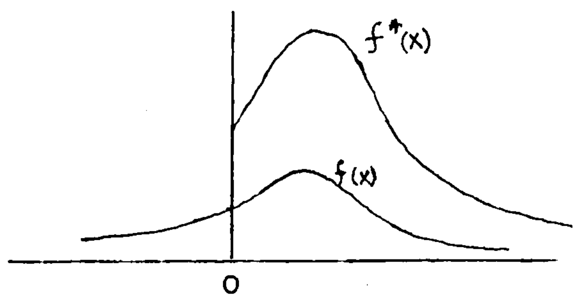

Figure 6-2. The relationship between the truncated distribution f*(x) and f(x).

$$\int_{a_i}^{a_{i+j}} f^*(x)dx = \int_{a_i}^{a_{i+j}} f(x)dx \Big/ \int_{0}^{+\infty} f(x)dx$$

where

$$\int_{0}^{+\infty} f(x)dx < 1 .$$

Hence,

$$\int_{a_i}^{a_{i+j}} f^*(x)dx > \int_{a_i}^{a_{i+j}} f(x)dx$$

for all cases of eroded sequences. For the rare case in which a sequence has suffered no erosion $f(x) = f^*(x)$.

Restrictions

Kolmogorov's theory provides a rigorous statistical technique by which $f(x)$ may be calculated. However, there are certain decisions that must be made and certain requirements that must be met before this analysis can validly be applied.

Target Population

The choice of a target population is the first decision. Kolmogorov's analysis has been applied to sand, to shale, and the sand-shale couplet thickness distributions in turbidite sequences

(Mizutani and Hattori, 1972). In light of geological understanding of the formation of turbidite sequences such a procedure is ill-advised because it is difficult to see how processes that deposit shale (shale deposition events in the earlier matrix) can erode sand; yet, this is the assumption implicitly necessary for applying Kolmogorov's methods to turbidite sands in which the sand-shale couplet is ubiquitous. Indeed, the presence of a sand-shale couplet and the continuous grading of grain sizes up through the turbidite is important empirical evidence that the sand was not eroded after emplacement. It is certainly possible for sand to be eroded by turbulent currents transporting sand. In this case, however, there is generally no longer a sand-shale couplet but rather a sand-sand transition. In any case, it is not the quiet settling out of fines (shale deposition) that accomplishes erosion.

A geologically more reasonable target population is the shales. Qualitative criteria such as sole markings in the overlying sands, as well as an understanding of the mechanics of sand emplacement in turbidites, indicate that shale beds are indeed eroded by the currents emplacing the overlying sandstones but are not themselves erosive agents. Amalgamated sandstones and Bouma sequences with divisions D and E missing provide field evidence of the erosion of entire beds of shale.

Randomness

A second consideration is purely theoretical but adds weight to the decision to use the shales as the target population. According to the theory, the distribution of bed thicknesses must be random. In many turbidite sequences, however, the thicknesses of sandstone beds are not random. Indeed, in Chapter 4, Markov analysis shows well-developed trends of thinning-upward in the turbidites of LSHDS. The thickness of a sandstone depends to some finite probability on the thickness of the underlying bed. The sequence possesses memory. In such an obviously nonrandom system, Kolmogorov's theory is inapplicable.

This consideration also invalidates application of the Kolmogorov apparatus to the couplet as a whole. The nonrandomness of the sandstones introduces a systematic element into the couplet's thickness that falsifies the results of the statistical analysis to a greater or lesser degree depending upon the strength of the trend in the sands. While it is probably not the case that well-developed trends exist in all turbidite, it is reasonable to assume that there may always be a nonrandom control of thicknesses in turbidites. What is deposited from a given flow simply depends upon the configuration of the basin at the time of the flow, a configuration controlled strongly by previous deposits.

Geological consideration of the manner in which shales are emplaced, however, indicates that, in general, their deposition is not strongly influenced by what has already been deposited. The thicknesses of shales, especially those containing the E and interturbidite divisions, are randomized and rendered independent of previous deposits in two ways. First, shales accumulate through randomly distributed time intervals that are only terminated by the next turbidity flow. While it is not known whether there are larger nonrandom controls on time intervals between flows, there is at present no compelling empirical evidence to that effect. (This statement will be qualified later.) Second, the variable size of the turbulent cloud of suspended fines from which the turbidite fraction of the shales is deposited, as well as bottom currents that act to resuspend and keep particles in suspension for periods far greater than their settling velocities in quiet water would dictate, served as "error" terms that randomize shale bed thickness accumulation.

A measure of certitude concerning the independence of the shale bed thickness distribution from either associated sandstone bed thicknesses or other shale bed thicknesses is possible by the calculation of the autocorrelation coefficient r_k for the sequence. If a trend exists in the sands, an r_1 value close to 0 for sand-shale couplets indicates that neither this trend nor a reverse trend is present in the shales. The autocorrelation coefficient up to a given lag k (Agterberg, 1974) can be calculated for the shales themselves. Low values for r_k will indicate substantial independence (trendlessness) among the shale bed thicknesses themselves.

Distribution Form

The third and final decision is the choice of the general form of f(x). Kolmogorov's theory does not specify what f(x) will be; it only suggests a means of relating a truncated distribution f*(x) to some f(x) that extends to the left of the ordinate. Mizutani and Hattori (1972) simply show a shale bed thickness distribution curve and argue that it is very similar to the overall form of the normal distribution curve though now truncated. But, to make this model of sedimentation-erosion more creditable from the geological standpoint requires a bit more ingenuity. Are there compelling geological reasons for assuming that shale bed thicknesses should follow a normal distribution? A possible model for shale formation in turbidite sequences will be considered with the goal of assessing the geological rationale behind a normal distribution of shale thickness. Of course, from a strictly mathematical standpoint, any curve that fits will be suitable; but, for this curve to model an empirical process, it must at least be physically explicable.

General Mathematical Model of Shale Deposition

Consider the incursion of a turbidity current into a basin at time t_n. Sand and coarser material will be deposited almost instantaneously. Following the deposition of coarser materials, suspended clastic fines dominate the formation of the pelitic interval. Later, the dominant sediment source for the shales becomes the fallout from the overlying water column. The deposition of fine sediment will continue until the next turbulent cloud moves through the basin at time t_{n+o}.

The next unit will be deposited in an interval of time $(n + o) + p$ which we will assume for simplicity has a length independent from the previous time length of t_{n+o} (independence assumption). This assumption makes an incursion following a given point of time equally probable regardless of whether a great amount of time or a small amount of time has elapsed from the last flow. This assumption is problematic, though. In some cases, turbulent currents may be set off by, for example, *annual* stream flooding. Thus, while certain turbidity current-triggering mechanisms are thought to be best modeled by an independent processes model, for example, earthquakes (Till, 1974), certain systematic temporal regularities may also be operative. Consequently, the model as presented below should be qualified. Empirical data will fit well or less well depending upon the strength of the systematic regularities in the timing of turbulent flows.

If we look at the time line for a great period of time, it would be possible to compute an average value λ for the number of incursions that occur in a given time length. We will further assume that the occurrence probability for any time interval of given length is the same for any other period of the same length no matter when such time periods are taken to begin (assumption of stationarity).

Such a temporal distribution as described above is the Poisson distribution. The probability distribution of this process is:

$$P(x) = \frac{\exp^{-\lambda t}(\lambda t)}{x!}$$

This equation gives the probability of exactly x occurrences of turbidity incursions into the basin at a fixed interval of duration t, where λ may be called the intensity or average value of x for a given time length. What will the distribution of bed thicknesses look like under the operation of this independent, stationary distribution of time intervals?

There is an important point to consider: Shale beds are the sum of two types of sediments and the result of two types of processes. The majority of the turbidite fraction is deposited at the end of physical sorting of the grain sizes present in the original turbulent cloud. The pelagic fallout sediments drop out of the overlying water column based simply on their becoming available to the basin. For the sake of simplicity, we shall assume that the deposition of the pelagic portion only commences following the practical completion (failure) of the turbidite sedimentation process. The term "failure" is used here to denote the completion of a process in conformity with the usage given to such completions in reliability mathematics. See, for example, Amstadter (1971). This is not strictly true as the background sediments are presumably also sedimented along with turbidite sediments. However, considering the quantity of turbidite versus pelagic sediments shortly after the incursion of a turbulent cloud, it is *practically* true. Again, for the sake of simplicity, we shall assume that the failure rate is constant in both processes. This is certainly true for pelagic deposition but probably is not generally true for the turbidite sedimentation process. It is likely that the turbidite shale sedimentation process should be modeled by an increasing failure rate. The resulting distribution would be a Weibull distribution in which $\beta > 1$ in the general formula

$$f(x) = (\lambda\beta)x^{\beta-1}\exp^{-\lambda x^{\beta}} \quad , \quad x > 0 \ .$$

(Amstadter, 1971; Meyer, 1972). The exponential distribution is simply a special case of the Weibull distribution in which $\beta = 1$. But, again for simplicity, only the exponential distribution will be considered.

Now, under the assumption of stationary, independent time intervals of sedimentation where the length of time intervals is distributed by the Poisson distribution, the thicknesses of turbidite as well as pelagic sediments will be distributed according to the exponential distribution (though each will probably have different parameters λ). The general equation for the exponential distribution is

$$
\begin{aligned}
f(x) &= \lambda \exp^{-\lambda x} , && x > 0 \\
&= 0 , && \text{elsewhere} .
\end{aligned}
$$

In the above equation, $f(x)$ represents the thickness distribution of *either* turbidite or pelagic shale sediments. The exponential distribution is defined on the space series (bed thicknesses) produced by the Poisson distributed time series.

Yet, the actual shale bed thickness distribution is the *sum* of turbidite as well as pelagic sediments. What is the likely distribution of the sum of two random variables which follow the exponential distribution?

The sum of two random variables X and Y is known as the convolution of the variables (Meyer, 1972) and the convolution integral $g*h$ gives the distribution of the sum $X + Y$ where $g(x)$ and $h(y)$ are the distributions of X and Y respectively. If we let

$z = x + y$, and $w = x$,

then $g{*}h$ is

$$s(z) = \int_{-\infty}^{+\infty} g(w)h(z - w)dw \; .$$

The convolution of two exponential distributions for the case in which $\lambda_g > \lambda_h$ [the likely situation for the pelagic h(y) versus the turbidite g(x)] is the distribution of the sum s(z):

$$s(z) = \frac{\lambda_g \lambda_h}{\lambda_h - \lambda_g} \left(\exp^{-z\lambda_g} - \exp^{-z\lambda_h}\right) \; .$$

The general graph of this equation is shown in Figure 6-3. What this graph essentially shows is the distribution of bed thicknesses that is expected to result if we assume that upon the failure of turbidite sedimentation, pelagic sedimentation commences and that both are independent, randomly distributed processes. Notice that λ is average bed thickness per given interval (space series), though it reflects the temporal intensity parameter λ of the Poisson time series.

This graph (Figure 6-3) closely approximates the normal distribution. Yet, it is a graph of *uneroded* (and uncompacted--a point to which we shall return presently) shale bed thicknesses. How can we approximate this original distribution form from the data which we possess, the thickness distribution of eroded beds? It is at this point that Kolmogorov's techniques become valuable, for it is not the problem of

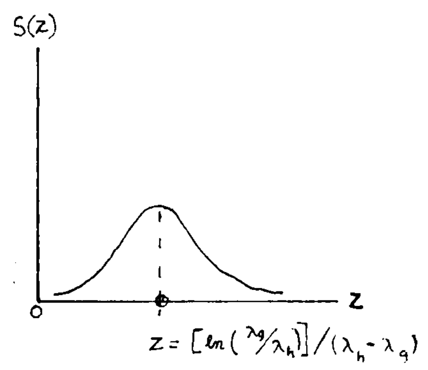

Figure 6-3. Graph of the convolution of the two exponential distributions.

producing $f^*(x)$ from $f(x)$ (erosion has done that for us) but of estimating $f(x)$ from $f^*(x)$ that is to be accomplished. Before we return to the details of this analysis, however, we should not a subtle but very significant shift in the approach used in this study from that adopted by Kolmogorov (1951) and Mizutani and Hattori (1972).

These earlier workers assumed that bed thickness distributions could be best understood by assuming a truncated normal distribution. Now, while the proposed model portrays shale bed thickness distributions as truncated from a normal distribution, it in no way assumes that they are *derived* from a normal distribution. In fact, as we have seen, a geologically more plausible origin lies in the convolution of two exponentially distributed random sedimentation variables. Mathematical analysis does not require that our normal distribution be a convolution, but geologically, it is more understandable. See Appendix C for further comments on shale distributions.

General Method of Application

When the three preliminaries noted earlier are resolved, Kolmogorov's statistical theory can be applied to a bed thickness distribution. Schematically, the analysis proceeds as follows. The details of this analysis can be found in Mizutani and Hattori (1972).

What we are presented with in an actual thickness distribution is the truncated distribution $f^*(x)$. Since we have already determined in the preliminaries the general form of the complete, uneroded distribution, $f(x)$, we can approximate this $f(x)$ by using the data of the empirical

$f^*(x)$. Since we are dealing with a truncated normal distribution, the problem resolves itself into the problem of estimating the values for the mean and standard deviation of the original curve $f(x)$.

Having calculated these values, if we then compute the ratio of $\int_0^{+\infty} f(x)dx$ to $\int_{-\infty}^{+\infty} f(x)dx$, the resulting quantity, p, called Kolmogorov's coefficient, represents the degree of preservation of beds in a sequence. A p value of 0.89, for example, indicates that 89 out of 100 originally deposited beds are preserved. Eleven have been eliminated by erosion. A further quantity, q, called Kolmogorov's ratio, is obtained from the ratio of $\int_0^{+\infty} xf(x)dx$ to $\int_{-\infty}^{+\infty} |x|f(x)dx$. This quantity is a statistical estimate of the percentage of a sequence actually preserved in outcrop relative to that total thickness that would have been present if erosion had not removed some material. A q value of 0.92, for example, indicates that of 100 meters of possible outcrop deposit, 92 meters are preserved. Of course, compaction has reduced the thickness of the original deposit. But, assuming that compaction acted similarly on all portions of the outcrop, the *ratio* of uncompacted, eroded shales to uncompacted, uneroded shales should equal the ratio of compacted, eroded shale thickness to that thickness which would have been present (compacted) in outcrop had the sequence suffered no erosion. There is a further difficulty with compaction that will be addressed later. The absolute value of x in the denominator is used since some of the "thicknesses" of the total distribution $f(x)$ take on negative values. Thus, the problem posed in the introductory section of this chapter for computing the proportion of preserved shales is solved.

Application

Kolmogorov's analysis is applied here to the turbidite sequence lying above the conglomerates at South Holston Dam (LSHDS). The outcrop was divided in the field into three portions based on the appearance of major bodies of sand. Group A, stratigraphically lowest, comprises an interval approximately 20 m thick; Group B, 40 m; and Group C, stratigraphically highest, 30 m.

Particular care was taken in measuring the shales. Thin punctuations of very fine sand to sandy silt were noted and excluded from shale thickness tabulations since they indicate the termination of a *bona fide* shale unit and the incursion of fresh clastic material. Since such a measurement procedure is possible only on well-exposed outcrops, beds from the few places where weathering or vegetation had obscured their definition have been excluded from the tabulation. While it was clear that such beds were shales and fine sandstones and while this suffices for general field description, the biasing effect of including as one thick shale unit what may have been multiple depositional events is too large to allow for the determination of accurate statistical parameters. (There are qualifications inherent in this technique that will be addressed later.)

The first task is the determination of the correlation coefficient between sand and shale and the autocorrelation coefficients for successive shale beds. For sand-shale pairs from Group B(the best exposed of the three groups), the correlation coefficient between sand and shale was r = 0.249. This indicates a rather insignificant positive correlation between sand and shale. The variation of sand thicknesses explains 6.2% $[(0.249)^2 = 0.062 \times 100\%]$ of the thickness variance of the shale. There is no significant covariation of the two. The autocorrelation coefficients (Agterberg, 1974) for 52 beds of shale are shown in graphical form (known as a correlogram) in Figure 6-4. They were calculated up to lag N/4 where N = 52. In order for a significant correlation to exist the autocorrelation coefficient must be greater than 2 (1/N) (Schwarzacher, 1975). None of the calculated autocorrelation coefficients obtain this value. We are statistically justified, therefore, in regarding the shales to be trendless with respect to thickness. The assumptions of randomness and stationarity are satisfied.

A summary of thickness data and calculated f(x) and f*(x) are shown in Table 6-1. For f(x), the estimators μ of mathematical expectation and σ of standard deviation are given at the bottom of the table. Curves based on these data are shown for each section in Figures 6-5, 6-6, and 6-7. A word of explanation regarding the curve f*(x) is in order.

The empirical data define the actual f*(x). From this f*(x) we estimate f(x). As a check on this procedure, f*(x) may be *re*calculated from the theoretical f(x) by truncating f(x) at zero and dividing all the positive values of f(x) by p. The resulting f*(x) should approximate the original distribution if the assumptions of our method and the calculations upon which it is based are correct. As the diagrams show, a rather close approximation has been achieved between the empirical and theoretical values for f*(x).

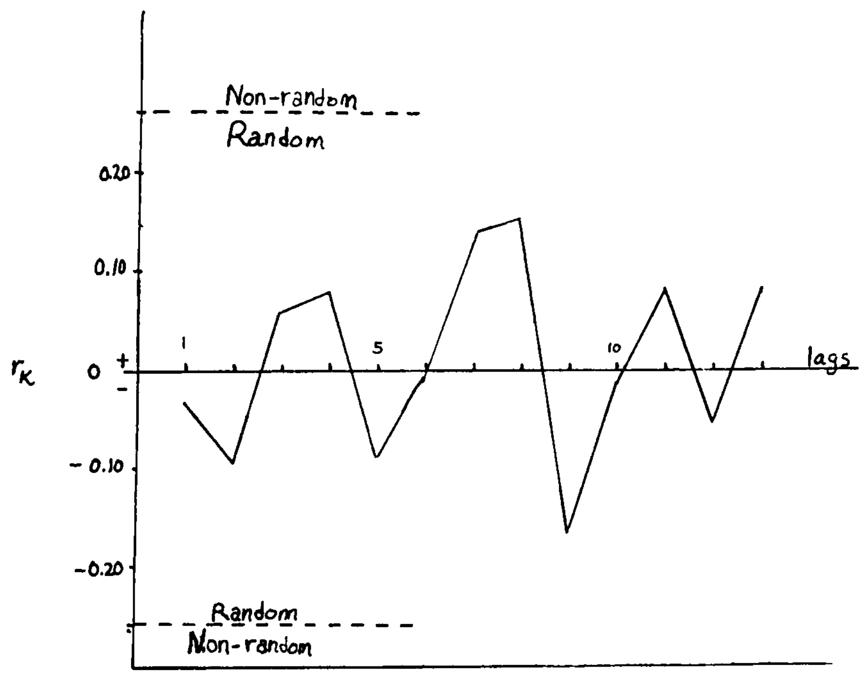

Figure 6-4. Correlogram for 52 shale beds.

Table 6-1. Empirical and Kolmogorov frequencies for the three groups of shales

	Group A				Group B							
Interval (cm)	n	n/N	f(x)	f*(x)	n	n/N	f(x)	f*(x)	n	n/N	f(x)	f*(x)
0 - 2	38	0.43	0.23	0.41	69	0.22	0.16	0.23	15	0.14	0.14	0.18
2 - 4	13	0.15	0.18	0.32	89	0.27	0.16	0.23	29	0.27	0.15	0.20
4 - 6	10	0.12	0.10	0.18	56	0.18	0.14	0.20	19	0.18	0.16	0.21
6 - 8	4	0.05	0.04	0.07	44	0.14	0.11	0.15	15	0.14	0.12	0.16
8 - 10	5	0.06	0.01	0.02	22	0.07	0.07	0.09	15	0.14	0.09	0.12
10 - 12	3	0.03	--	0.01	14	0.04	0.04	0.05	4	0.04	0.06	0.08
12 - 14	4	0.05	--	--	12	0.04	0.02	0.02	3	0.03	0.03	0.04
14 - 16	2	0.02	--	--	7	0.02	0.01	0.01	2	0.02	0.01	0.01
16 - 18	2	0.02	--	--	4	0.01	--	--	2	0.02	--	--
18 - 20	1	0.01	--	--	3	0.01	--	--	1	0.01	--	--
20 - 22	4	0.05	--	--	3	0.01	--	--	1	0.01	--	--
22 - 24	0	0.00	--	--	0	0.00	--	--	0	--	--	--
>24	2	0.02	--	--	0	--	--	--	2	0.02	--	--
(-2) - 0	--	--	0.21	--	--	--	0.13	--	--	--	0.10	--
(-4) - (-2)	--	--	0.14	--	--	--	0.09	--	--	--	0.07	--
(-6) - (-4)	--	--	0.07	--	--	--	0.05	--	--	--	0.04	--
(-8) - (-6)	--	--	0.02	--	--	--	0.03	--	--	--	0.01	--
(-10) - (-8)	--	--	0.01	--	--	--	0.01	--	--	--	0.01	--
(-12) - (-10)	--	--	--	--	--	--	--	--	--	--	0.01	--
<(-12)	--	--	--	--	--	--	--	--	--	--	--	--
	N = 88				N = 321				N = 108			
	f(x) = N(0.5, 3.40)				f(x) = N(2.4, 4.95)				f(x) = N(3.7, 5.05)			

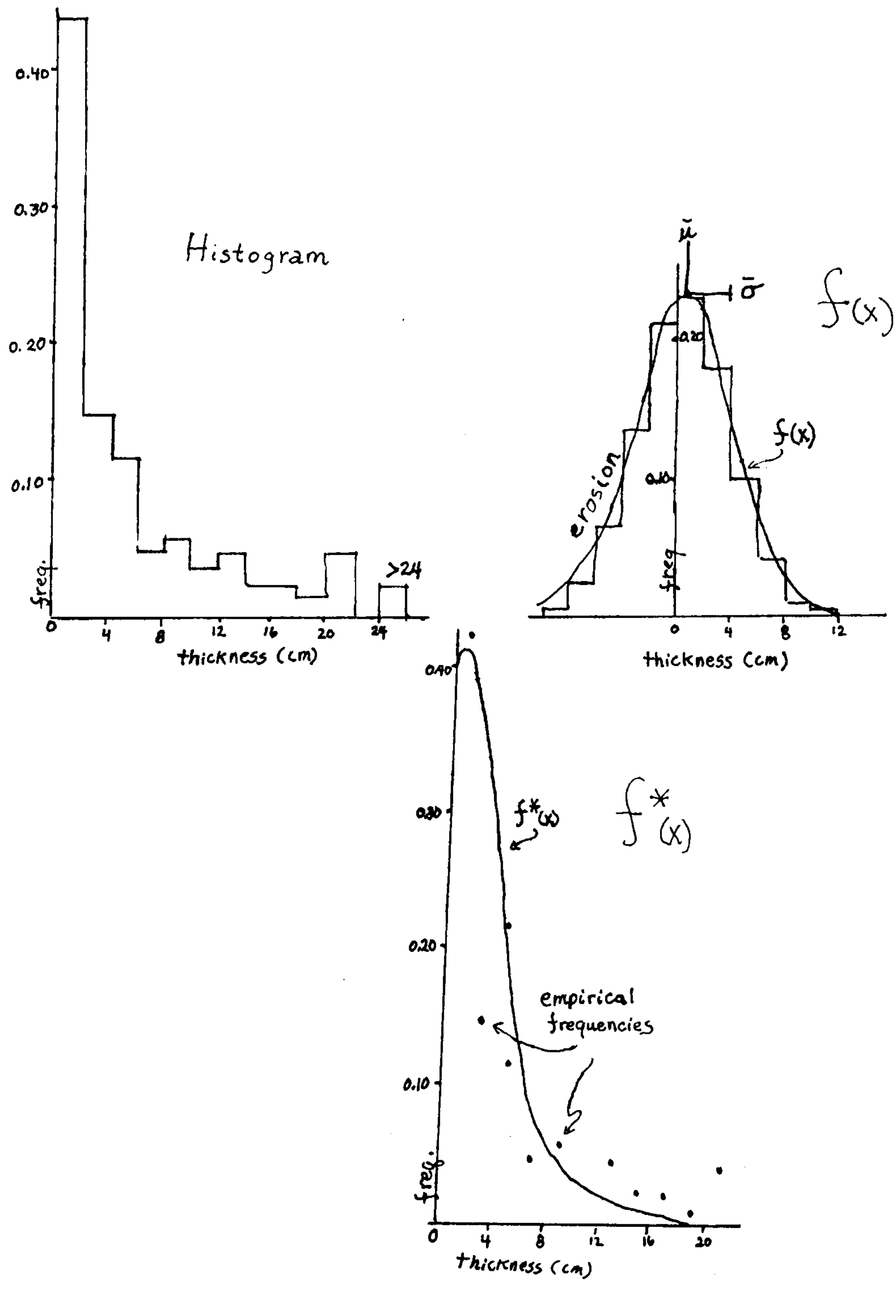

Figure 6-5. Histogram, f(x), and f*(x) for Group A shales.

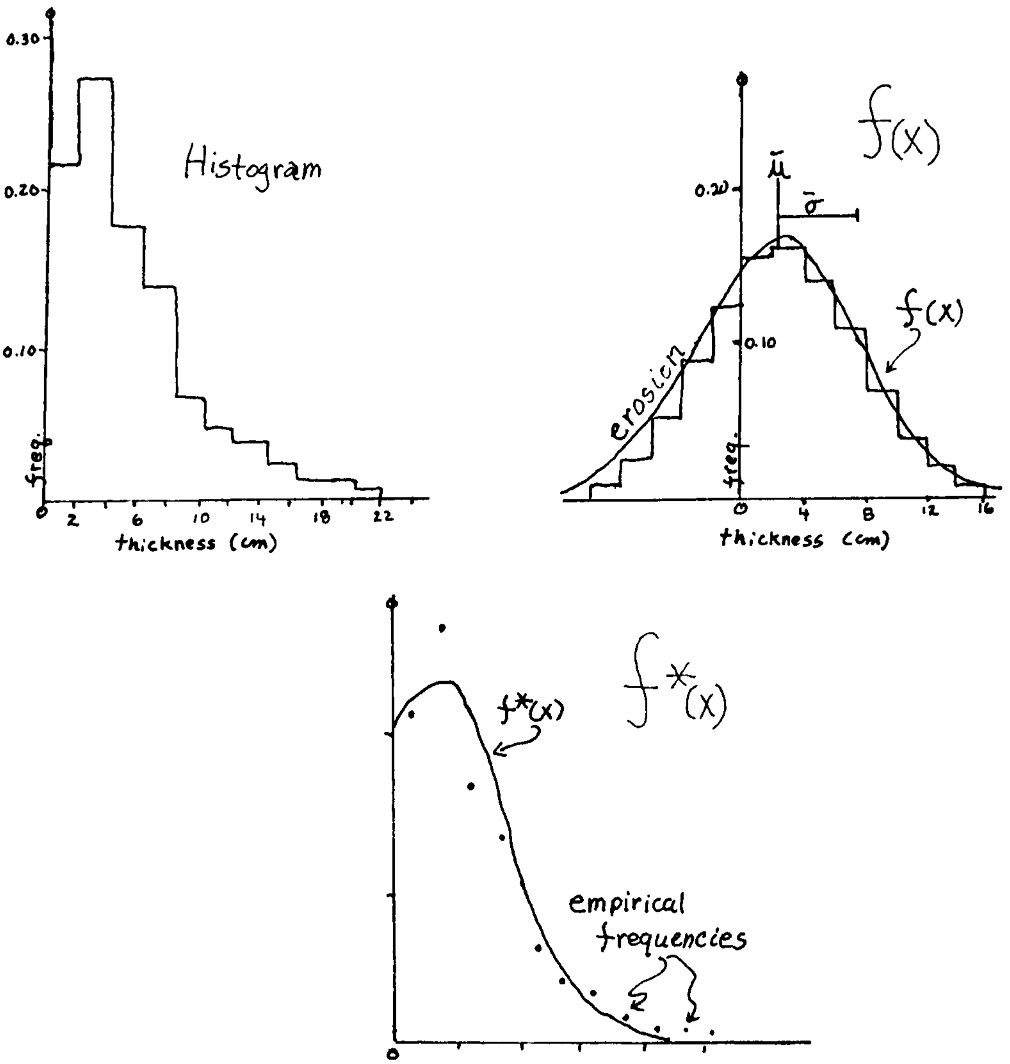

Figure 6-6. Histogram, f(x), and f*(x) for Group B shales.

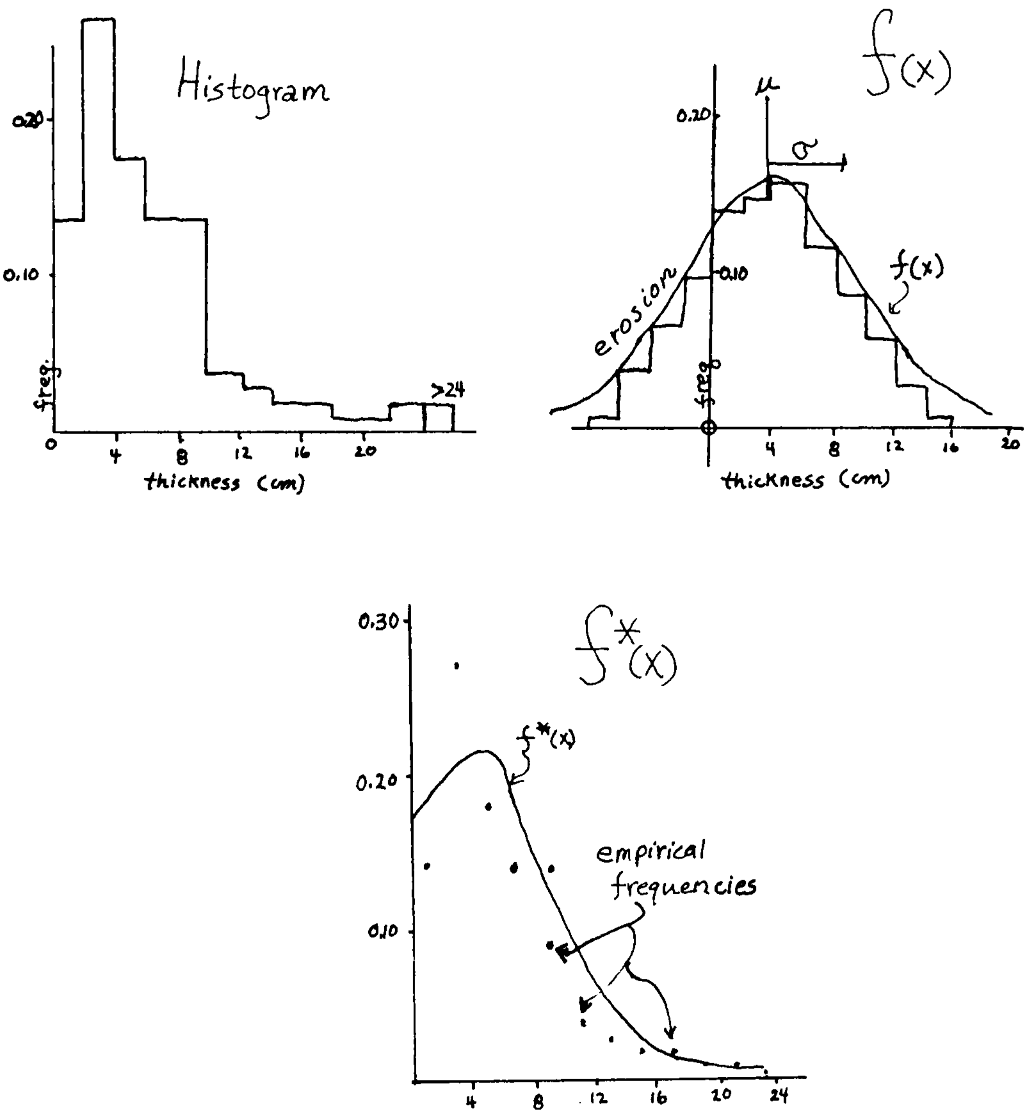

Figure 6-7. Histogram, f(x), and f*(x) for Group C shales.

Table 6-2 gives a summary of the values of p and q calculated for the three groups of shales. The graph in Figure 6-8 plots the p and q values of the three groups at the midpoints of their stratigraphic thicknesses. If we extend this graph as shown in the hypothetical extension to include the conglomerates of SHDC (whose values for p and q must approach 0), a trend emerges for the deposits. With respect to the shales, we pass from conditions of almost complete erosion (and/or nondeposition) to predominantly depositional conditions. There was an apparent slow evolution of this part of the basin with time into a less erosive, more stable condition. This transition from lower p and q values to higher p and q values is, then, essentially a quantitative profile of the relative depositional-erosional activity of this portion of the basin through time.

Table 6-2. Summary of Kolmogorov calculations

Group	Number of Measurements	Mean	Std. Dev.	p	q
Group A	88	0.5	3.40	0.56	0.59
Group B	321	2.4	4.95	0.69	0.77
Group C	108	3.7	5.05	0.77	0.86

Physical Interpretation

As we saw in Chapter 4, the outcrop LSHDS is dominated by fining-upward sequences and/or monotonous successions of sand and shale. In light of this and the overall facies packages, these cycles were

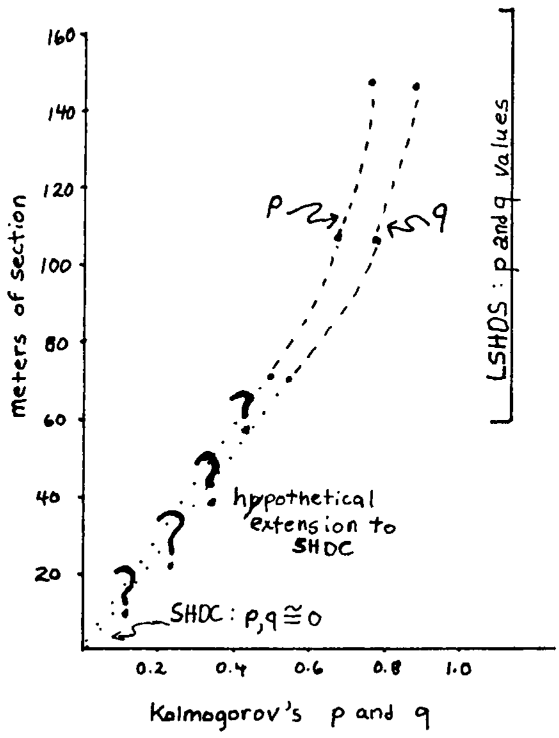

Figure 6-8. Graph of p, q against stratigraphic position.

interpreted to represent the filling/shifting of inner-to-mid-fan channels with interspersed periods of overbank sedimentation. However, Kolmogorov analysis raises the interpretation of this sequence to a broader scale.

The entire suite of beds in this sequence (including the conglomerates of SHDC) appears on the basis of Kolmogorov analysis to be undergoing a slow, evolutionary pattern of depositional development. Such a large scale development is probably characteristic of what Ricci-Luchi (1975) has termed (somewhat misleadingly) a recessional suite--dominance of thinning-up cycles, evidence of overall fining up of grain sizes, and a shift to less "proximal" facies packages.

Morphologically, it might be hypothesized that this corresponds with the gradual maturing of a suprafan lobe in the mid-fan division of a submarine fan or a general recession that takes place through the lives of several lobes. As the lobe is constructed we would expect this morphological development to exert a control on the relative dominance of erosive or depositional processes. As the lobe matures, erosion will play a diminishing role in the dynamics of sedimentation. If this is the case, one should expect to find other empirical evidence to substantiate the claim. If erosion is diminishing in importance it would be reasonable to assume that sandstone should diminsih in quantity upward and thinner, finer beds should become more abundant up section.

A weighted plot of the frequency of the coarse division (Ricci-Luchi, 1975) was computed. The thickness ratio (t.r.) was obtained for 5 m intervals by:

$$\text{t.r.} = \frac{\text{\% coarse sand in interval}}{\text{number of coarse beds in interval}}$$

The purpose of dividing the simple frequency percent by the number of beds contributing to that percent was to provide a weighting factor for intervals with thicker sand units. While, for example, two intervals of 5 m each might both have 300 cm of coarse division and thus have equal percentages (60%), one interval might have this 300 cm distributed over many small beds while the other might have only one 300 cm thick bed. By dividing by the number of beds, a distinction is made between these two cases and the thicker-bedded unit will have a higher t.r. than the other interval.

As Figure 6-9 shows, there is a decline in t.r. up through the section. By smoothing these ratios (5×5 moving average over the t.r. scores) the overall trend is emphasized and mode more comparable in scale to the large intervals used in calculating Kolmogorov's coefficient and ratio. These smoothed averages as well as a regression line on their values is shown in Figure 6-10. The regression line should be interpreted cautiously since there appears to be a systematic departure from linearity in the middle section of the section. The correlation coefficient between smoothed ratios and vertical position is $r = -0.765$. This shows a relatively strong negative correlation between bed thickness and height in the section. This is exactly what we would expect if the p and q values do indeed represent some actual, slow evolution of the depositional systems operative in this part of the basin.

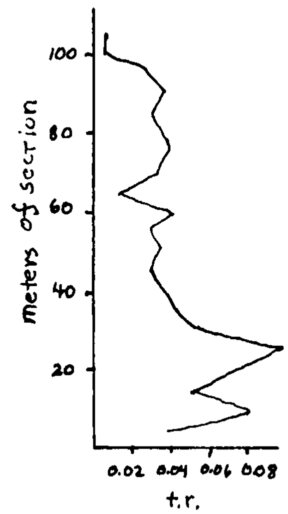

Figure 6-9. Thickness ratios for LSHDS.

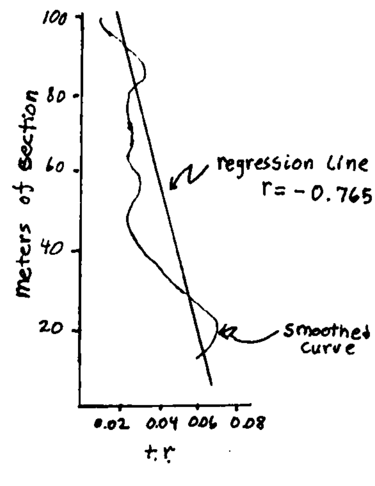

Figure 6-10. Smoothed thickness ratios and regression line for LSHDS.

The outcrop thus shows two important, inversely related trends. On the one hand, erosive activity is lessening up through the section. The beds of shale have an increasing probability of survivial the higher their position in the section. On the other hand, beds of coarse material are declining in frequency and thickness up through the section. It is likely that these two trends are evidence of an overall morphological maturation of the suprafan division of a submarine fan system.

A more direct field method of checking the reliability of the values of p and q would be to tally the number of amalgamation surfaces observed between sands. This is direct empirical evidence of shale erosion (or nondeposition). Ideally (assuming that each amalgam represents no more than one shale bed removal), the number tallied on 100 successive sandstone transitions (to either sand or shale) would equal $(1 - p) \times 100$. For example, in section A ($p = 0.56$), ideally there would be 44 sand-to-sand transitions and 56 sand-to-shale transitions tallied over 100 sand transitions.

There are three complicating factors here however. First, a sand bed might remove *more* than one shale bed. Second, an erosive event might erode away a shale, then a sandstone, and then only part of the next shale beneath. The result in a tally would be a sand-shale succession. Observational tallies, then, can consistently be expected to show higher p values than the Kolmogorov p values. Third, amalgamations are not always obvious in the field. This difficulty probably results in overlooking some amalgamations.

In a single sequence, however, we may tentatively assume that the biases entering into the tally on account of the three factors mentioned above should not affect the *relative* values of the amalgamations seen (equal biasing). The tally of observed amalgamations, total number of sand transitions, "observed" p, and calculated p are shown in Table 6-3. Calculated and observed values of p (standardized scores) are plotted in Figure 6-11. As the graph shows, there is a reasonably close relationship between the two. The correlation coefficient between the values of observed and calculated p's was +0.876 indicating strong similarity in the relative behaviors of these values.

Table 6-3. Data on amalgamations and Kolmogorov's p

Group	Number of Observed Amalgamations	Total Number of Sand Transitions	"Observed" p	Kolmogorov p
A	21	109	$\frac{109}{109 + 21} = 0.838$	0.56
B	41	362	$\frac{362}{362 + 41} = 0.898$	0.69
C	8	116	$\frac{116}{116 + 8} = 0.935$	0.77

Qualifications and Discussion

There are two very important qualifications to the analysis attempted in this chapter.

The values for p and q (as mentioned earlier) are derived from *compacted* sediments. While the value for these two parameters represent

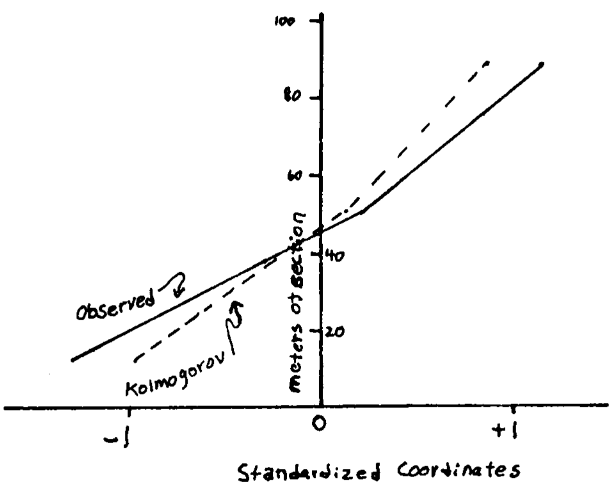

Figure 6-11. Standardized amalgamations and Kolmogorov's p scores.

ratios which might not change during compaction, the possibility that differential compaction might "unnormalize" the shale bed thickness distribution should not be overlooked. The thickness of the final, compacted shale bed varies with many parameters: calcium carbonate content (McCrosson, 1961); grain size (Teodorovich and Chernov, 1968); clay composition (Chilingarian and Rieke, 1968); and, many other variables (Rieke and Chilingarian, 1974). The model has proposed a normal or near normal distribution for *initially* deposited sediments, but any or all of the above may differentially alter this thickness distribution during diagenesis-compaction.

There is no easy way to assess the effects of compaction on the proposed theoretical distribution of thicknesses. Detailed chemical, petrographic, and experimental work would be necessary. In the absence of this data, the question is not empirically solvable. However, there is one formal property of probability distributions which can be appealed to in this regard. This property is stated in the Central Limit Theorem (Meyer, 1972). In the absence of any *compelling* reasons to the contrary, the Central Limit Theorem states that the convolution of *many* random variables (e.g., those parameters mentioned above) asymptotically approaches a normal distribution as the resultant. Thus, while it is hardly proved, the statistically likely probability density resulting from the convolution of multiple random variables will be normal. Since the "values" of these random variables on eroded beds are "negative" (strictly, meaningless), the truncated character of the bed thickness distribution will be preserved (Meyer, 1972). (This, of course, is highly speculative.)

A second problem is likewise imponderable from the data at hand. It is known that shales may be internally complex at a level below that visible to the naked eye. Small scale erosive events and depositional events occur within what may appear in the field to be a single unit (Shanmugam and Walker, 1978). While it is not known whether the shales examined in the study area are complex or indeed whether this would matter for the gross determination of the proportion of missing section at the outcrop level, the phenomenological limits to the data collected suggest that the analysis cannot be taken as a definite determination of "real" values of p and q. In light of this, Kolmogorov's p and q may have relative meaning but may be biased as estimates of the actual values of p and q.

Although these qualifications are serious and restrictive, the model does seem to follow in a regular way the behavior of independently determined physical parameters. The theoretical assumptions made by the model, though broad and at times perhaps subject to oversimplification, nevertheless are capable of disclosing valuable geological information. The verification and confirmation of the model by basic, empirical observation make this elegant mathematical system a helpful geological tool.

CHAPTER 7

CONCLUSIONS

The coarse clastics of the study area have been described, interpreted, and quantitatively treated.

The deposits are most comprehensively described as submarine fan sediments. The lithotypes and bed properties provide evidence for this interpretation and reflect the particular processes favored by their specific environmental setting.

Though there are definite limitations to the quantitative methodology used in this work, in general, it seems capable of complementing and refining more descriptive or conceptual efforts. Markov chains, factors, grading types, and Kolmogorov coefficients all are useful in clarifying the terms and rigor of our descriptive terminology and conceptual systems.

The conclusions specific to this study are as follows:

1. The distinction between coarse fraction and distribution grading is statistically valid. They represent two different styles of vertical variation.

2. Distribution graded beds show statistically significant variation in clast size vertically. This variation, however, is only weakly linear. Measures of grading involving mean clast size or D/10 are strongly linear. These measures do not appear, then, to reflect the variation style of the clast population as a whole.

3. The study of textural variation in massive sandstone beds suggests an extension of the Bouma A division into inversely graded, massive, and normally distribution graded intervals.

4. The pebbly sandstone lithotype exhibits inverse grading and imbrication contrary to what has been reported in the literature (Walker and Mutti, 1973). Aside from clast size, it lacks any distinct attributes proper to it alone. It is suggested that this lithotype be dropped from coarse clastic classificational schemes.

5. Markov analysis of conglomerates suggests that there is a preferred sequence of conglomeratic types in a vertical succession. This sequence is disorganized conglomerate to inverse-to-normally graded conglomerate to normally graded (or normally graded-stratified) conglomerate to nonconglomeratic lithotypes. This vertical sequence may represent likely lateral transitions in the original depositional environment.

6. Matrix-supported beds exhibit a descriptive spectrum from slumps to diamictites. It is thought that the debris-flow mechanism was important in the transport of the sediments making up these beds.

7. The associational and sequential regularities in the outcrops studied suggest likely paleoenvironmental settings for each outcrop. SHDC is interpreted as an incised-channel deposit; AFC, as an upper mid-fan braided-channel deposit; USHDS, as a progradational to recessional suite of mid-fan massive sandstone deposits; LSHDS, as suprafan lobe sediments, deposited during predominantly recessional conditions; and, LLCD and ULCD, as deposits of relatively inactive upper-fan channels in which mass-movement processes were dominant.

8. R-mode factor analysis gives most weight to physical mechanism as the primary explanatory factor accounting for the most variance in the attributes of coarse clastic beds. Measures of scale, shape, time competency, and concentration successfully explain most of the variance in the properties unaccounted for or not contingent upon this first, genetic factor.

9. Q-mode factor analysis provides an ordination of beds and properties which is probably based upon general spatial relationships of proximality and distality for a given flow. The ordination is not based upon clast size along but takes into account other properties, especially those that are most likely tied to physical transport mechanism such as matrix support.

LIST OF REFERENCES

LIST OF REFERENCES

Aalto, K. R., 1976, Sedimentology of a melange: Franciscan of Trinidad, California: Jour. Sed. Petrology, v. 46, pp. 913-929.

Ackermann, E., 1951, Geröllton: Geol. Rundshau, v. 39, pp. 237-239.

Agterberg, F. P., 1974, Geomathematics, Elsevier, New York, 596p.

Allen, J. R. L., 1968, On criteria for the continuance of flute marks and their implications: Geol. Mijnbouw, v. 47, pp. 3-16.

Allen, J. R. L., 1970, Physical processes of sedimentation, George Allen and Unwin Ltd., London, 248p.

Amstadter, B. L., 1971, Reliability mathematics, McGraw-Hill, New York, 408p.

Bagnold, R. A., 1954, Experiments on a gravity-free dispersion of large solid spheres in a Newtonian fluid under shear: Royal Soc. Proc., ser. A, v. 225, pp. 49-63.

Bardsley, W. E., 1978, An extreme value model for expressing grain size and bed thickness as functions of the spatial variation of grain frequency: Math. Geol., v. 10, pp. 463-654.

Bouma, A. H., 1962, Sedimentology of some flysch deposits, Elsevier, Amsterdam, 196p.

Butts, C., 1940, Geology of the Appalachian Valley in Virginia; pt 1, geologic text and illustrations: Va. Geol. Survey Bull., 52, 568p.

Campbell, M. R., 1899, Description of the Bristol quadrangle: U.S. Geol. Survey Geol. Atlas, Folio 59.

Cas, R., 1979, Mass-flow arenites from a Paleozoic interarc basin, New South Wales, Australia: mode and environment of emplacement: Jour. Sed. Petrology, v. 49, pp. 29-44.

Chilingarian, G. V., and Rieke, H. H., 1968, Data on consolidation of fine-grained sediments: Jour. Sed. Petrology, v. 38, pp. 811-816.

Chipping, D. H., 1972, Sedimentary structures and environments of some thick sandstone beds of turbidite type: Jour. Sed. Petrology, v. 42, pp. 587-595.

Choi, S. C., 1978, Introductory applied statistics in science, Prentice-Hall, Englewood Cliffs, 278p.

Collins, S. L., 1976, Submarine-fan deposits in the Shields Formation (Precambrian, Ocoee Series of East Tennessee, unpublished thesis, The University of Tennessee, Knoxville, 114p.

Crowell, J. C., 1957, Origin of pebbly mudstones: Bull. Geol. Soc. America, v. 68, pp. 993-1010.

Curry, J. C., 1966, Observations of alpine mudflows in the Tenmile Range, central Colorado: Geol. Soc. America Bull., v. 77, pp. 771-776.

Dahlberg, E. C., and Griffiths, J. C., 1967, Defining gradients in a sample of sedimentary rock: Sedimentology, v. 8, pp. 291-309.

Davies, I. C., and Walker, R. G., 1974, Transport and deposition of resedimented conglomerates: the Cap Enrage formation, Cambro-Ordovician, Gaspe, Quebec: Jour. Sed. Petrology, v. 44, pp. 1200-1216.

Dzulynski, S., and Walton, E. D., 1965, Sedimentary features of flysch and greywacke, Elsevier, New York, 274p.

Fisher, R. V., 1971, Features of coarse-grained, high-concentration fluids and their deposits: Jour. Sed. Petrology, v. 41, pp. 916-927.

Folk, R. L., 1974, Petrology of sedimentary rocks, Hemphill Publishing Company, Austin, 182p.

Hampton, M. A., 1972, The role of subaqueous debris flow in generating turbidity currents: Jour. Sed. Petrology, v. 42, pp. 775-793.

Hampton, M. A., 1975, Competence of fine-grained debris flows: Jour. Sed. Petrology, v. 45, pp. 834-844.

Harbaugh, J. W., and Bonham-Carter, G., 1970, Computer simulations in geology, Wiley and Sons, New York, 575p.

Harman, H. H., 1967, Modern factor analysis, University of Chicago Press, Chicago, 471p.

Hattori, I., 1973, Mathematical analysis to discriminate two types of sandstone-shale alternations: Sedimentology, v. 20, pp. 331-345.

Hendry, H. E., 1972, Breccias deposited by mass flow in the Breccia Nappe of the French pre-Alps: Sedimentology, v. 18, pp. 277-292.

Hesse, R., 1975, Turbiditic and nonturbiditic mudstones of Cretaceous flysch sections of the east Alps and other basins: Sedimentology, v. 22, pp. 387-416.

Hill, M. O., 1974, Correspondence analysis: a neglected multivariate method: Appl. Statistics, v. 23, pp. 340-354.

Howard, R. A., 1971, Dynamic probabilistic systems: Markov models, John Wiley, New York, 576p.

Icaacson, D. L., and Madsen, R. W., 1976, Markov chains theory and applications, John Wiley, New York, 256p.

Imbrie, J., and Purdy, E. G., 1962, Classification of modern Bahamian carbonate sediments: Am. Assoc. Petrol. Geol. Mem. 1, pp. 253-272.

Ingram, R. L., 1954, Terminology for the thickness of stratification and parting units in sedimentary rocks: Geol. Soc. America Bull., v. 65, pp. 937-938.

Johnson, A. M., 1970, Physical processes in geology, Freeman, Cooper and Co., San Francisco, 557p.

Joreskog, K. G., Klovan, J. E., and Reyment, R. A., 1976, Geological factor analysis, Elsevier, New York, 178p.

Keith, A., 1907, Description of the Roan Mountain quadrangle, U.S. Geology Survey Geol. Atlas, Folio 151.

Kellberg, J. M., and Grant, L. F., 1956, Coarse conglomerates of the Middle Ordovician series in the southern Appalachian Valley: Geol. Soc. America Bull., v. 67, pp. 697-716.

Klovan, J. E., R- and Q-mode factor analysis, *in* McCammon, R. B., ed., Concepts in geostatistics, Springer-Verlag, New York, pp. 21-61.

Kolmogorov, A. N., 1951, Solution of a problem in probability theory connected with the problem of mechanism of stratification: Trans. Am. Math. Soc., 53, pp. 171-177.

Krumbein, W. C., 1967, FORTRAN IV computer program for Markov chain experiments in geology: Kansas Geol., Sur. Comp. Contributions, 13, pp. 1-38.

Krumbein, W. C., and Graybill, F. A., 1965, An introduction to statistical models in geology, McGraw-Mill, New York, 475p.

Lajoie, J., 1972, Slump fold axis orientations: an indication of paleoslope?: Jour. Sed. Petrology, v. 42, pp. 584-586.

Leible, K. A., 1975, The paleotectonic significance of two Middle Ordovician polymictic conglomerates near South Holston Dam, Tennessee, and Avens Bridge, Virginia, unpublished thesis, Blacksburg, 89p.

Lindsay, J. F., 1966, Carboniferous subaqueous mass movement in the Manning-Macleay Basin, Kempur, New South Wales: Jour. Sed. Petrology, v. 36, pp. 719-732.

Lindsay, J. F., 1968, The development of clast fabric in mud flows: Jour. Sed. Petrology, v. 38, pp. 1242-1252.

Link, M. H., 1975, Matilija sandstone: a transition from deep-water turbidite to shallow marine deposition in the Eocene of California: Jour. Sed. Petrology, v. 45, pp. 63-78.

Lumsden, D. N., 1971, Markov chain analysis of carbonate rocks: applications, limitations, and implications as exemplified by the Pennsylvanian System in southern Nevada: Geol. Soc. America Bull., v. 82, pp. 447-462.

McCammon, R. B., 1969, Multivariate methods in geology, *in* Fenner, P. F., covener, Models of geologic processes, American Geol. Inst. Short Course, Philadelphia, pp. RM-A-1-RM-E-11.

McCrossan, R. G., 1961, Resistivity mapping and petrophysical study of upper Devonian inter-reef clacereous shales of central Alberta, Canada: Bull. American Assoc. Petrol. Geol., v. 45, pp. 441-470.

Meyer, P. L., 1972, Introductory probability and statistical applications, Addison-Wesley, Reading, 367p.

Middleton, G. V., 1967, Experiments on density and turbidity currents. III. Deposition of sediment: Canadian Jour. Earth Sci., v. 4, pp. 475-505.

Middleton, G. V., 1970, Experimental studies related to problems of flysch sedimentation, *in* Lajoie, J., ed., Flysch sedimentology in North America, Geol. Assoc. Canada Spec. Pub. 7, pp. 253-272.

Middleton, G. V., and Hampton, M. A., 1973, Sediment gravity flows: mechanics of flow and deposition, *in*, Middleton, G. V., and Bouma, A. H. (cochairmen), Turbidites and deep water sedimentation: Pacific Coast Section, Soc. Econ. Paleontologists and Mineralogists, Los Angeles, pp. 1-38.

Miller, R. L., and Kahn, J. S., 1962, Statistical analysis in the geological sciences, John Wiley, New York, 483p.

Mitzutani, S., and Hattori, I., 1972, Stochastic analysis of bed-thickness distribution of sediments: Jour. Int. Ass. Math. Geology, v. 4, pp. 123-146.

Mutti, E., and Ricci-Luchi, F., 1972, Le torbiditi dell' Appennino settentrionale: introduzione all'-analisi di facies: Mem. Soc. Geol. Italia, v. 11, pp. 161-199.

Nelson, C. H., Mutti, E., and Ricci-Luchi, F., 1974, Criteria for distinguishing thin-bedded turbidites deposited in proximal overbank and distal basin plain environments (abstr): Geol. So. America, Abst. with Programs, v. 6, pp. 887-888.

Neuman, R. B., 1955, Stratigraphy of the Middle Ordovician series of the type Tellico-Sevier belt: U.S. Geol. Survey Prof. Paper 274-F, 136p.

Nie, W. H., Hull, C. H., Jenkins, J. G., Steinbrenner, K., and Brent, D. H., 1975, SPSS: statistical package for the social sciences, McGraw-Hill, New York, 675p.

Normark, W. R., 1970, Growth patterns of deep-sea fans: American Assoc. Petrol. Geol. Bull., v. 54, pp. 2170-2195.

Normark, W. R., 1974, Submarine canyons and fan valleys: factors affecting growth patterns of deep-sea fans, *in* Dott, R. H., and Shaver, R. H., eds., Modern and ancient geosynclinal sedimentation, SEPM Spec., Pub. 19, pp. 56-68.

Normark, W. R., 1978, Fan valleys, channels, and depositional lobes on modern submarine fans: characters for recognition of sandy turbidite environments: Am. Assoc. Petrol. Geol. Bull., v. 62, pp. 912-931.

Otto, G. H., 1938, The sedimentation unit and its use in field sampling: Jour. Geol., v. 46, pp. 569-582.

Pearson, Karl, 1901, On lines and planes of closest fit to systems of points in space: Philosophical Magazine, v. 6, pp. 559-572.

Pett, J. W., and Walker, R. G., 1971a, Relationship of flute cast morphology to internal sedimentary structures in turbidites: Jour. Sed. Petrology, v. 41, pp. 1156-1158.

Pett, J. W., and Walker, R. G., 1971b, "Relationship of flute cast morphology to internal sedimentary structures in turbidites," a reply: Jour. Sed. Petrology, v. 41, pp. 1156-1158.

Pettijohn, F. J., 1975, Sedimentary rocks, Harper and Row, New York, 628p.

Rao, J. S., and Sengupta, S., 1972, Mathematical techniques for paleocurrent analysis: Mathematical Geology, v. 4, pp. 235-247.

Rees, A. I., 1968, The production of preferred orientation in a concentrated dispersion of elongated and flattened grains: Jour. Geology, v. 76, pp. 457-465.

Ricci-Luchi, F., 1975, Depositional cycles in two turbidite formations of northern Apennines (Italy): Jour. Sed. Petrology, v. 45, pp. 3-43.

Rieke, H. H., and Chilingarian, G. V., 1974, Compaction of argillaceous sediments, Elsevier, New York, 424p.

Rivlina, T. S., 1970, A stochastic model of stratification (The case of unlimited interstratal erosion), *in* Romanova, M. A., and Sarmonova, eds., Topics in mathematical geology, Consultants Bureau, New York, pp. 142-150.

Rocheleau, M., and Lajoie, J., 1974, Sedimentary structures in resedimented conglomerates of the Cambrian flysch, L' Islet, Quebec Appalachians: Jour. Sed. Petrology, v. 44, pp. 826-836.

Rummel, R. J., 1970, Applied factor analysis, Northwestern University Press, Evanston, 617p.

Rust, B. R., 1972, Pebble orientation in fluvial sediments: Jour. Sed. Petrology, v. 42, pp. 384-388.

Sallenger, A. A., 1979, Inverse grading and hydraulic equivalence in grain-flow deposits: Jour. Sed. Petrology, v. 49, pp. 553-562.

Scheidegger, A. E., and Potter, P. E., 1965, Textural studies of graded bedding: observation and theory: Sedimentology, v. 5, pp. 265-276.

Schwarzacher, W., 1975, Sedimentation models and quantitative stratigraphy, Elsevier, New York, 382p.

Selley, R. C., 1979, Dipmeter and log motifs in North Sea submarine fans: American Assoc. Petrol. Geol. Bull., v. 63, pp. 905-917.

Shanmugan, G., 1978, The stratigraphy, sedimentology, and tectonics of the Middle Ordovician Sevier Shale basin in East Tennessee, unpublished dissertation, The University of Tennessee, Knoxville, 222p.

Shanmugan, G., and Walker, K. R., 1978, Tectonic significance of distal turbidites in the Middle Ordovician Blockhouse and lower Sevier Formations in East Tennessee: Am. Jour. Sci., v. 278, pp. 551-578.

Stanley, D. J., 1974, Pebbly mud transport in the head of Wilmington Canyon: Marine Geology, v. 16, pp. M1-M8.

Stanley, D. J., and Bertrand, J. P., 1979, Penrose Conference report: submarine slope, fan, and trench sedimentation--new concepts and problem solving: Geology, v. 7, pp. 49-52.

Stanely, D. J., and Unrug, R., 1972, Submarine channel deposits, fluxoturbidites, and other indicators of slope and base-of slope environments in modern and ancient marine basins, *in* Rigby, J, K., and Hamblin, W. K., eds., Recognition of ancient sedimentary environments, SEPM Spec. Pub., 16, pp. 287-340.

Stauffer, P. H., 1967, Grain flow deposits and their implications, Santa Ynez Mountains, California: Jour. Sed. Petrology, v. 37, pp. 487-508.

Teodorovich, G. I., and Chernov, A. A., 1968, Character of changes with depth in productive deposits of Apsheron oil-gas-bearing region: Soviet Geol., v. 4, pp. 83-93.

Till, R., 1974, Statistical methods for the earth scientist, John Wiley and Sons, New York, 154p.

van Olphen, H., 1963, An introduction to clay colloid chemistry, Interscience, New York, 301p.

Walker, K. R., and Keller, F. B., 1977, Tellico formation; submarine fan, proximal to distal turbidite environments, *in* Ruppel, S. C., and Walker, K. R., The ecostratigraphy of the Middle Ordovician of the southern Appalachians (Kentucky, Tennessee, and Virginia), U.S.A.: a field excursion, The University of Tennessee, Knoxville, pp. 134-140.

Walker, R. G., 1967, Turbidite sedimentary structures and their relationship to proximal and distal depositional environments: Jour. Sed. Petrology, v. 37, pp. 25-43.

Walker, R. G., 1970, Review of the geometry and facies organization of turbidites and turbidite-bearing basins, *in* Lajoie, J., ed., Flysch sedimentology of North America, Geol. Assoc. Canada Spec. Paper 7, pp. 219-251.

Walker, R. G., 1975, Generalized facies models for resedimented conglomerates of turbidite association: Geol. Soc. America Bull., v. 86, pp. 737-748.

Walker, R. G., 1977, Deposition of upper Mesozoic resedimented conglomerates and associated turbidites in southwestern Oregon: Geol. Soc. America Bull., v. 88, pp. 273-285.

Walker, R. G., 1978, Deep-water sandstone facies and ancient submarine fans: Models for exploration for stratigraphic traps: American Assoc. Petro. Geol., v. 62, pp. 932-966.

Walker, R. G., and Mutti, E., 1973, Turbidite facies and facies associations, *in* Middleton, G. V., and Bouma, A. H. (cochairmen), Turbidites and deep water sedimentation: Pacific Coast Section, SEPM, Los Angeles, pp. 119-157.

Winkler, R. L., and Hays, W. L., 1975, Statistics, probability, inference, and decision, Holt Rinehart, New York, 889p.

Woodcock, N. H., 1976, Structural style in slump sheets: Ludlow series, Powys, Wales: Jour. Geol. Soc. London, v. 132, pp. 399-415.

APPENDIXES

APPENDIX A

OUTCROP LOCATIONS AND MEASURED SECTIONS

The following tables contain measured sections from four of the six outcrops studied. ULCD and LLCD are not included since only a single bed from each, the large diamictite-slump bed, was examined closely. Description of these diamictite beds is contained in Chapter 3. The tables show bed number, thickness, cumulative thickness, and the classification of the bed in Walker's (1978) terminology where 1 represents classical turbidites; 2, massive sandstones; 3, pebbly sandstones; 4, clast-supported conglomerates; 5, matrix-supported beds. In the case of the turbidites, the Bouma (1962) notation is used with D, E, and interturbidite divisions all simply labeled as "D" (adapted from Walker, 1967). Problematic assignments have an accompanying question mark in their identification cell. Since maximum bed thickness is the parameter of bed thickness used, some cumulative thicknesses exceed actual stratigraphic thickness. This is especially true for SHDC and AFC.

SHDC, Table A-1, is located on the access road to South Holston Dam. It is approximately 1 km west from the dam in a steep cut on the north side of the road.

AFC, Table A-2, is located 1-1/2 km southeast of Avens Bridge on Virginia Route 672. It is located on the south side of the road.

Table A-1. Measured section, outcrop SHDC

Bed Number	Bed Thickness (cm)	Cumulative Thickness (cm)	Lithotype	Conglomerate Identification
1	base unexposed	1.00	4	I
2	150	2.50	4	II,III
3	350	6.00	4	IV,VI
4	130	7.30	4	V
5	250	9.80	5	(IX)?
6	100	10.80	4	VII
7	150	12.30	4	VIII
8	250	14.80	4	X
9	100	15.80	3	
10	120	17.00	3	
11	70	17.70	3	
12	30	18.00	2	
13	40	18.40	2	
14	125	19.65	3	
15	60	20.25	2	
16	55	20.80	2	
17	45	21.25	2	
18	30	21.55	2	
covered	400	25.55	--	
19	77	26.32	2	
20	25	26.57	2	
21	30	26.87	2	
covered	400	30.87	--	
22	45	31.32	2	
covered	100	32.32	--	
23	45	32.77	2	
24	35	33.12	2	
25	18	33.30	1 D's	
26	25	33.55	1 AD	
27	20	33.75	1 AD	
28	30	34.05	2	
29	70	34.75	2	
30	145	36.20	1 AD	
31	40	36.60	1 D's	
32	110	37.70	2	
33	45	38.15	1 D's	
34	65	38.80	1 ACD	

Table A-2. Measured section, outcrop AFC

Bed Number	Bed Thickness (cm)	Cumulative Thickness (m)	Lithotype
1	45	0.45	4
2	30	0.75	3
3	85	1.60	3,4
4	500	6.60	5
5	42	7.02	3
6	30	7.32	3
7	9	7.41	3
8	55	7.96	3
9	60	8.56	5
10	20	8.76	3
11	16	8.92	3
12	61	9.53	2
13	13	9.66	2
14	25	9.91	3
15	40	10.31	2
16	32	10.63	2
17	27	10.90	2
18	17	11.07	2
19	15	11.22	2
20	7	11.29	2
21	55	11.84	3
22	28	12.12	2
23	70	12.82	2
24	30	13.12	2
25	20	13.32	2
26	30	13.62	3
27	210	15.72	5
28	30	16.02	4
29	81	16.83	4
30	60	17.43	3
31	30	17.73	3
32	165	19.38	2
33	20	19.58	3
34	28	19.86	3
35	18	20.04	4
36	15	20.19	3
37	15	20.34	3
38	24	20.58	2
39	35	20.93	4
40	30	21.23	2
41	23	21.46	3
42	300	24.46	2
43	200	26.46	5

Table A-2. (continued)

Bed Number	Bed Thickness (cm)	Cumulative Thickness (m)	Lithotype
44	130	27.76	2
45	13	27.89	2
46	60	28.49	3
47	45	28.94	2
48	400	32.94	5
49	32	33.26	3
50	52	33.78	2
51	105	34.83	4
52	31	35.14	3
53	50	35.64	2
54	15	35.79	4
55	90	36.69	2
56	45	37.14	3
57	20	37.34	3
58	90	38.24	2
59	35	38.59	4
60	130	39.89	4
61	80	40.69	2

USHDS, Table A-3, is located in an exposure approximately 275 m above South Holston Dam on the north side of the river (now lake), and is plainly visible from the top of the dam itself.

LSHDS-A (Table A-4), LSHDS-B (Table A-5), and LSHDS-C (Table A-6) compose a stratigraphic section that begins approximately 3/4 km west of the dam on the north side of the access road. LSHDS-A is lowest in the section; LSHDS-C is highest and is terminated by a shale unit that adjoins, and is mostly covered, by the dam itself.

ULCD is located approximately 3.6 km south of the US 421 Bridge across South Holston Lake. The outcrop is on US 421 on the north side of the road.

LLCD is located approximately 3.2 km south of the US 421 Bridge across South Holston Lake. The outcrop is on US 421 on the south side of the road.

Table A-3. Measured section, outcrop USHDS

Bed Number	Bed Thickness (cm)	Cumulative Thickness (m)	Lithotype
1	10	0.10	2
2	102	1.12	1 AD
3	18	1.20	5
4	40	1.60	1 AD
5	12	1.72	5
6	92	2.64	2
7	30	2.94	5
8	80	3.74	3
9	60	4.34	2
10	15	4.49	5
11	75	5.24	3
12	10	5.34	5
13	17	5.51	1 AD
14	70	6.21	2
15	150	7.71	2
16	30	8.01	2
17	7	8.08	2
18	26	8.34	2
19	18	8.52	2
20	20	8.72	2
21	27	8.99	2
22	10	9.09	2
23	115	10.24	2
24	55	10.79	2
25	34	11.13	2
26	70	11.83	2
27	78	12.61	2
28	30	12.91	2
29	100	13.91	5
30	80	14.71	2
31	175	16.46	2
32	150	17.96	2
33	80	18.76	3
34	24	19.00	3
35	20	19.20	3
36	170	20.90	2
37	130	22.20	2
38	520	27.40	2 (3)
39	500	32.40	2 (3)
40	80	33.20	2
41	150	34.70	2
42	190	36.60	2
43	100	37.60	2

Table A-3. (continued)

Bed Number	Bed Thickness (cm)	Cumulative Thickness (m)	Lithotype
44	108	38.68	2
45	104	39.72	2
46	60	40.32	2
47	20	40.52	1 AD
48	6	40.58	1 AD
49	30	40.88	1 AD
50	45	41.33	1 AD
51	18	41.51	1 AD
52	53	42.04	2
53	12	42.16	2
54	17	42.33	2
55	15	42.48	1 D(?)
56	14	42.62	1 D
57	40	43.02	2
58	10	43.12	1 D
59	10	43.22	1 D
60	40	43.62	5
61	120	44.82	3
62	30	45.12	2
63	60	45.72	1 AD(?)
64	18	45.90	1 AD
65	83	46.73	2
66	13	46.86	1 ACD
67	7	46.93	1 ACD
68	10	47.03	1 AD
69	175	48.78	5
70	10	48.88	1 AD

Table A-4. Measured section, outcrop LSHDS-A

Bed Number	Bed Thickness (cm)	Cumulative Thickness (m)	Lithotype
1	21.0	0.210	1 AD
2	18.0	0.390	1 CD
3	25.0	0.640	1 D
4	1.5	0.655	1 D
5	1.0	0.665	1 D
6	2.2	0.687	1 D
7	4.0	0.727	1 D
8	2.4	0.751	1 D
9	1.0	0.761	1 D
10	1.9	0.780	1 D
11	10.0	0.880	1 D
12	10.0	0.980	1 A
13	60.0	1.580	1 AD
14	11.7	1.697	1 D
15	2.0	1.717	1 D
16	1.2	1.729	1 D
17	14.5	1.874	1 D
18	6.4	1.938	1 D
19	10.0	2.038	1 AD
20	5.3	2.091	1 D
21	3.9	2.130	1 D
22	11.4	2.244	1 D
23	11.6	2.360	1 ACD
24	4.7	2.407	1 AD
25	3.8	2.445	1 AD
26	12.0	2.565	1 ACD
27	4.7	2.612	1 D
28	5.7	2.669	1 D
29	5.3	2.722	1 D
30	10.9	2.831	1 AD
31	2.8	2.859	1 D
32	3.5	2.894	1 D
33	5.0	2.944	1 D
34	4.7	2.991	1 D
35	1.9	3.010	1 D
36	1.1	3.021	1 D
37	14.0	3.161	1 D
38	17.0	3.331	1 AD
39	20.0	3.531	1 ACD
40	18.0	3.711	1 A
41	13.0	3.841	1 ACD
42	5.5	3.896	1 D
43	3.0	3.926	1 D

Table A-4. (continued)

Bed Number	Bed Thickness (cm)	Cumulative Thickness (m)	Lithotype
44	16.0	4.086	1 CD
45	8.5	4.171	1 AD
46	13.0	4.301	1 AD
47	14.0	4.441	1 AD
48	1.0	4.451	1 D
49	2.0	4.471	1 D
50	0.6	4.477	1 D
51	0.9	4.486	1 D
52	2.0	4.506	1 D
53	1.1	4.517	1 D
54	1.1	4.528	1 D
55	1.4	4.542	1 D
56	1.0	4.552	1 D
57	1.2	4.564	1 D
58	10.4	4.668	1 D
59	130.0	5.968	1 AD
60	48.5	6.453	1 AD
61	41.0	6.863	1 AD
62	80.0	7.663	1 AD
63	16.0	7.823	1 CD
64	10.0	7.923	1 AD
65	53.0	8.453	1 ACD
66	14.3	8.596	5 (?)A
67	18.0	8.776	1 AD
68	12.5	8.901	1 D
69	7.0	8.971	1 D
70	10.0	9.071	1 D
71	13.0	9.201	5 (?)A
72	20.0	9.401	1 D
73	4.0	9.441	5 (?)
74	3.0	9.471	1 D
75	7.0	9.541	1 D
76	7.0	9.611	1 D
77	8.0	9.691	1 D
78	26.0	9.951	1 AD
79	21.1	10.162	1 AD
80	3.5	10.197	1 D
81	12.0	10.317	1 ACD
82	30.5	10.622	1 ACD
83	34.0	10.962	1 ACD
84	37.0	11.332	1 AD
85	8.0	11.412	1 D
86	6.0	11.472	1 D

Table A-4. (continued)

Bed Number	Bed Thickness (cm)	Cumulative Thickness (m)	Lithotype
87	14.0	11.612	1 ACD
88	12.0	11.732	1 ACD
89	62.0	12.352	1 ACD
90	57.0	12.922	1 ACD
91	10.0	13.022	1 CD
92	29.0	13.312	1 D
93	44.5	13.757	1 D's
94	88.0	14.637	1 AD
95	65.0	15.287	1 AD
96	29.0	15.577	1 AD
97	22.0	15.797	1 ACD
98	4.5	15.842	1 D
99	3.5	15.877	1 D
100	4.0	15.917	1 D
101	6.0	15.977	1 D
102	12.0	16.097	1 D
103	33.0	16.427	1 AD
104	30.0	16.727	1 AD
105	31.0	17.037	1 AD
106	45.7	17.494	1 D's
107	6.5	17.559	1 D
108	10.0	17.659	1 AD
109	8.0	17.739	1 AD
110	27.0	18.009	1 AD
111	117.0	19.179	1 ACD
112 equals LSHDS-B-1			

Table A-5. Measured section, outcrop LSHDS-B

Bed Number	Bed Thickness (cm)	Cumulative Thickness (m)	Lithotype
1	91.0	0.910	1 ACD
2	26.0	1.170	1 D
3	30.0	1.470	1 D's
4	14.5	1.615	1 D
5	9.0	1.705	1 D
6	12.0	1.825	1 CD
7	64.0	2.465	1 ACD
8	72.0	3.185	1 AD
9	8.0	3.265	1 AD
10	6.0	3.325	1 D
11	8.0	3.405	1 CD
12	5.0	3.455	1 D
13	23.0	3.685	1 CD
14	58.0	4.265	1 BD
15	40.0	4.665	5
16	24.0	4.905	1 D
17	58.0	5.485	1 AD
18	42.0	5.905	1 AD
19	16.0	6.065	1 AD
20	13.0	6.195	1 AD
21	6.5	6.260	1 D
22	15.0	6.410	1 D
23	30.0	6.710	1 AD
24	4.2	6.752	1 D
25	53.0	7.282	1 AD
26	8.0	7.362	1 D
27	2.5	7.387	1 D
28	24.0	7.627	1 D
29	7.0	7.697	1 D
30	15.0	7.847	1 CD
31	28.0	8.127	1 ACD
32	8.5	8.212	1 D
33	17.0	8.382	5
34	14.0	8.522	1 D
35	7.0	8.592	1 D
36	38.0	8.972	1 A
37	15.0	9.122	5
38	18.0	9.302	1 D
39	57.0	9.872	1 ACD
40	15.5	10.027	1 D
41	6.0	10.087	1 D
42	33.0	10.417	1 AD
43	26.0	10.677	1 AD
44	58.0	11.257	1 AD

Table A-5. (continued)

Bed Number	Bed Thickness (cm)	Cumulative Thickness (m)	Lithotype
45	17.0	11.427	1 D
46	27.0	11.697	1 ACD
47	12.0	11.817	1 AD
48	11.0	11.927	1 AD
49	40.0	12.327	1 AD
50	9.0	12.417	1 D
51	5.0	12.467	1 D
52	6.0	12.527	1 D
53	6.0	12.587	1 D
54	5.0	12.637	1 D
55	26.0	12.897	1 ACD
56	20.0	13.097	1 AD
57	12.0	13.217	1 D
58	11.0	13.327	1 D
59	41.0	13.737	5
60	20.0	13.937	1 D
61	6.0	13.997	1 D
62	15.0	14.147	1 D
63	12.0	14.267	1 D
64	5.5	14.322	1 D
65	11.0	14.432	1 D
66	7.0	14.502	1 D
67	8.0	14.582	1 D
68	1.0	14.592	1 D
69	7.0	14.662	1 D
70	26.0	14.922	1 AD
71	18.0	15.102	1 ACD
72	12.0	15.222	5
73	7.0	15.292	1 D
74	11.0	15.402	1 D
75	60.0	16.002	1 AD
76	9.5	16.097	1 D
77	9.0	16.187	1 D
78	5.0	16.237	1 D
79	8.5	16.322	1 D
80	25.0	16.572	1 A
81	16.0	16.732	1 AD
82	10.0	16.832	1 A
83	27.0	17.102	1 CD
84	25.0	17.352	1 AD
85	9.0	17.442	1 ACD
86	5.0	17.492	1 D
87	8.0	17.572	1 D
88	6.0	17.632	1 D

Table A-5. (continued)

Bed Number	Bed Thickness (cm)	Cumulative Thickness (m)	Lithotype
89	5.5	17.687	1 D
90	11.0	17.797	5
91	17.0	17.967	1 AD
92	18.0	18.147	1 AD
93	20.0	18.347	1 ACD
94	4.5	18.392	1 D
95	7.5	18.467	1 D
96	7.0	18.537	1 AD
97	3.0	18.567	1 AD
98	11.0	18.677	1 D
99	7.0	18.747	1 D
100	6.0	18.807	1 D
101	18.0	18.987	1 CD
102	61.0	19.597	1 AD
103	15.0	19.747	1 CD
104	11.0	19.857	1 CD
105	8.0	19.937	1 D
106	13.0	20.067	1 D
107	7.5	20.142	1 D
108	20.0	20.342	1 AD
109	17.0	20.512	1 AD
110	14.0	20.652	1 A
111	19.0	20.842	1 A
112	5.0	20.892	1 AD
113	5.0	20.942	1 D
114	2.4	20.966	1 D
115	2.0	20.986	1 D
116	8.0	21.066	1 D
117	20.0	21.266	1 AD
118	8.0	21.346	1 D
119	2.0	21.366	1 D
120	6.0	21.426	1 D
121	4.5	21.471	1 D
122	20.5	21.676	1 D
123	7.0	21.746	1 D
124	14.0	21.886	1 D
125	12.0	22.006	1 D
126	8.0	22.086	1 D
127	11.5	22.201	1 D
128	13.0	22.331	1 D
129	6.0	22.391	1 D
130	6.0	22.451	1 D
131	33.0	22.781	5
132	5.6	22.837	1 AD

Table A-5. (continued)

Bed Number	Bed Thickness (cm)	Cumulative Thickness (m)	Lithotype
133	7.3	22.910	1 D
134	6.0	22.970	1 D
135	5.0	23.020	1 D
136	2.5	23.045	1 D
137	4.0	23.085	1 D
138	12.0	23.205	1 D
139	12.0	23.325	1 D
140	15.0	23.475	1 D
141	4.0	23.515	1 D
142	7.0	23.585	1 D
143	13.0	23.715	1 D
144	10.0	23.815	1 AD
145	9.0	23.905	1 AD
146	5.0	23.955	1 AD
147	3.5	23.990	1 AD
148	22.0	24.210	1 ACD
149	2.5	24.265	1 D
150	5.0	24.315	1 D
151	7.0	24.385	1 D
152	4.0	24.425	1 D
153	4.0	24.465	1 D
154	3.0	24.495	1 D
155	2.5	24.520	1 D
156	1.5	24.535	1 D
157	2.0	24.555	1 D
158	2.0	24.575	1 D
159	23.5	24.810	1 A
160	23.0	25.040	1 A
161	31.0	25.350	1 AD
162	23.0	25.580	1 ACD
163	11.0	25.690	1 AD
164	7.0	25.760	1 D
165	9.0	25.850	1 D
166	2.5	25.875	1 D
167	6.5	25.940	1 D
168	8.0	26.020	5 A(?)
169	12.0	26.140	1 CD
170	40.0	22.540	1 ACD
171	22.0	22.760	1 A
172	14.0	22.900	1 A
173	56.0	23.460	1 ABCD
174	10.0	23.560	1 AD
175	8.0	23.640	1 ACD
176	13.0	23.770	1 ACD

Table A-5. (continued)

Bed Number	Bed Thickness (cm)	Cumulative Thickness (m)	Lithotype
177	63.0	24.400	1 AD
178	6.0	24.460	1 D
179	7.0	24.530	1 D
180	69.0	25.220	1 ACD
181	14.0	25.360	1 AD
182	9.0	25.450	1 AD
183	5.0	25.500	1 CD
184	28.0	25.780	1 ACD
185	14.0	25.920	1 CD
186	17.0	26.090	1 ABCD
187	8.0	26.170	1 D
188	5.0	26.220	1 D
189	8.0	26.300	1 D
190	25.0	26.550	1 ACD
191	15.0	26.700	1 ACD
192	9.0	26.790	1 ACD
193	4.0	26.830	1 D
194	9.0	26.920	1 D
195	8.5	27.005	1 CD
196	6.5	27.070	1 CD
197	5.0	27.120	1 ACD
198	4.0	27.160	1 CD
199	4.5	27.205	1 D
200	9.5	27.300	1 D
201	4.0	27.340	1 D
202	3.0	27.370	1 D
203	2.5	27.395	1 D
204	5.0	27.445	1 D
205	4.5	27.490	1 D
206	3.5	27.525	1 D
207	1.5	27.540	1 D
208	3.5	27.575	1 D
209	7.0	27.645	1 D
210	19.0	27.835	5 (?)
211	12.0	27.955	1 CD
212	25.0	28.205	1 A
213	16.0	28.365	1 CD
214	18.0	28.545	1 AD
215	4.0	28.585	1 D
216	5.0	28.635	1 D
217	7.0	28.705	1 D
218	8.5	28.790	1 CD
219	10.0	28.890	1 D

Table A-5. (continued)

Bed Number	Bed Thickness (cm)	Cumulative Thickness (m)	Lithotype
220	2.5	28.915	1 D
221	13.5	29.050	1 ACD
222	5.5	29.105	1 D
223	4.0	29.145	1 D
224	15.5	29.300	1 A
225	7.5	29.375	1 AD
226	6.0	29.435	1 CD
227	8.0	29.515	1 CD
228	25.0	29.765	1 ACD
229	9.0	29.855	1 D
230	55.0	30.405	1 ACD
231	65.0	31.055	1 ACD
232	30.0	31.355	1 CD
233	27.0	31.625	1 CD
234	9.0	31.715	1 D
235	8.0	31.795	1 D
236	7.0	31.865	1 D
237	12.0	31.985	5 (?)
238	19.0	32.175	1 CD
239	23.0	32.405	1 CD
240	11.0	32.515	1 D
241	12.0	32.635	1 D
242	4.5	32.680	1 D
243	3.0	32.710	1 D
244	3.5	32.745	1 D
245	6.0	32.805	1 AD
246	31.0	33.115	1 AD
247	7.0	33.185	1 AD
248	6.0	33.245	1 AD
249	4.0	33.285	1 D
250	19.0	33.475	5
251	7.0	33.545	1 D
252	6.0	33.605	1 D
253	8.0	33.685	1 D
254	6.0	33.745	1 D
255	13.0	33.875	1 D
256	11.5	33.990	1 D
257	3.0	34.020	1 D
258	13.0	34.150	1 D
259	12.5	34.275	1 D
260	13.5	34.410	1 D
261	3.0	34.440	1 D
262	7.0	34.510	1 D

Table A-5. (continued)

Bed Number	Bed Thickness (cm)	Cumulative Thickness (m)	Lithotype
263	14.0	34.650	1 D
264	3.0	34.680	1 D
265	8.0	34.760	1 D
266	4.0	34.800	1 D
267	7.0	34.870	1 D
268	11.0	34.980	1 D
269	5.5	35.035	1 D
270	8.0	35.115	1 D
271	8.0	35.195	1 AD
272	14.0	35.335	1 D
273	2.0	35.355	1 D
274	4.0	35.395	1 D
275	3.5	35.430	1 D
276	3.5	35.465	1 D
277	13.0	35.595	1 ACD
278	15.0	35.745	1 ACD
279	8.0	35.825	1 ACD
280	13.5	35.960	1 D
281	2.0	35.980	1 D
282	4.0	36.020	1 D
283	11.5	36.135	1 D
284	11.5	36.250	1 D
285	10.0	36.350	1 D
286	4.0	36.390	1 D
287	4.0	36.430	1 D
288	12.0	36.550	1 D
289	7.0	36.620	1 D
290	6.0	36.680	1 D
291	7.5	36.755	1 D
292	4.0	36.795	1 D
293	3.5	36.830	1 D
294	1.5	36.845	1 D
295	6.0	36.905	1 D
296	2.0	36.925	1 D
297	10.0	37.025	1 D
298	0.9	37.034	1 D
299	1.5	37.049	1 D
300	4.5	37.094	1 D
301	11.5	37.209	1 D
302	4.5	37.254	1 D
303	5.5	37.309	1 D
304	1.0	37.319	5 (?)
305	1.0	37.329	5 (?)

Table A-5. (continued)

Bed Number	Bed Thickness (cm)	Cumulative Thickness (m)	Lithotype
306	3.5	37.364	1 D
307	3.5	37.399	1 D
308	2.0	37.419	1 D
309	3.0	37.449	1 D
310	3.0	37.479	1 D
311	10.0	37.579	1 CD
312	9.0	37.669	1 D
313	7.0	37.739	1 D
314	4.0	37.779	1 D
315	5.0	37.829	1 D
316	3.0	37.859	1 D
317	6.0	37.919	1 D
318	3.5	37.954	1 D
319	2.5	37.979	1 D
320	4.0	38.019	1 D
321	5.0	38.069	1 D
322	2.0	38.089	1 D
323	8.0	38.169	1 D
324	7.0	38.239	1 D
325	5.0	38.289	1 D
326	4.5	38.334	1 D
327	5.0	38.384	1 D
328	4.0	38.424	1 D
329	3.0	38.454	1 D
330	6.5	38.519	1 D
331	6.5	38.584	1 D
332	2.5	38.609	1 D
333	1.5	38.624	1 D
334	2.5	38.649	1 D
335	2.0	38.669	1 D
336	3.0	38.699	1 D
337	10.0	38.799	1 D
338	2.5	38.824	1 D
339	18.0	39.004	5 (?)
340	7.0	39.074	1 D
341	5.0	39.124	1 D
342	4.0	39.164	1 D
343	1.8	39.182	1 D
344	3.0	39.212	1 D
345	5.5	39.267	1 D
346	1.5	39.282	1 D
347	5.0	39.332	1 D
348	3.0	39.362	1 D

Table A-5. (continued)

Bed Number	Bed Thickness (cm)	Cumulative Thickness (m)	Lithotype
349	4.5	39.407	1 D
350	2.0	39.427	1 D
351	4.0	39.467	1 D
352	5.0	39.517	1 D
353	7.0	39.587	1 D
354	3.5	39.622	1 D
355	2.3	39.645	1 D
356	4.5	39.690	1 D
357	3.2	39.722	1 D
358	4.3	39.765	1 D
359	5.5	39.820	1 D
360	12.0	39.940	1 D
361	5.0	39.990	1 D
362	2.0	40.010	1 D
362	2.5	40.035	1 D
363	3.5	40.070	1 D
364	2.5	40.095	1 D
365	2.5	40.120	1 D
366	4.5	40.165	1 D
367	10.0	40.265	1 D
368	7.0	40.335	1 D
369	6.0	40.395	1 D
370	9.0	40.485	1 D
371	11.0	40.595	1 D
372	3.5	40.630	1 D
373	5.5	40.685	1 D
374	18.0	40.865	1 D
375 = LSHDS-C-1			

Table A-6. Measured section, outcrop LSHDS-C

Bed Number	Bed Thickness (cm)	Cumulative Thickness (m)	Lithotype
1	34.0	0.340	1 AD
2	7.0	0.410	1 D
3	36.0	0.770	1 ACD
4	18.0	0.950	1 CD
5	11.3	1.063	1 D
6	6.5	1.128	1 CD
7	5.5	1.183	1 CD
8	9.0	1.273	1 CD
9	2.6	1.299	1 D
10	1.3	1.312	1 D
11	1.2	1.324	1 D
12	1.5	1.339	1 D
13	7.0	1.409	1 D
14	4.0	1.449	1 D
15	11.0	1.559	1 D
16	3.3	1.592	1 D
17	7.5	1.667	5 ?
18	11.2	1.779	1 D
19	8.0	1.859	1 AD
20	46.0	1.905	1 ABCD
21	33.0	2.235	5
22	38.0	2.615	1 ABCD
covered	30.0	2.915	--
23	15.0	3.065	1 AD
covered	150.0	4.565	--
24	5.0	4.615	1 D
25	24.0	4.855	1 D
26	41.5	5.270	1 A
27	26.0	5.530	1 AD
28	12.5	5.655	1 AD
29	25.0	5.905	1 ACD
covered	40.0	6.305	--
30	140.0	7.705	1 ACD
31	23.5	7.940	1 ACD
covered	30.0	8.240	--
32	12.0	8.360	1 AD
33	12.0	8.480	1 CD
34	9.5	8.575	1 CD
covered	25.0	8.825	--
35	32.5	9.150	1 ACD
36	4.5	9.195	1 D
37	4.5	9.240	1 CD
covered	20.0	9.440	--

Table A-6. (continued)

Bed Number	Bed Thickness (cm)	Cumulative Thickness (m)	Lithotype
38	4.2	9.482	1 CD
39	2.5	9.507	1 D
40	1.1	9.518	1 D
41	5.2	9.570	1 D
42	4.2	9.612	1 D
43	5.0	9.662	5
44	28.8	9.950	1 A
45	12.0	10.070	1 AD
46	28.0	10.350	1 AD
47	28.0	10.630	1 ACD
48	24.0	10.870	1 ACD
49	9.5	10.965	1 CD
50	5.0	11.015	1 D
51	7.0	11.085	1 D
52	7.4	11.159	1 D
53	6.8	11.227	1 D
54	2.7	11.254	1 D
55	6.0	11.314	1 D
56	12.0	11.434	1 D
57	8.0	11.514	1 D
58	6.8	11.582	1 D
59	10.3	11.685	1 CD
60	15.0	11.835	1 CD
61	7.5	11.910	1 D
62	90.5	12.815	1 AD
63	19.0	13.005	1 CD
64	6.5	13.070	1 CD
covered	25.0	13.320	--
65	46.5	13.785	1 AD
66	13.5	13.920	1 D
67	7.4	13.994	1 CD
68	5.9	14.053	1 D
69	23.0	14.283	1 D
70	20.0	14.483	1 D
covered	40.0	14.883	--
71	7.0	14.953	1 D
covered	60.0	15.553	--
72	6.0	15.613	1 D
73	9.6	15.709	1 D
74	6.5	15.774	1 D
75	5.0	15.824	1 D
76	8.0	15.904	1 D
77	14.0	16.044	1 D

Table A-6. (continued)

Bed Number	Bed Thickness (cm)	Cumulative Thickness (m)	Lithotype
78	8.0	16.124	1 D
covered	300.0	19.124	--
79	12.0	19.244	1 D
80	6.0	19.304	1 D
81	10.0	19.404	1 D
82	18.0	19.584	1 CD
83	10.5	19.689	1 ACD
covered	25.0	19.939	--
84	27.0	20.209	1 ACD
85	35.0	20.559	1 ACD
86	47.5	21.034	1 ACD
87	35.7	21.391	1 AD
covered	50.0	21.891	--
88	42.0	22.311	1 ACD
89	14.0	22.451	1 D
90	21.0	22.661	1 D
91	6.0	22.721	1 D
92	12.0	22.841	1 CD
93	9.0	22.931	1 CD
94	17.5	23.106	1 D
95	7.0	23.176	1 D
96	5.0	23.226	1 D
97	16.0	23.386	5
covered	160.0	24.986	--
98	45.0	25.436	1 ACD
covered	30.0	25.736	--
99	81.0	26.546	1 ACD
100	12.0	26.666	1 CD
101	5.0	26.716	1 CD
102	18.0	26.896	5
103	12.0	27.016	1 D
104	10.0	27.116	1 CD
105	7.2	27.188	1 CD
106	1.8	27.206	1 D
107	10.0	27.306	1 D
108	15.5	27.461	1 CD
109	12.0	27.581	1 D
110	28.0	27.861	1 CD
111	10.0	27.961	5
112	13.0	28.091	1 D
+ ≃ 10 m thin bedded shale--not individually measured.			

--Unexposed.

APPENDIX B

FACTOR ANALYSIS: DATA AND METHODS

Procedures and Methods of Factor Analysis

The basic problem in factor analysis concerns establishing the simplest, most parsimonious factors that can be adduced to explain the correlations in a given body of variables. The basic assumption is that a variable X can be represented by factor scores (F) and factor loadings (A) as

$$X = FA' \quad \text{or} \quad X' = AF'$$

where the symbol "'" denotes the transpose of a matrix. The correlation matrix R can be represented (Klovan, 1975) by the standardized variable and its transpose X' (ignoring the divisor 1/N) as:

$$R = X'X \ .$$

Then, with substitution

$$R = AF'FA' \ .$$

Since we want the factors to be uncorrelated (orthogonal) the condition on F is:

$$F'F = I$$

where I is the identity matrix. Hence,

$$R = AA' .$$

We set

$$A'A = \Lambda$$

where Λ are the eigenvalues of the correlation matrix. U is the square, orthonormal matrix containing the eigenvectors associated with Λ. Hence,

$$U'RU = \Lambda .$$

The eigenvalues are the numerical solutions to equations which maximize variance. The associated eigenvectors are geometrically the orthogonal axes whose lengths are proportional to their eigenvalues. Multiplying the above equation by U:

$$UU'RU = U\Lambda$$

$$RU = U\Lambda .$$

Then, multiplying by U'

$$RUU' = U\Lambda U'$$

$$R = U\Lambda U' .$$

Because the R matrix has a certain property (Gramian or positive semidefiniteness):

$$R = U\Lambda U' = U\Lambda^{1/2}\Lambda^{1/2}U' = AA'$$

$$A = U\Lambda^{1/2}$$

$$X = FA'$$

$$XA = FA'A$$

$$XA = F$$

$$F = XA \ .$$

Thus, both F and A are solved numerically and values can be placed in the equation

$$X = FA' \ .$$

In this manner, the perplexing problem of knowing neither the variables for the right side of the equation nor their values can be solved for any set of variables X on any number of observations N. (The above presentation follows Kolvan, 1975, closely.)

Data Matrix

The data to which the above analysis is applied is shown in Table B-1. The evaluation of dichotomous and ordinal properties is discussed in the text (pp. 130-132). A list of the properties with the abbreviations with which they will be referred to in all the following factor matrices is shown in Table B-2.

The data as shown in Table B-1 are ideally arranged for R-mode analysis. For Q-mode analysis, the reader should imagine this matrix on its side: the properties become the observations, the beds become the variables.

	.cates		Other Information (Not used in factoring)		
Bed # ig	Partly Preserved Beds	Induration	Bed ID	*Walker (1978)	**Process(es)
1	0	2	Ideal turbidite	1	1
2	0	1	High density turbidite	1	1
3	0	1	Ideal grain flow	1 (?)	2
4	1	0	Ideal debris flow	5	3
5	0	2	SHDC-I	4	1 (?)
6	0	2	SHDC-II	4	1 (?)
7	0	2	SHDC-III	4	1
8	0	2	SHDC-IV	4	1
9	0	1	SHDC-V	4	1 (2)
10	0	2	SHDC-VI	4	1 (2)
11	0	2	SHDC-VII	4	1
12	0	1	SHDC-VIII	4	1
13	0	2	SHDC-IX	4	1
14	0	2	SHDC-X	4	1 (2)
15	0	2	AFC-1	4	1 (2)
16	0	2	AFC-3	4	1
17	0	2	AFC-28	4	1
18	0	2	AFC-29	4	1
19	0	2	AFC-35	4	1
20	0	2	AFC-39	4	1
21	0	2	AFC-51	4	1
22	0	2	AFC-54	4	1
23	0	2	AFC-59	4	1
24	0	2	AFC-60	4	1
25	1	0	AFC-4	5	3
26	1	0	AFC-9	5	3
27	1	0	AFC-27	5	3
28	1	0	AFC-48	5	3
29	2	0	ULCD	5	3 (4)
30	2	0	LLCD	5	3 (4)
31	0	2	LSHDS-B-1	1	1
32	0	1	LSHDS-B-6	1	1
33	0	2	LSHDS-B-7	1	1
34	0	1	LSHDS-B-8	1	1 (2?)
35	0	1	LSHDS-B-9	1	1 (2,3?)
36	0	1	LSHDS-B-11	1	1
37	1	0	LSHDS-B-15	5	4 (3?)
38	0	2	LSHDS-B-17	1	1
39	0	2	LSHDS-B-18	1	1
40	0	1	LSHDS-B-19	1	1
41	1	1	LSHDS-B-20	1	1
42	0	0	LSHDS-B-23	1	1 (3?)
43	0	2	LSHDS-B-25	1	1 (2)
44	0	1	LSHDS-B-30	1	1
45	0	2	LSHDS-B-31	1	1
46	0	0	LSHDS-B-33	5	4 (3)
47	0	1	LSHDS-B-36	1	1 (3?)
48	2	--	LSHDS-B-37	5	4
49	0	2	LSHDS-B-39	1	1 (2)
50	0	2	LSHDS-B-42	1	1
51	0	2	LSHDS-B-43	1	1
52	0	2	LSHDS-B-44	1	1
53	0	2	USHDS-1	2	1 (2)
54	0	2	USHDS-6	2	1
55	0	2	USHDS-9	2	1
56	0	2	USHDS-14	2	1
57	0	2	USHDS-15	2	1

	ates		Other Information (Not used in factoring)		
Bed #	Partly Preserved Beds	Induration	Bed ID	*Walker (1978)	**Process(es)
58	0	2	USHDS-16	2	1
59	0	2	USHDS-17	2	1 (2)
60	0	2	USHDS-18	2	1
61	0	2	USHDS-19	2	1
62	0	2	USHDS-20	2	1
63	0	2	USHDS-21	2	1
64	0	2	USHDS-22	2	1
65	0	2	USHDS-23	2	1
66	0	2	USHDS-24	2	1
67	0	2	USHDS-25	2	1
68	0	2	USHDS-26	2	1
69	0	1	USHDS-27	2	1
70	0	1	USHDS-28	2	1
71	0	2	USHDS-30	2	1
72	0	2	USHDS-31	2	1
73	0	2	USHDS-32	2	1
74	0	2	USHDS-36	2	1
75	0	2	USHDS-37	2	1
76	0	2	AFC-2	3	1 (2)
77	0	1	AFC-33	3	1 (2)
78	0	2	AFC-49	3	1 (2)
79	0	2	AFC-12	2 (3)	1
80	0	2	AFC-14	2 (3)	1
81	0	2	AFC-5	3	1 (2)
82	0	2	AFC-6	3	1
83	0	2	AFC-7	3	1 (2)
84	0	2	AFC-8	3	1
85	0	2	AFC-11	2 (3)	1
86	0	2	AFC-31	3	1
87	0	2	LSHDS-B-46	1	1
88	1	0	USHDS-3	5	3,4
89	1	0	USHDS-5	5	3,4
90	1	0	USHDS-7	5	3,4
91	0	2	LSHDS-B-173	1	1
92	0	2	LSHDS-B-186	1	1
93	2	0	USHDS-29	5	3,4
94	0	2	LSHDS-B-170	1	1
95	2	1	AFC-43	5	4 (3)
96	2	1	SHDC-B	5 (4)	3,4
97	0	1	LSHDS-B-304	?	3 (?)
98	2	0	LSHDS-B-168	1 (?)	3 (?)
99	2	--	USHDS-69	5	4

*

Table B-2. Property abbreviations in factor analysis

Property	Abbreviation	Number
Bed thickness	THICK	1
Maximum clast diameter	DMAX	2
D/10	DID	3
Mean grain size	MEAN	4
Massive texture	MASS	5
Normal distribution grading	NORM	6
Coarse-fraction grading	COFRAC	7
Inverse-to-normal grading	INNORM	8
Stratification	STRAT	9
Matrix-supported	MATRIX	10
Low-flow regime features	LOFLOW	11
Bedding-parallel features	PARLAM	12
Lenticular bed geometry	LENTIC	13
Erosive bed base	EROS	14
Sorting	SORT	15
Partially-preserved beds	PREBED	16
Induration	INDUR	17

Correlation Matrix: R-Mode

The properties of beds in R-mode analysis, recast in the form of a correlation matrix between properties (17 × 17) is shown in Table B-3. The correlation coefficients between pairs of entries are simply computed values of Pearson's r. The values of these coefficients along the diagonal of the matrix, though, bear further treatment. As shown, these values are less than one, even though common sense would suggest to us that the variance of a variable to itself (termed communality) is equal to unity. The difficulty is that the correlation matrix represents a correlation of variables based on underlying *common* factors. Since for any given variable, the common factors may nonuniquely be combined, the communality must in general be less than one. This may be reexpressed by stating that the structure (ontology) of a particular variable is the result of the combinatory interaction of nonuniquely combined common factors plus a unique factor. The communality values are estimated by iterating values of Pearson's r from the factor analysis. Five iterative analyses yielded stable, unchanging values for the communalities, assuming initial values of one. The interpretation of communality is exactly the same as that of variance: it is the square of the correlation values. Consequently, the figures shown in the diagonal of the correlation matrix are the square roots of the communalities.

Under this interpretation of communalities as that percentage of a variable that may be regarded as explainable by the interaction of the other variables, the best communality value for bed thickness "behavior," for example, is 0.50322. This indicates that 50.3% of the thickness

Table B-3. Correlation matrix for R-mode factor analysis

	THICK	DMAX	DID	MEAN	MASS	NORM	COFRAC	INNORM	STRAT	MATRIX	LOFLOW	PARLAM	LENTIC	EROS	SORT	PREBED	INDUR
Thick	.7094																
Dmax	.7725	.9995															
DID	.5495	.9022	.9095														
Mean	.6368	.8839	.9039	.9557													
Mass	.1772	.1167	.1297	-.0299	.7432												
Norm	-.2763	-.2898	-.2405	-.2462	-.4411	.7810											
Cofrac	-.0261	-.1312	-.1105	-.1220	-.1734	-.0877	.6950										
Innorm	.0242	-.0088	.0290	.1323	-.2199	-.2702	.0948	.6732									
Strat	-.0139	-.1514	-.1041	-.0433	-.1306	-.0014	.2062	.3849	.6080								
Matrix	.3029	.3336	.2635	.1521	.3088	-.3734	.3863	-.1177	-.2101	.8884							
Loflow	-.2330	-.2434	-.2124	-.2614	-.2283	.4696	-.0978	-.1687	-.3160	-.2345	.8902						
Parlam	.5236	.6025	.4962	.3922	.4327	-.2994	-.1313	-.1245	-.2332	.5677	-.1869	.7888					
Lentic	.9092	.2274	.2694	.3075	-.0572	-.0854	-.0734	.2243	.3630	-.0762	-.6342	.0097	.9047				
Eros	-.2993	-.2892	-.2178	-.0941	-.5048	.4196	-.1153	.2022	.2038	-.6500	.1682	-.5752	.3769	.8933			
Sort	-.2368	-.2996	-.2454	-.2051	-.2898	.4615	-.2495	.1330	.0245	-.6274	.4649	-.3585	-.0893	.5643	.7894		
Prebed	.4209	.6240	.5510	.4277	.3076	-.3552	-.1019	-.1477	-.2767	.6020	-.2217	.6681	-.0800	-.6824	-.5221	.8529	
Indur	-.2714	-.2966	-.1673	-.1088	-.3121	.3458	-.1546	.0883	.2694	-.7763	.1328	-.5888	.2732	.7607	.6213	-.7339	.8937

Square roots of communalities in diagonal. 0's omitted before decimals since all r's are $-1 < r < 1$.

behavior of the 99 beds can be predicted from knowing the control (loadings) of the other 16 variables on the common factors. Unrelated to that control is 49.7%. Apparently, bed thickness is related to other bed properties but also contains a strong independent element that cannot be predicted from knowledge of the other variables. The table of communality estimates is shown in Table B-4.

The Factor Matrices: R-Mode

Table B-5 shows the list of factors, associated eigenvalues, and the percentage of variance for which each factor accounts in the iterative analysis. The first factor pattern gives the largest pattern of relationships in the data; the second delineates the next largest pattern that is independent of the first (orthogonal or uncorrelated); the other factors give increasingly smaller patterns of relationships. The amount of variance in the data described by each pattern decreases successively with each factor.

The factor loadings are shown in Table B-6. These loadings measure the degree of involvement of each variable in a particular pattern. The square of the loading time 100 gives the percent that a variable has in common (or is explainable by) a given factor. For example, in the factor loading table, thickness has a loading of 0.61600 on the first factor. This means that $(0.61600)^2 \times 100 = 37.9\%$ of the variation of thickness in the 99 beds can be reliably predicted from knowledge of the particular pattern picked out by the first factor. By looking at the values of the loadings (including important negative as well as positive

Table B-4. Communality estimates, R-mode factor analysis

Variable	Communality
THICK	0.50322
DMAX	0.99898
DID	0.82712
MEAN	0.91331
MASS	0.55238
NORM	0.60989
COFRAC	0.48296
INNORM	0.45314
STRAT	0.36963
MATRIX	0.80710
LOFLOW	0.79253
PARLAM	0.62215
LENTIC	0.81842
EROS	0.79800
SORT	0.62313
PREBED	0.72738
INDUR	0.79867

Table B-5. Factors, eigenvalues, percent of variance explained, and cumulative variance explained, R-mode analysis

Factor	Eigenvalue	% of Var	Cum %
1	5.75097	49.2	49.2
2	2.66352	22.8	71.9
3	1.78749	15.3	87.2
4	0.90038	7.7	94.9
5	0.59563	5.1	100.0

Table B-6. Unrotated factor loadings, R-mode analysis

	Factor 1	Factor 2	Factor 3	Factor 4	Factor 5
THICK	0.61600	0.29786	0.13683	0.06942	-0.10727
DMAX	0.80376	0.50384	0.30541	0.07578	-0.00893
DID	0.68506	0.52839	0.26808	0.07760	0.02691
MEAN	0.61783	0.66626	0.23691	0.17057	-0.04983
MASS	0.43095	-0.25370	-0.08355	-0.52938	-0.12283
NORM	-0.52684	0.01063	0.39265	0.14808	0.39511
COFRAC	0.02488	-0.19020	-0.38555	0.54376	0.04289
INNORM	-0.07892	0.32634	-0.32226	0.21048	-0.43848
STRAT	-0.20003	0.29855	-0.46698	0.09954	-0.11182
MATRIX	0.71860	-0.38819	-0.20430	0.26311	0.17047
LOFLOW	-0.39451	-0.31333	0.68952	0.22085	-0.12042
PARLAM	0.75704	-0.06759	0.15155	-0.14497	0.02238
LENTIC	0.05446	0.67671	-0.46107	-0.18650	0.33190
EROS	-0.71493	0.51748	0.03592	0.05199	0.12287
SORT	-0.63655	0.21194	0.37312	-0.06304	-0.17269
PREBED	0.82711	-0.14298	0.13575	-0.02795	0.06019
INDUR	-0.71821	0.50702	0.06409	-0.14627	-0.01639

loadings) the particular variables that are strongly related to the factor can be determined and the factor may be interpretable in light of which variables participate in the pattern that it delineates.

Factor Rotation: R-Mode

Figure B-1 graphically shows the first and second R-mode factor axes determined for the data by the above procedure. Loadings of the variables on these two factors are represented by the orthogonal projections of each vector onto the factor axes. Now, while factor 1, for example, lies about the center of gravity of the data, the values of factor loadings for each property clearly show that distinct clusters in the properties cannot be distinguished. In this position, the factor 1 axis only accounts for maximal variation in the data.

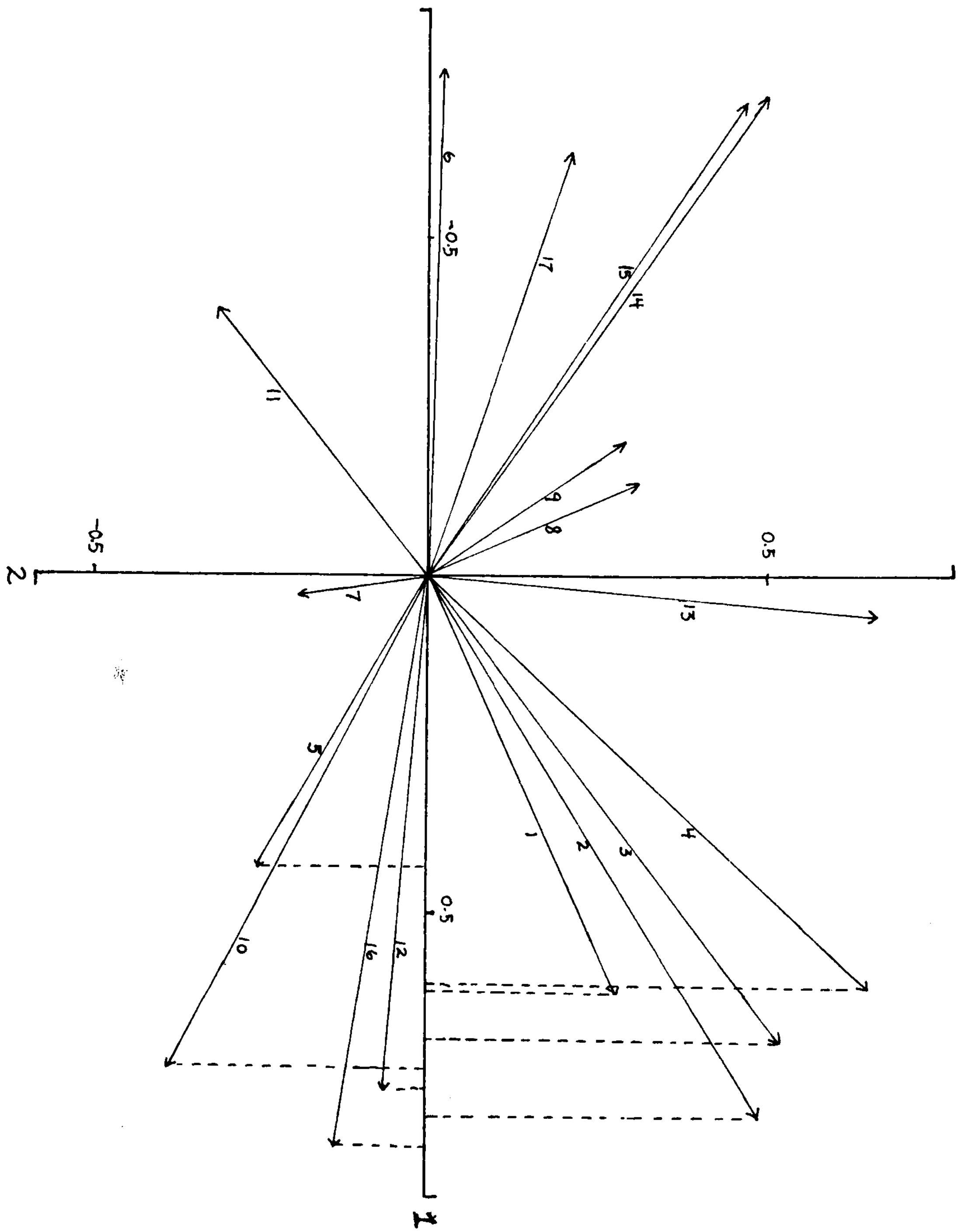

Figure B-1. Unrotated factor axes 1 and 2.

The contribution of distinct data clusters to each factor can more clearly be distinguished by rotating the factor axes, while maintaining their orthogonality (independence), until the simplest, most straightforward clustering of the data that correlates with them is achieved. In this manner, loadings of the properties (orthogonal projections onto the factor axes) are driven either to very high or very low values. Such a rotation is termed a varimax rotation (Rummel, 1970) and is graphically shown for factors 1 and 2 in Figure B-2. The transformation matrix by which the original is multiplied to rotate the axes is given in Table B-7. The transformed loadings are given in Table B-8. Graphical presentations of all varimax rotated factors are presented in Chapter 5 of the text.

It is possible to ease the restriction of orthogonality for factor axes and allow the axes to correlate with each other through rotation. In general, the angle between axes will no longer be 90°. This style of rotation is known as oblique rotation (Rummel, 1970). It was performed for the data but none of the obliquely rotated axes were sufficiently far from orthogonality to pick out the clusters of variance more clearly than the varimax rotation. Consequently, the oblique values and plots are not given in this work.

The Q-Mode Analysis

The factor tables for the Q-mode analysis are presented in Tables B-9 through B-18 without explanatory text. Their interpretation and meaning are the same as those for the R-mode except row beds rather

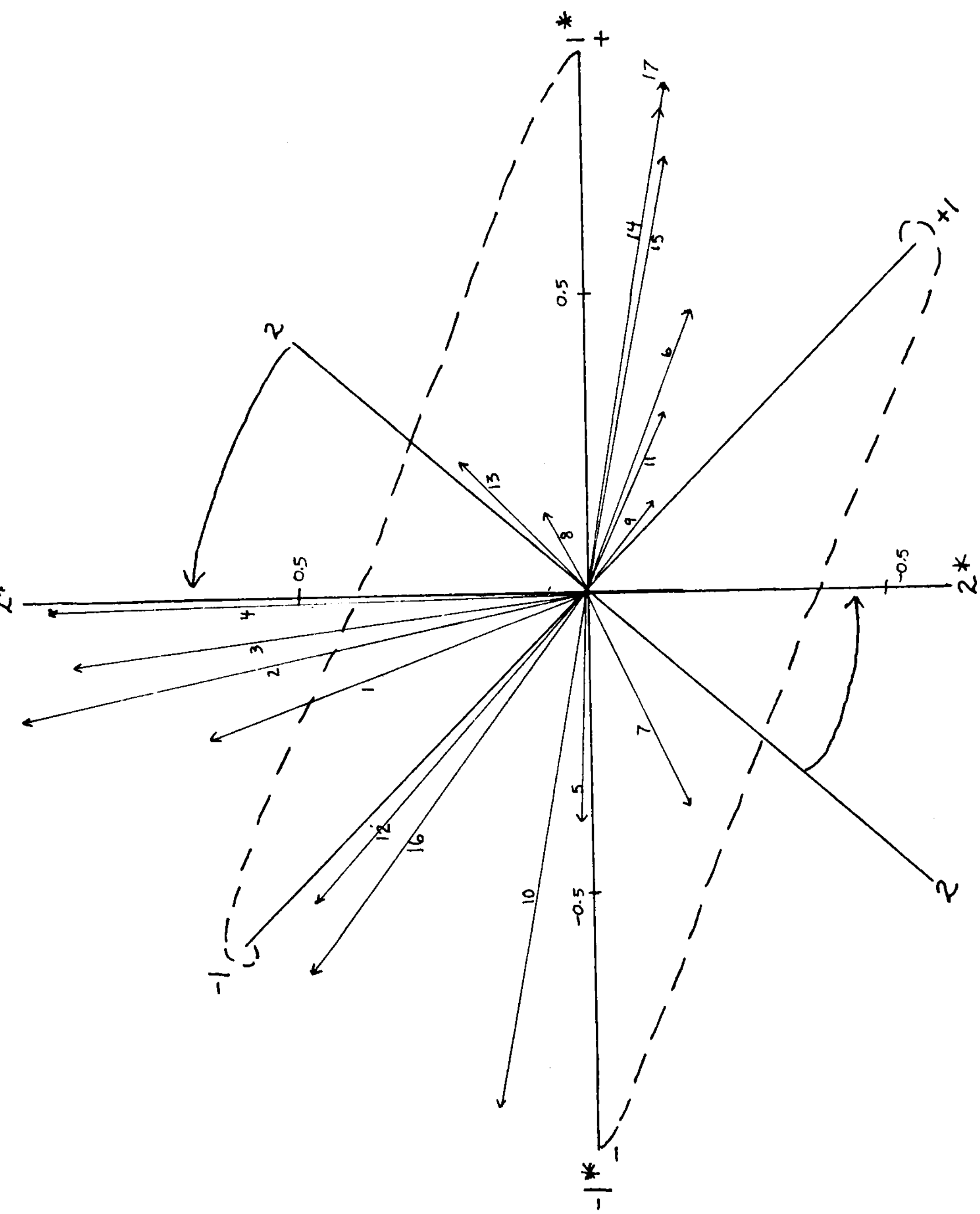

Figure B-2. Rotated varimax factor axes 1 and 2.

Table B-7. Transformation matrix, R-mode analysis

	Factor 1	Factor 2	Factor 3	Factor 4	Factor 5
Factor 1	-0.72342	0.64788	0.08679	-0.22121	-0.02130
Factor 2	0.57693	0.61987	0.47186	0.09198	0.22761
Factor 3	0.32698	0.41221	-0.68593	-0.08341	-0.49569
Factor 4	-0.17808	0.15352	-0.27479	0.90121	0.23880
Factor 5	-0.07207	-0.05028	0.47308	0.35138	-0.80312

Table B-8. Varimax factor loadings, R-mode analysis

	Factor 1	Factor 2	Factor 3	Factor 4	Factor 5
THICK	-0.23367	0.65618	0.03033	-0.09541	0.08958
DMAX	-0.20376	0.97103	0.07297	-0.09178	-0.02856
DID	-0.11884	0.89244	0.11631	-0.04591	-0.03029
MEAN	-0.01188	0.93962	0.13505	0.04106	0.10180
MASS	-0.38231	0.01241	0.06237	-0.63193	-0.05327
NORM	0.46079	-0.17002	-0.16381	0.35705	-0.46295
COFRAC	-0.35372	-0.17939	0.04774	0.51427	0.24270
INNORM	0.13411	0.07268	0.10291	0.10997	0.63811
STRAT	0.15459	-0.11612	0.36357	0.16108	0.41727
MATRIX	-0.86974	0.17255	0.02768	0.11940	-0.07647
LOFLOW	0.29943	-0.12563	-0.77271	0.15766	-0.25526
PARLAM	-0.51289	0.48766	-0.01971	-0.30910	-0.15922
LENTIC	0.20955	0.21937	0.84856	0.03720	0.07032
EROS	0.80937	-0.12581	0.20132	0.29278	0.02894
SORT	0.72844	-0.12823	-0.27555	0.01169	0.00048
PREBED	-0.63580	0.49588	-0.05264	-0.21147	-0.17247
INDUR	0.86026	-0.14625	0.16539	0.06258	0.07717

Table B-9. Communality estimates, Q-mode analysis, odd-numbered beds

Variable	Communality	Variable	Communality
BED1	0.96954	BED51	0.99813
BED3	1.46543	BED53	0.92844
BED5	1.74799	BED55	1.01347
BED7	1.00374	BED57	1.02707
BED9	0.95661	BED59	0.81552
BED11	0.97871	BED61	0.97634
BED13	1.01284	BED63	0.98879
BED15	0.97740	BED65	1.02413
BED17	0.98229	BED67	1.01531
BED19	0.99092	BED69	1.01956
BED21	0.99811	BED71	0.92064
BED23	1.01327	BED73	0.96940
BED25	0.91957	BED75	0.98390
BED27	0.93743	BED77	0.96882
BED29	0.93231	BED79	0.96229
BED31	1.02154	BED81	0.92292
BED33	1.02461	BED83	0.94666
BED35	0.93178	BED85	0.93784
BED37	0.95310	BED87	0.98968
BED39	0.97235	BED89	0.97694
BED41	0.95784	BED91	0.83503
BED43	1.02462	BED93	0.92861
BED45	0.98771	BED95	0.97577
BED47	1.00032	BED97	0.93061
BED49	1.02714	BED99	1.80885

Table B-10. Factors, eigenvalues, percent of variance explained, and cumulative variance explained, Q-mode analysis, odd-numbered beds

Factor	Eigenvalue	% of Var	Cum %
1	34.15021	68.3	68.3
2	15.11292	30.2	98.5
3	1.38871	2.8	101.3

Table B-11. Unrotated factor loadings, Q-mode analysis, odd-numbered beds

	Factor 1	Factor 2	Factor 3
BED1	0.85899	0.48129	0.00648
BED3	1.16657	0.04066	-0.32075
BED5	1.09420	-0.03698	0.74119
BED7	0.77382	-0.63529	-0.03668
BED9	0.77942	-0.59065	0.01571
BED11	0.78407	-0.60291	-0.02086
BED13	0.78544	-0.62888	-0.02092
BED15	0.76798	-0.62253	-0.00742
BED17	0.76113	-0.63450	-0.01941
BED19	0.75850	-0.64446	-0.01632
BED21	0.79679	-0.60115	-0.04309
BED23	0.77950	-0.63687	-0.00658
BED25	0.75413	-0.57657	-0.13572
BED27	0.77800	-0.56505	-0.11338
BED29	0.75738	-0.58749	-0.11631
BED31	0.69517	0.73364	-0.00744
BED33	0.67468	0.75294	-0.05006
BED35	0.91199	-0.30363	0.08870
BED37	0.97038	0.09093	0.05651
BED39	0.96040	0.20335	0.09295
BED41	0.89581	0.39255	0.03566
BED43	0.67139	0.75400	-0.07311
BED45	0.87069	0.47583	0.05651
BED47	0.82036	0.57041	0.04432
BED49	0.66591	0.76006	-0.07755
BED51	0.81774	0.57332	0.02693
BED53	0.84471	0.46353	0.00633
BED55	0.75392	0.66693	0.01645
BED57	0.64453	0.78113	-0.03874
BED59	0.81609	0.38548	-0.03023
BED61	0.92295	-0.34746	0.06149
BED63	0.85772	0.50077	0.04821
BED65	0.66988	0.75829	-0.01970
BED67	0.72886	0.69512	-0.02960
BED69	0.69853	0.72911	-0.00408
BED71	0.94617	-0.13148	0.09009
BED73	0.91008	0.36736	0.07873
BED75	0.88339	0.44574	0.06955
BED77	0.79938	-0.57100	-0.06143
BED79	0.96025	0.17460	0.09858
BED81	0.81980	-0.49883	0.04489
BED83	0.77839	-0.57987	0.06723
BED85	0.85925	-0.44108	0.07060

Table B-11. (continued)

	Factor 1	Factor 2	Factor 3
BED87	0.85294	0.50993	0.04617
BED89	0.75574	-0.63641	-0.02782
BED91	0.67020	0.61850	-0.05756
BED93	0.78563	-0.54563	-0.11698
BED95	0.76440	-0.62539	0.01886
BED97	0.69901	-0.60427	0.27724
BED99	1.14589	0.03756	-0.70312

Table B-12. Transformation matrix, Q-mode analysis, odd-numbered beds

	Factor 1	Factor 2	Factor 3
Factor 1	0.71534	0.69852	0.01907
Factor 2	-0.69839	0.71559	-0.01370
Factor 3	-0.02322	-0.00352	0.99972

Table B-13. Varimax factor loadings, Q-mode analysis, odd-numbered beds

	Factor 1	Factor 2	Factor 3
BED1	0.27819	0.94440	0.01626
BED3	0.81355	0.84509	-0.29897
BED5	0.79134	0.73524	0.76236
BED7	0.99808	0.08604	-0.01321
BED9	0.96969	0.12172	0.03867
BED11	0.98243	0.11633	0.00236
BED13	1.00155	0.09870	0.00269
BED15	0.98431	0.09100	0.01577
BED17	0.98805	0.07769	0.00380
BED19	0.99305	0.06872	0.00698
BED21	0.99081	0.12655	-0.01964
BED23	1.00254	0.08878	0.01701
BED25	0.94529	0.11466	-0.11340
BED27	0.95380	0.13950	-0.09076
BED29	0.95479	0.10905	-0.09379
BED31	-0.01491	1.01059	-0.00423
BED33	-0.04206	1.01024	-0.04749
BED35	0.86237	0.41945	0.11023
BED37	0.62933	0.74269	0.07376
BED39	0.54283	0.81604	0.10845
BED41	0.36583	0.90651	0.04736
BED43	-0.04461	1.00878	-0.07062
BED45	0.28921	0.94849	0.06658
BED47	0.18744	0.98106	0.05214
BED49	-0.05267	1.00931	-0.07525
BED51	0.18394	0.98137	0.03467
BED53	0.28038	0.92172	0.01609
BED55	0.07315	1.00382	0.02169
BED57	-0.08358	1.00931	-0.03714
BED59	0.31527	0.84601	-0.01994
BED61	0.90145	0.39584	0.08384
BED63	0.26271	0.95731	0.05769
BED65	-0.04993	1.01061	-0.01731
BED67	0.03661	1.00664	-0.02522
BED69	-0.00942	1.00969	-0.00075
BED71	0.76657	0.56651	0.10991
BED73	0.39263	0.89831	0.09103
BED75	0.31901	0.93578	0.08027
BED77	0.97203	0.14999	-0.03834
BED79	0.56268	0.79535	0.11447
BED81	0.93377	0.21553	0.06735
BED83	0.96023	0.12853	0.09000
BED85	0.92106	0.28432	0.09301

Table B-13. (continued)

	Factor 1	Factor 2	Factor 3
BED87	0.25294	0.96053	0.05544
BED89	0.98572	0.07258	-0.00468
BED91	0.04881	0.91094	-0.05324
BED93	0.94577	0.15874	-0.09449
BED95	0.98313	0.08636	0.04201
BED97	0.91560	0.05489	0.29878
BED99	0.80980	0.82977	-0.68158

Table B-14. Communality estimates, Q-mode analysis, even-numbered beds

Variable	Communality	Variable	Communality
BED2	0.96452	BED52	1.01316
BED4	1.48028	BED54	0.95535
BED6	0.97137	BED56	0.96592
BED8	1.00518	BED58	1.00143
BED10	0.98668	BED60	0.97573
BED12	0.96478	BED62	1.00447
BED14	0.95651	BED64	0.93697
BED16	0.95959	BED66	1.01673
BED18	0.96030	BED68	1.04124
BED20	0.99925	BED70	0.99528
BED22	1.00666	BED72	0.96440
BED24	0.96699	BED74	1.04738
BED26	0.99375	BED76	0.97922
BED28	0.96356	BED78	0.96179
BED30	0.99266	BED80	0.99828
BED32	0.99476	BED82	0.94105
BED34	0.99507	BED84	0.94497
BED36	0.97639	BED86	0.96644
BED38	1.00078	BED88	0.98116
BED40	0.99529	BED90	0.98149
BED42	0.98699	BED92	0.99124
BED44	1.02068	BED94	1.02572
BED46	0.97873	BED96	0.98592
BED48	1.46524	BED98	0.96750
BED50	1.02248		

Table B-15. Factors, eigenvalues, percent of variance explained, and cumulative variance explained, Q-mode analysis, even-numbered beds

Factor	Eigenvalue	% of Var	Cum %
1	34.62541	70.7	70.7
2	13.54608	27.6	98.3
3	1.07983	2.2	100.5

Table B-16. Unrotated factor loadings, Q-mode analysis, even-numbered beds

	Factor 1	Factor 2	Factor 3
BED2	0.82916	0.52630	0.00451
BED4	1.16385	0.20768	0.28743
BED6	0.87033	-0.46238	0.01002
BED8	0.86893	-0.48992	0.10063
BED10	0.86527	-0.48331	0.06642
BED12	0.88035	-0.43486	-0.02572
BED14	0.88257	-0.40960	-0.09903
BED16	0.87780	-0.42839	-0.07447
BED18	0.87787	-0.43483	-0.02380
BED20	0.86682	-0.49732	0.02330
BED22	0.85260	-0.51644	0.11417
BED24	0.87060	-0.45347	0.05842
BED26	0.87687	-0.47411	0.00883
BED28	0.92599	-0.30880	0.10360
BED30	0.85992	-0.47346	0.17040
BED32	0.67964	0.73011	0.00499
BED34	0.71129	0.69922	-0.01540
BED36	0.66379	0.73192	0.00789
BED38	0.70683	0.70788	-0.00870
BED40	0.74291	0.66407	-0.04884
BED42	0.98103	0.03552	-0.15270
BED44	0.57552	0.82492	0.09475
BED46	0.87734	0.42245	-0.17474
BED48	1.15479	0.20469	0.29967
BED50	0.57729	0.82506	0.09218
BED52	0.62709	0.78551	0.05381
BED54	0.96923	0.00176	-0.12624
BED56	0.88036	-0.43498	-0.04102
BED58	0.94937	0.22352	-0.22399
BED60	0.95830	0.15217	-0.18503
BED62	0.96389	0.12209	-0.24592
BED64	0.92586	0.08836	-0.26821
BED66	0.60232	0.80534	0.07330
BED68	0.51208	0.86975	0.15020
BED70	0.70961	0.70095	-0.02014
BED72	0.94692	0.15731	-0.20734
BED74	0.49301	0.88080	0.16883
BED76	0.85913	-0.48835	0.05124
BED78	0.90310	-0.35032	0.15323
BED80	0.97372	-0.05927	-0.21598
BED82	0.88818	-0.35605	-0.15942
BED84	0.91374	-0.30273	-0.13566
BED86	0.91753	-0.29715	-0.19049

Table B-16. (continued)

	Factor 1	Factor 2	Factor 3
BED88	0.82222	-0.48611	0.26231
BED90	0.84983	-0.48087	0.16748
BED92	0.66537	0.74056	0.00908
BED94	0.55983	0.83724	0.10643
BED96	0.86002	-0.49148	-0.06886
BED98	0.76923	-0.48330	0.37710

Table B-17. Transformation matrix, Q-mode analysis, even-numbered beds

	Factor 1	Factor 2	Factor 3
Factor 1	0.82677	0.55633	0.08331
Factor 2	-0.55918	0.82893	0.01390
Factor 3	0.06132	0.05808	-0.99643

Table B-18. Varimax factor loadings, Q-mode analysis, even-numbered beds

	Factor 1	Factor 2	Factor 3
BED2	0.39151	0.89782	0.07190
BED4	0.86373	0.83633	-0.18655
BED6	0.97874	0.10149	0.05610
BED8	0.99853	0.08314	-0.03469
BED10	0.98971	0.08461	-0.00082
BED12	0.96944	0.12781	0.09292
BED14	0.95265	0.14572	0.16651
BED16	0.96072	0.12891	0.14137
BED18	0.96749	0.12656	0.09081
BED20	0.99619	0.07135	0.04208
BED22	1.00069	0.05287	-0.04991
BED24	0.97694	0.11184	0.00802
BED26	0.99063	0.09534	0.05766
BED28	0.94462	0.26520	-0.03038
BED30	0.98616	0.09583	-0.10474
BED32	0.15380	0.98351	0.06178
BED34	0.19614	0.97442	0.08433
BED36	0.14001	0.97646	0.05761
BED38	0.18802	0.97951	0.07740
BED40	0.23989	0.96093	0.11980
BED42	0.78186	0.56635	0.23437
BED44	0.02036	1.00948	-0.03499
BED46	0.47842	0.82812	0.25308
BED48	0.85867	0.82952	-0.19955
BED50	0.02158	1.01043	-0.03229
BED52	0.08252	1.00312	0.00955
BED54	0.79261	0.53334	0.20656
BED56	0.96857	0.12682	0.10817
BED58	0.46419	0.70043	0.30539
BED60	0.69586	0.64853	0.26632
BED62	0.71357	0.62316	0.32704
BED64	0.69962	0.57275	0.34561
BED66	0.05214	1.00691	-0.01166
BED68	-0.05376	1.01457	-0.09491
BED70	0.19350	0.97464	0.08893
BED72	0.68221	0.64516	0.28767
BED74	-0.07457	1.01421	-0.11491
BED76	0.98653	0.07613	0.01373
BED78	0.95195	0.22093	-0.08232
BED80	0.82494	0.48004	0.29550
BED82	0.92364	0.18973	0.22789
BED84	0.91642	0.24952	0.20709
BED86	0.91307	0.25307	0.26212

Table B-18. (continued)

	Factor 1	Factor 2	Factor 3
BED88	0.96770	0.06971	-0.19963
BED90	0.98178	0.08391	-0.10277
BED92	0.13656	0.98457	0.05668
BED94	0.00121	1.01165	-0.04777
BED96	0.98164	0.06705	0.13343
BED98	0.92936	0.04923	-0.31838

than properties are the variables. There are a few points which should be noted, however.

First, the correlation matrix (cosine values) is not included in the text because of its size: 99 × 99 = 9801 entries. The major characteristic of interest is that most correlation coefficients are quite high, reflecting, the author thinks, the strong kinship of beds in the coarse-clastic family.

Second, a few communality estimates are greater than one. This statistical oddity occurs for those beds in which missing data was treated by substituting the value of the mean of the particular property for that missing entry. Since the correlations are generally so high, the substitution of a *common* mean value causes the bed's communality to rise above one. This does not mean, of course, that the bed is excessively explained! It merely reflects calculative eccentricity due to missing data.

Third, the correlation matrix had to be divided for the capacity of the computer. An odd-even division of beds was used. As the tables show, there is no substantial difference between the factor results.

Technical Information

The factor program was run on the Dec-10 computer at The University of Tennessee. The program used was that contained in SPSS (Nie, et al., 1975).

APPENDIX C

THE GENERAL PROBLEM OF EMPIRICAL PROBABILITY DISTRIBUTIONS AND ITS RELATIONSHIP TO THE SHALE BED THICKNESS DISTRIBUTION

One of the very real problems that faces the theoretician is the nature of the available data itself. Often, a number of theoretical curves can be fitted to a given data set. Usually, the quantity of information that would define an unambiguous distribution is simply not available. This problem, thus, resolves itself into which one of a group of distributions provide the most likely or most reasonable interpretation of the data.

For quite some time, it has been fashionable to normalize geological distributions by applying a log transform to the data. This generally straightens cumulative curves and approximately normalizes frequency curves. Yet, as far as a fit to the untransformed data, an exponential curve can often provide an equally good approximation. Which distribution, then, makes the best geological sense?

If we regard elapsed time between turbidity incursions (pelagic sediments) an exponential distribution makes the most sense. In general, it is not possible to identify this background sediment. But, in turbidite sequences in which the turbidite portion is carbonate rich and which lie below the lysocline, a distinctly calcite depleted pelagic division will accumulate on top of the turbidite division. Due to the slow fallout from the overlying water column, most of the calcite should dissolve before it is sedimented. In such a case, there will be a definite difference between the turbidite and pelagic shales.

Hesse (1975) has studied such a system in the Alps and has drawn cumulative curves for turbidite and pelagic shales. Keeping in mind that the curves may have been altered somewhat by erosion and compaction, the frequency curves that may be constructed from Hesse's cumulative curves are astonishingly close to exponential distributions.

For example, his data for the Hällritzer formation pelagic shales and an exponential curve the author fitted for it ($t = x/3$) are shown in Figure C-1. The data for the turbidite portion of the shales, likewise, seems to define an exponential curve as shown in Figure C-2. Unfortunately, Hesse does not give the curve for couplets of the two types of shale. But, if we convolute them by the formula suggested earlier:

$$s(z) = \frac{\lambda_g \lambda_h}{\lambda_h - \lambda_g} \left(\exp^{-z\lambda_g} - \exp^{-z\lambda_h} \right)$$

the curve shown in Figure C-3 is formed with mode at around 10.5 cm. It is a slightly skewed curve which, given the rough data on hand, could reasonably be interpreted as a skewed normal curve. There is, therefore, some empirical justification for the suggested model of shale sedimentation.

As a refinement, it might be noted that turbidite and pelagic sedimentation can proceed at the same time. In this case, the distribution is formed by:

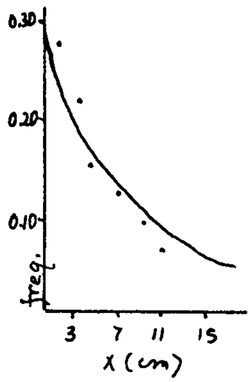

Figure C-1. Pelagic shale distribution and fitted exponential distribution function.

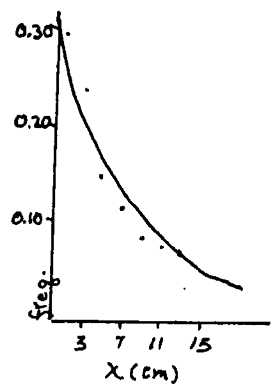

Figure C-2. Turbiditic shale distribution and fitted exponential distribution function.

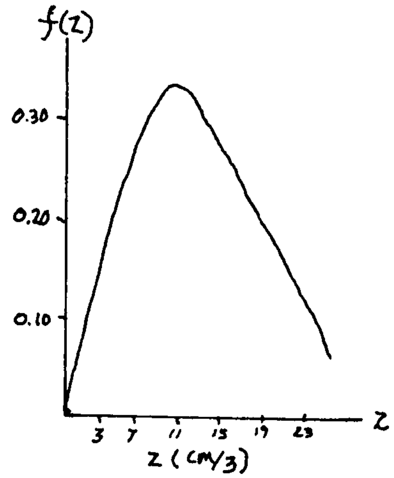

Figure C-3. Convolution of two exponential shale distributions.

$z = \max(x, y)$;

which in our case resolves itself into:

$$s(z) = \lambda_g \exp^{-\lambda_g z} + \lambda_h \exp^{-\lambda_h z} - (\lambda_g + \lambda_h) \exp^{-(\lambda_g + \lambda_h) z}$$

However, in the case of Hesse's data, the beds apparently were deposited *essentially* separately. And, due to the extreme differences in sedimentation rates, we would, for all practical purposes, expect the sum $g*h$ rather than $\max(x, y)$.

VITA

Benjamin Kyle Bowlin was born in Hancock County, Tennessee, on January 8, 1950. He attended elementary schools in that county and was graduated from Hancock County High School in June 1967. He entered The University of Tennessee, Knoxville, in September of 1967 and received the Bachelor of Arts degree in Philosophy in June of 1971. In the fall of 1971, he entered The University of Notre Dame and worked toward a degree of Master of Arts in Philosophy with specialities in Metaphysics and Symbolic Logic. This degree was conferred in August of 1974.

From the fall of 1974 until June of 1976, he worked as a remedial reading specialist with the Hancock County School System. He entered The University of Tennessee, Knoxville, in June of 1976 to begin work on the Master of Science degree in Geology. He received this degree in December of 1979.

The author is a member of Phi Beta Kappa, Phi Kappa Phi, Sigma Gamma Epsilon, the American Liszt Society, and a fellow of the International Franz Liszt Society.